Technische Universität München
Fakultät für Medizin

Abteilung für experimentelle Radioonkologie und Strahlenbiologie

Immunological Aspects of the major Heat-Shock Protein 70 and its Role as a Tumor Biomarker in the NSCLC

Sophie Gunther

Vollständiger Abdruck der von der Fakultät für Medizin der Technischen Universität München zur Erlangung des akademischen Grades eines Doktors der Medizin (Dr. med.) genehmigten Dissertation.

Vorsitzende(r): Prof. Dr. Jürgen Schlegel

Prüfer der Dissertation:

1. Prof. Dr. Gabriele Multhoff

2. apl. Prof. Dr. Philipp J. Jost

Die Dissertation wurde am 27.08.2019 bei der Technischen Universität München eingereicht und durch die Fakultät für Medizin am 01.01.2020 angenommen.

This dissertation is dedicated to the people who helped to initiate the lung cancer study keeping in mind that behind every blood sample there is a human mind who has to bear the diagnosis of cancer.

Contents

I. List of Abbreviations

APC, allophycocyanin; AJCC, American Joint Committee on Cancer; AUC, area under the curve; BD, Becton Dickinson Biosciences; BC, Beckmann; BSP-1, bone sialoprotein I; BNSP, bone sialoprotein I; CA IX, carbonic anhydrase IX; CD, cluster of differentiation; COPD, chronic obstructive pulmonary disease; CT, computed tomography; Ctrl, control; CYFRA 21-1, cytokeratin-19 fragment; ELISA, Enzyme-linked Immunosorbent Assay; FITC, fluorescein isothiocyanate; GM-CSF, granulocyte-macrophage colony stimulating factor; HLA-E, Hsp70, heat shock protein 70; HIF1α, Hypoxia-inducible factor 1α; IASLC, International Association for the Study of Lung Cancer; IL-1 β, interleukin-1β; IL-2, interleukin 2; IL-10, interleukin 10; LDH, lactate dehydrogenase; MHC, major histocompatibility complex; MIP-1α, macrophage inflammatory protein-1 α; NK cells, natural killer cells; NSCLC, non-small-cell lung cancer; NSE, neuron specific enolase; OPN, osteopontin; PBL, peripheral blood lymphocytes; pRb, Retinoblastoma protein; PBS, phosphate buffered saline; PD-1, programmed cell death protein 1; PD-L1, programmed death ligand 1; PET, positron emission tomography; PS, phosphatidylserine; RANTES, regulated upon activation, normal T cell expressed and secreted; RNA, Ribonucleic acid; RT, radio(chemo)therapy; ROC-curve, receiver operating characteristic; SCC, squamous cell carcinoma; SCCHN, squamous cell carcinoma of the head and neck; TH2 cell, T helper cell; Treg, regulatory T cells; TNFα, tumor necrosis factor α; VDRE, vitamin D response element; VEGF, vascular endothelial growth factor; WHO, world health organization;

II. Abstract

The heat-shock protein 70 (Hsp70) is a physiologically conserved protein which maintains protein homeostasis by preventing aggregation or misfolding. Apart from its overexpression in the cytosol, Hsp70 is frequently found on the cell surface of many different tumor entities and actively secreted into the blood circulation in exosomes by malignant cells. The expression of Hsp70 on tumor cells represents an enhanced aggressiveness on the one hand, on the other hand, this protein has great immunogenic potential and serves as an activator of NK cell-mediated immunity after stimulation with Hsp70-peptide TKD plus low-dose interleukin-2. Based on these findings, a current proof-of-concept phase II clinical trial with radiochemotherapy (RCT) following ex vivo stimulation of autologous NK cells in squamous cell carcinoma of the lung with stage IIIA/IIIB has been initiated. In the context of this study, blood samples of NSCLC patients were collected to determine the Hsp70 status in the plasma using the lipHsp70 ELISA. The novel ELISA enables the quantification of both lipid bound and free Hsp70 in the blood. A comparison of Hsp70 in NSCLC patients and healthy volunteers confirmed significantly elevated levels in the blood of tumor patients. Further investigations on Hsp70 which are based on a different patient collective of NSCLC patients revealed a significant correlation with the gross tumor volume. The immune phenotype was evaluated with fluorescence-activated cell sorting (FACS). Significantly elevated ratios of NK cells with the activation markers $CD69^{+}/CD94^{+}$ were associated with low serum Hsp70 levels in squamous cell NSCLC patients. These findings might indicate that the adeno NSCLC is less immunogenic than the squamous cell NSCLC.

Since the overall survival of lung cancer patients is unsatisfactory due to a lack of specific symptoms leading to a delay of first diagnosis, the role of Hsp70 was investigated in the therapy monitoring of tumor patients and compared to the tumor biomarker osteopontin. Similar to Hsp70, osteopontin is physiologically expressed especially by osteoblasts and serves as a component of the extracellular bone matrix. It has also been found to be enhanced in the blood of tumor patients and indicates tumor hypoxia concomitant with a disadvantageous prognosis. Hypoxia mediates resistance to radio(chemo)therapy by stimulating the transcription of hypoxia-related genes, including the major stress-inducible Hsp70. With respect to the opposing traits of Hsp70, its clinical role in the therapy monitoring of patients

with advanced, non-metastasized non-small-cell lung cancer (NSCLC) was assessed. Plasma levels before (T1) and 4-6 weeks after RT (T2) were compared and evaluated in relation to OPN concerning its function as a tumor biomarker. Plasma levels of Hsp70 correlated with those of OPN at T1, and high OPN levels were significantly associated with a decreased overall survival (OS). Hsp70 plasma levels dropped significantly at T2 ($p = 0.016$) when the tumor volume decreased after RT. Nevertheless, with respect to the immunostimulatory capacity of Hsp70 released by dying tumor cells, patients with higher post-therapeutic Hsp70 levels showed a significantly better response to RT ($p = 0.034$) than those with lower levels at T2.

In summary, high OPN plasma levels at T1 are indicative of poor OS, whereas elevated post-therapeutic Hsp70 plasma levels, together with a drop of Hsp70 between T1 and T2, successfully predict favorable responses to RT. Monitoring the dynamics of Hsp70 in NSCLC patients before and after RT can provide additional predictive information for clinical outcome and therefore might allow a more rapid therapy adaptation.

1 INTRODUCTION

Lung cancer is the tumor entity with the highest number of cancer-related deaths and the second most common cancer among both men and women [141]. It is a growing concern especially in countries like China, Asia and Africa [84]. According to the GLOBOCAN report 2000 [103], the incidence of lung cancer worldwide is 1,238,900 with a mortality of 1,103,100 and a 5-year prevalence of 1,394,400. Frequently, the patients already have an advanced stage at the time of first diagnosis as the symptoms of lung tumors are unspecific and can be covered by additional secondary pulmonal diseases like COPD (chronic obstructive pulmonary disease) or pneumonia that are accompanied by clinical symptoms like dyspnea, coughing or chest pain [142]. State of the art therapies, such as radical surgery, chemo- and/or radiotherapy, could not improve the outcome of locally advanced tumor stages. Among all kinds of lung tumors, the Non-Small Cell Lung Cancer (NSCLC) is the most common type with 80-85% [143]. The progression-free and overall survival of NSCLC patients in stage IIIA and IIIB is often less than 16 months [98]. Consequentially, there is a high medical need to explore new treatment modalities to increase life expectancy of NSCLC patients and to develop minimal invasive methods for an early tumor detection.

1.1 Lung Cancer

Lung cancer is the most frequent tumor associated cause of death worldwide [144]. Regarding mortality, it surpasses the mamma carcinoma, prostate cancer and the colon carcinoma. The majority of the patients are male, although the number of female patients is constantly growing [98] due to an increasing percentage of female smokers since the late 20th century. The average age of onset is 70 years [145].

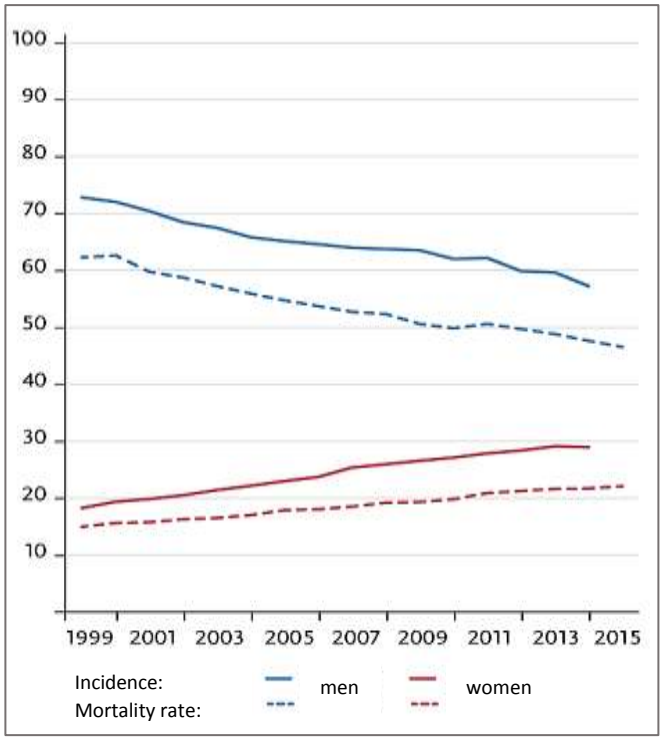

Figure 1:

Age-adjusted rates of incidence and deaths in lung cancer patients, subdivided by gender, ICD-10 C33-34, Germany 1999-214/2015; numbers per 100 000 people;

The majority of lung cancer patients are male, although the number of female patients is constantly growing due to an increasing number of female smokers.

[146]

Smoking is the most significant risk factor of developing lung cancer. In the United States, 87% of all lung cancers are smoking-related [147]. The reason for this is that tobacco smoke includes many different carcinogens like nitrosamines and N-nitroso compounds, benzopyrene and mutagenic metallic substances (e.g. cadmium hydroxide) [121]. However, not only the intentional consumption of cigarettes evokes carcinogenic processes. Also the frequent exposition to second-hand smoking has equal toxic effects [148]. The risk of developing lung cancer when living together in a household with a smoker increases by 20 to 30% [106].

In most cases of non-smoking related cancers, the formation of tumor cells is genetically determined. Alterations in oncogenes and tumor suppressor genes as well as genetical polymorphisms, which are responsible for tumor metabolism and DNA repair, increase the risk of developing lung cancer. Especially mutations in the genes of the epidermal growth factors (EGFR) and anaplastic lymphoma kinase (ALK) have been detected predominantly in never smokers and oligo-smokers [114], whereas KRAS mutations occur more often in current or former smokers. Further, never-smokers frequently develop better-differentiated adenocarcinomas with less mutations in the tumor suppressor gene p53 [119].

Professional exposition to matters like asbestos particles, coke oven gases, arsenic or wood dust combined with tobacco consumption also increases the hazard of carcinogenesis [119]. Altogether, over 90% of work-related lung cancer incidences are caused by exposure to asbestos [117].

1.1.1 Clinical Symptoms and Diagnosis

Frequently, lung cancer is detected at advanced stages. The symptoms of this tumor entity are very unspecific at an early stage and can be associated with other pulmonary disorders like chronic obstructive pulmonary disease (COPD) or emphysemas that are mostly a result of smoking or pneumonia. Moreover, many lung tumors occur simultaneously with pathological tissue impairments like COPD and can be covered by them without reasonable diagnostic analysis. The symptoms include coughing, hemoptysis, wheezing and dyspnea. Apart from respiratory abnormalities, there can be systemic signs that are typical of malignant diseases and are referred to as B-symptoms, which are fever, weight loss of over 10 % in a period of six months and night sweats. In patients with an advanced stage, an infiltration of adjacent structures with tumor tissue can lead to bone and chest pain or difficulties with swallowing for example. Additionally, paraneoplastic syndromes can occur off the tumor sites or its metastases. The associated symptoms include a broad range of metabolic and hormonal changes. Electrolyte imbalance, osseous alterations like the hypertrophic pulmonary osteoarthropathy, Cushing syndrome and different disorders of the neurological system are only some of them [149]. Besides this, a formation of autoantibodies against autoantigens expressed by tumors can lead to neuromuscular syndromes. At an age over forty years, symptoms of asthma and bronchitis, recurring episodes with pneumonia and therapy-resistant coughs and sneezes are always suspicious of a bronchial carcinoma [142].
To reinforce a suspicion, chest x-ray in two planes is mostly the initial imaging to get an overview of potential alterations in a single area, of multifocal lesions or the enlargement of pulmonary nodules, a widened mediastinum or tracheobronchial narrowing for example [149]. The findings of CT imaging give a first hint on altered anatomic structures, but they are not specific to lung cancer and implicate further diagnostic methods like a mediastinoscopy with core needle biopsies of suspicious lesions followed by cytopathologic confirmation. Additionally, PET (positron emission tomography), which is a nuclear imaging technique mostly using fluorine-18 to detect high turnover metabolic processes in the body, can help to differentiate between inflammatory and malignant processes.

A laboratory analysis of the blood can support a suspected diagnosis, although ordinary blood values do not exclude the presence of a tumor. Possible variances might be found in the hemogram, the electrolytes, the lactate dehydrogenase (LDH) and serum uric acid or in the

liver parameters in the case of metastases for example. Additionally, there are tumor markers which can be elevated in patients with lung cancer, such as the neuron specific enolase (NSE) in the small cell lung cancer or CYFRA 21-1 (cytokeratin-19 fragment) especially in the NSCLC. Nevertheless, the stated sensitivity and specificity of these biomarkers varies significantly within the literature. They should not be used for diagnostic issues and rather play a role in the tumorous progress evaluation.

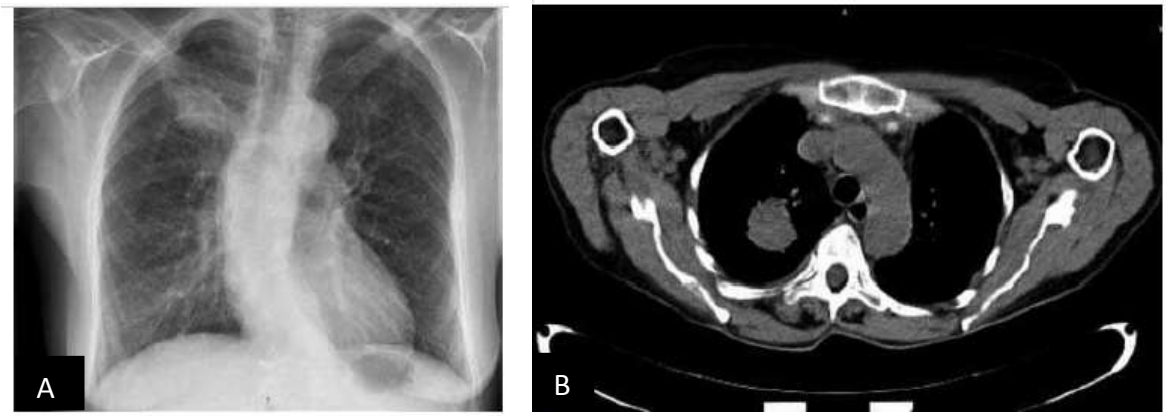

Figure 2:
Affirmation of the diagnosis lung cancer (adenocarcinoma) with medical imaging, Duale Reihe Innere Medizin 2009 [5]
A) Posterior-anterior chest X-ray of a 72 year old woman; tumor location in the right superior lobe
B) The related thoracic CT cross section: peripheral tumor in the right superior lobe

1.1.2 Histopathological Classification of Lung Tumors

Lung tumors consist of malignant cells originating from the bronchi, bronchioles and alveoli. They can be divided into different subgroups according to their histology. The two main types of lung cancer are the Small-Cell Lung Carcinoma (SCLC) and Non-Small Cell Lung Carcinoma (NSCLC). The latter is further classified into the adeno carcinoma, the squamous-cell carcinoma and the large-cell carcinoma.

At present, adenocarcinomas are the most frequent lung cancer type in highly industrialized countries with a rate of 50 % of all Non-Small Cell Lung Cancers [150]. As adenocarcinomas of the lung are highly heterogenous in their genetic aberrations [150], further subgroups can be distinguished. The acinar or papillary predominant adenocarcinoma, the solid predominant

and the invasive mucinous adenocarcinoma are only some of them. Tumor cells of the adeno carcinoma originate from glandular structures mostly in the peripheral lung tissue, whereas the squamous cell carcinoma in situ has its origin in a metaplasia or dysplasia of the squamous epithelium closer to the hilar centre of the lung (figure 4).

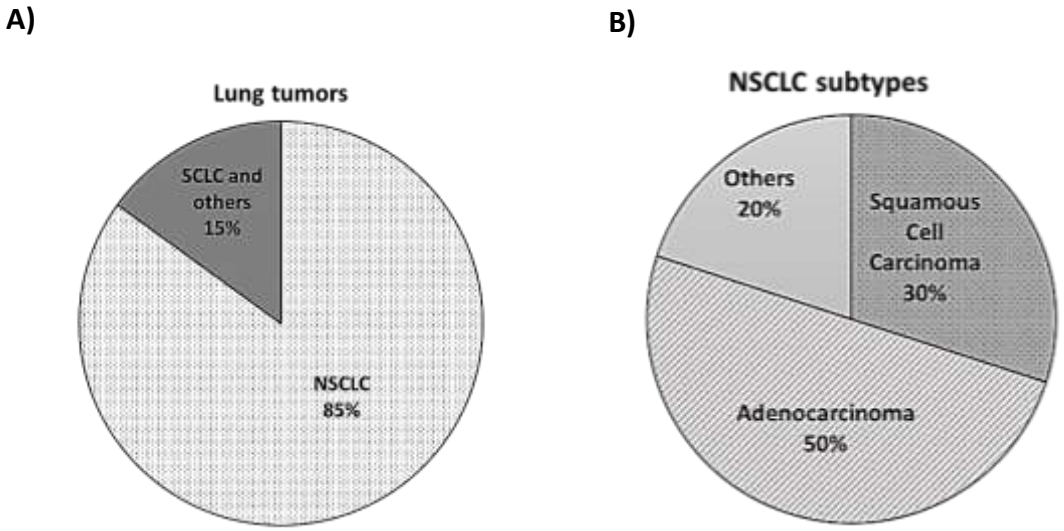

Figure 3:

Illustration of proportional distribution of different lung cancer subtypes

A) Classification of lung tumors: 85% of all lung tumors are NSCLC and 15% are SCLC or other subtypes [150]*; B) Subdivision of the NSCLC into squamous cell carcinoma (30%), adeno-carcinoma (50%) and others including the large cell carcinoma (20%)* [150]

According to the WHO-classification of 2004, carcinomas that distinctly lack glandular, small-cell like or squamous-cell like structures are defined as large cell carcinomas. Typical of this NSCLC subgroup are big cell nuclei (> 26 µm), prominent nucleoli and less cytoplasm. On the contrary, the small cell carcinoma is a poorly differentiated and highly malignant carcinoma with rather small cell nuclei and sparse cytoplasm. The tumor cells are barely cohesive which results in multiple metastases after a short time period and a highly limited survival time.

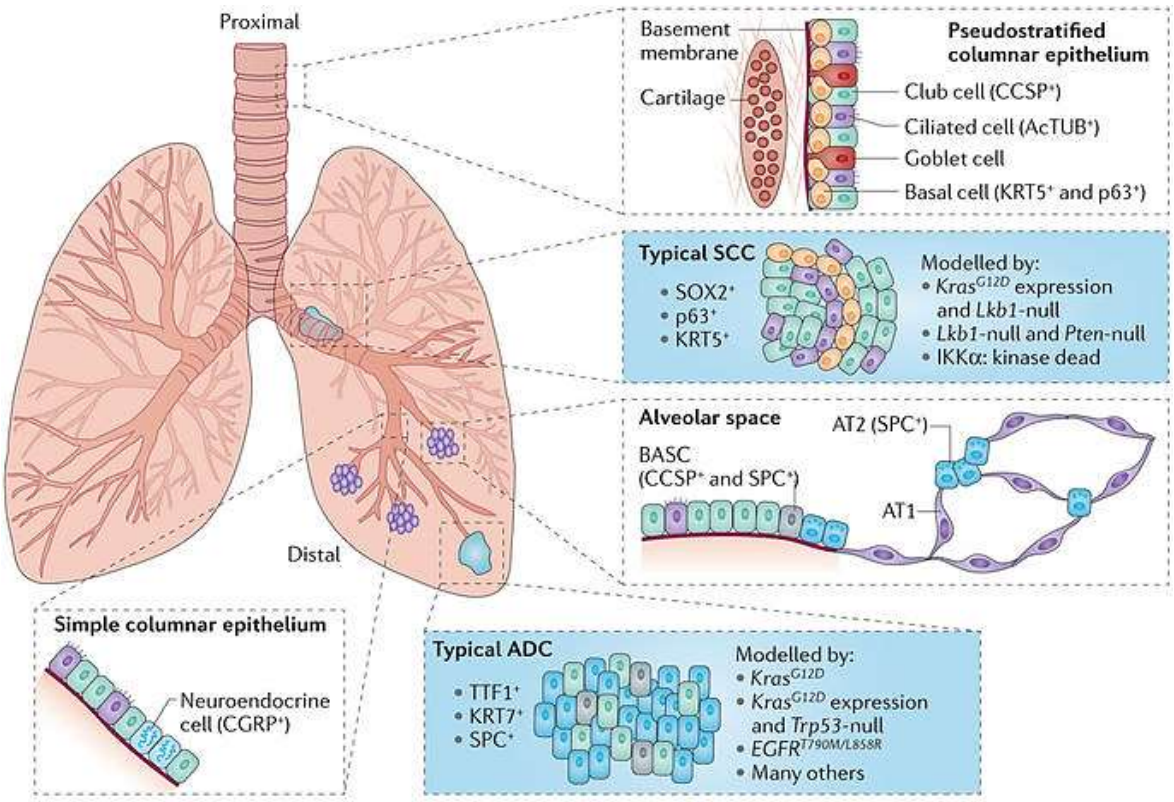

Figure 4:

Scheme of the structure of bronchial epithelium and lung cancer cells with different cellular origin along with markers that represent the respective tumor subtype

Lung cancer cells of the SCC originate from basal cells of the trachea close to the hilus of the lung. The basal cells as well as their metaplasia (in smokers) and cells of the SCC express p63, SRY-box 2 (SOX2) and keratin 5 (KRT5). Adenocarcinomas of the lung derive from respiratory cells which are located peripheral from the hilus and generate surfactant protein C (SPC), KRT7 and thyroid transcription factor 1 (TTF1). The markers KrasG12D, KrasG12D expression and Trp53-null, and epidermal growth factor receptor (EGFR)T790M/L858R are characteristic of adenocarcinomas of the lung.

AcTUB, acetylated tubulin; AT, alveolar epithelial type; CCSP, club cell secretory protein; CGRP, calcitonin gene-related peptide.[23]

1.1.3 Localization, Metastasis and Staging

The localization of bronchial carcinomas is variable and mainly depends on the histological subtype. With a percentage of 60-70%, tumors with a central position near the hilus are predominant. Most squamous carcinomas grow in this manner as their cells derive from the bronchial epithelium. The small cell carcinoma equally emanates from centrally located neuroendocrine cells of the bronchial mucosa. The second most common localization is in the periphery of the lung (30-40%) which is typical of the adenocarcinoma [86]. Diffuse infiltrating pneumonic carcinomas are less frequent.

The progression of the disease is crucially affected by metastasis. Mediastinal lymph nodes are infested frequently and early, continuing with intrapulmonary lymph nodes. Single lymph node stations can be skipped (skip lesion). The migrating tumor cells leave the lung passing parabronchial and hilar lymph nodes. Further sites of metastases are predominantly found in the brain, the suprarenal gland, the liver and the bone. In many cases, the symptoms of metastases become apparent before the primary tumor is identified. In contrast to the NSCLC, hematogenous spreading of the SCLC typically leads to the formation of metastases within a shorter time frame. In these cases, medical imaging shows multiple smaller spots of disseminated tumor tissue in the lung and the aforementioned locations.

For a better evaluation of prognosis and treatment adjustments, the bronchial carcinoma is categorized by the TNM classification which was developed by the Union for International Cancer Control (UICC). A similar classification was used by the American Joint Committee on Cancer (AJCC). In 1987, the staging systems of these federations were unified to create consensus on one international standard for classifying cancers regarding their spread. The TNM staging system was revised according to the IASLC (International Association for the Study of Lung Cancer)/UICC8 and is the present classification system since 1 January 2017. It considers the size of the primary tumor (T), the lymph node involvement (N) and the presence of distant metastases (M). The current staging is summarized in Table 1.

Table 1:

Summary of the staging system of the NSCLC according to the American Joint Committee on Cancer (AJCC)

A) Summary of the TNM staging system in the NSCLC and explanation of the short forms; each stage is a combination of the factors tumor size (T), the affected lymph nodes (N) and the presence of metastasis (M).
B) The combination of different TNM compositions determines the tumor stage of the NSCLC [46]

1A)

Primary Tumor (T) Classification	
TX	Primary tumor cannot be assessed or proven by the presence of malignant cells in sputum or bronchial washings but not visualized by imaging or bronchoscopy
T0	No evidence of primary tumor
Tis	Carcinoma in situ
T1	Tumor 3 cm or less in greatest dimension
T1a	Tumor 2cm or less in greatest dimension
T1b	Tumor more than 2 cm but 3cm or less in greatest dimension

T2	Tumor more than 3 cm but 7 cm or less or tumor with any of the following features (T2 tumors with these features are classified T2a if 5 cm or less): involves main bronchus, 2cm or more distal to the carina; invades visceral pleura (PL1 or PL2); associated with atelectasis or obstructive pneumonitis that extends to the hilar region but does not involve the entire lung
T2a	Tumor more than 3 cm but 5 cm or less in greatest dimension
T2b	Tumor more than 5 cm but 7 cm or less in greatest dimension
T3	Tumor more than 7 cm or one that directly invades any of the following: parietal pleural (PL3), chest wall (including superior sulcus tumors), diaphragm, phrenic nerve, mediastinal pleura, parietal pericardium; or tumor in the main bronchus less than 2 cm distal to the carina but without involvement of the carina; or associated atelectasis or obstructive pneumonitis of the entire lung of separate tumor nodule(s) in the same lobe
T4	Tumor of any size that invades any of the following: mediastinum, heart, great vessels, trachea, recurrent laryngeal nerve, esophagus, vertebral body, carina, separate tumor nodule(s) in a different ipsilateral lobe
Distant Metastasis (M) Classification	
M0	No distant metastasis
M1	Distant metastasis
M1a	Separate tumor nodule(s) in a contralateral lobe, tumor with pleural nodules or malignant pleural (or pericardial) effusion
M1b	Distant metastasis (in extrathoracic organs)
Regional Lymph Node (N) Classification	
NX	Regional lymph nodes cannot be assessed
N0	No regional lymph node metastases
N1	Metastasis in ipsilateral peribronchial and/or ipsilateral hilar lymph nodes and intrapulmonary nodes, including involvement by direct extension
N2	Metastasis in ipsilateral mediastinal and/or subcarinal lymph node(s)
N3	Metastasis in contralateral mediastinal, contralateral hilar, ipsilateral or contralateral scalene, or supraclavicular lymph node(s)

1B)

Anatomic stage/prognostic Groups			
Occult Carcinoma	TX	N0	M0
Stage 0	Tis	N0	M0
Stage IA	T1a	N0	M0
Stage IB	T1b		
	T2a		
Stage IIA	T2b	N0	M0
	T1a	N1	
	T1b		

	T2a		
Stage IIB	T2b	N1	M0
	T3	N0	M0
Stage IIIA	T1a	N2	M0
	T1b		
	T2a		
	T2b		
	T3	N1	
	T3	N2	
	T4	N0	
	T4	N1	
Stage IIIB	T1a	N3	M0
	T1b		
	T2a		
	T2b		
	T3		
	T4	N2	
	T4	N3	
Stage IV	Any T	Any N	M1a
			M1b

Due to the vast spread of metastatic tumor tissue of the SCLC, a different more abstract staging system is commonly used for this histological subtype (Table 1C). The SCLC is classified into “very limited-stage”, “limited-stage” and “extensive-stage disease” according to the Veterans Administration Lung Study. SCLC tumors with very limited-stage disease are confined to the hemithorax without an involvement of mediastinal lymph nodes. In limited-stage disease, tumor tissue is localized in one hemithorax and restricted to ipsilateral lymph nodes. In extensive-stage disease, that occurs in more than 60% of all SCLC cases (17), malignant tissue exceeds the hemithorax.

Table 1C): Classification of the SCLC according to the Veterans Administration Lung Study

SCLC stage	**Stage according to the TNM classification**
Very limited-stage	T1-2, N0-N1
Limited-stage	T1-4, N2-3
Extensive-stage disease	M1 (every T, every N)

The AJCC introduced prognostic stage groups in addition to the anatomical TNM staging system (Table 2a+b) which consider further important factors. These stage groups are abbreviated with prefix modifiers. The combination of the prefixes helps to shortly describe and assess the circumstances of diagnoses, a potential relapse, residual tissue after tumor therapy or the invasion of lymphatic vessels or veins. The tumor grading is a histological assessment of the differentiation grade of tumor cells. It ranges from G1, which describes still well differentiated, slowly growing tumor cells with equable epithelium but cellular atypia, to G4 tumor cells, which have completely lost the characteristics of their cell of origin and are characterized by a quick spread and necrosis or pseudocysts.

As an example, the combination pT4 pN1 M1 R1 G4 describes a tumor which has been diagnosed by a pathologist after surgical removal, it has a large tumor volume with an involvement of peribronchial or perihilar lymph nodes, it was not removed entirely, and the tumor cells are completely degenerated.

Table 2A): Prognostic stage groups according to the AJCC

Symbol	Term	Explanation
C	Clinical	Stage determined with clinical information
P	Pathologic	Stage determined with pathologic investigations after surgical resection
Y	Restaging	Reevaluation of the stage after therapy start
R	Recurrence	Stage at the time of relapse
A	Autopsy	Stage determined with an autopsy
G (1-4)	Grading of the malignant degeneration of cancer cells	
S (0-3)	Elevation of serum tumor markers	
L (0-1)	Invasion of lymphatic vessels	
V (0-2)	Invasion of veins	

Table 2B): Description of residual tumor tissue after treatment

Symbol	Term	Explanation
RX	Residual questionable	Tumor presence is not assessable
R0	No residual	No cancer cells at the resection margin
R1	Microscopic residual	Microscopical presence of cancer cells at the margin
R2	Gross residual	Macroscopic (visible/palpable) presence of tumor cells
R2a		Macroscopic tumor without microscopic affirmation
R2b		Macroscopic tumor with microscopic affirmation

Figure 5:

Schematic illustrations of the NSCLC stages IIIA and IIIB which are almost inoperable but still free from metastases. Patients with stages IIIA and IIIB were enrolled into a clinical phase II trial dealing with NK cell immunotherapy after RCTx (further descriptions of the study: see 1.3.3). [151]

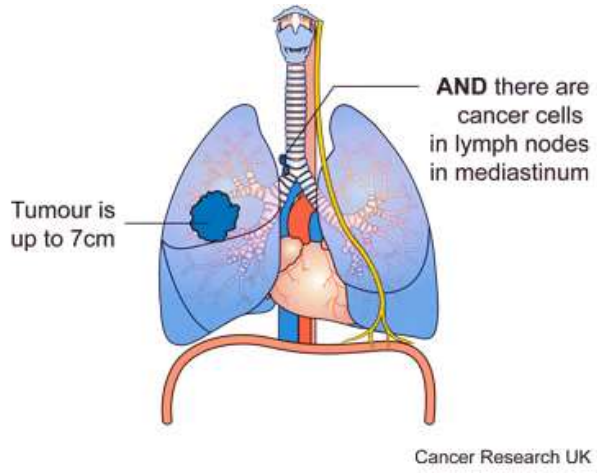

A) Localization pattern of NSCLC tumor tissue with stage IIIA

In stage IIIA, the tumor does not exceed a size of 7 centimeters and cancer cells are localized in the mediastinal lymph nodes.

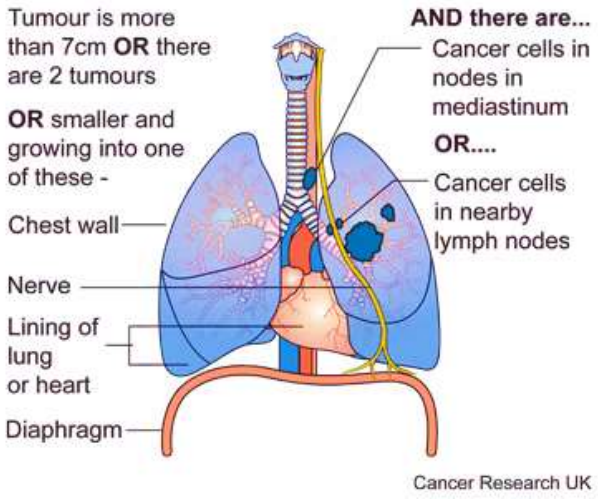

B) Localization pattern of NSCLC tumor tissue with stage IIIB
In stage IIIB, the tumor size surpasses 7 centimeters and tumor cells can be detected in the stated tissue.

1.1.4 Therapy and Prognosis

The bronchial carcinoma is a very heterogenous kind of neoplasia that differs in genetic, biological and clinical characteristics, such as therapy response for example. Therefore, the basis of an optimized therapy management is the correct classification of the lung cancer subtype and stage. The main difference between the two major groups NSCLC and SCLC is that in contrast to the SCLC, the therapy of choice for NSCLC patients is surgery as they show poor response to radio(chemo)therapy. On the contrary, the SCLC is more sensitive to radio(chemo)therapy and at diagnosis, the concerned patients already have an extensive stage with dispersed multifocal metastases making surgery abortive. The SCLC reaches double volume in 10-50 days, whereas the NSCLC needs 180-300 days. In addition, there are further patient factors that are independent from the tumor but nevertheless need to be considered for the choice of an optimal treatment. Even though there might be the chance of a recovery, impacting conditions like comorbidities (cytopenias or advanced psychiatric disorders e.g.), a poor cardiac and pulmonary function, frailty or a very poor general condition may affect a decision in the sense of preferring palliative care over curative treatment which would only be possible with aggressive therapy [149].

In principle, the treatment options of the NSCLC involve surgery, chemotherapy and/or radiotherapy and the decision for a type of treatment is tumor type- and stage-dependent. The radio sensitivity of adeno carcinomas is generally lower than of squamous subtypes. At

the early stages I and II, radical surgery including the resection of a pulmonary lobe or even pneumonectomy followed by a lymph node dissection. The extent of the surgical intervention is subordinate to the individual lung function. Patients with a poorer pulmonary capacity benefit from segmentectomy and wedge resections. At an early stage, neoadjuvant chemotherapy with 4 cycles of cisplatin and a further chemotherapy drug is frequently taken into consideration. Patients with the stages II and III are treated with an adjuvant chemotherapy after surgery consisting of cisplatin combined with a further chemotherapy drug (vinorelbine, docetaxel, paclitaxel, etoposide, gemcitabine or pemetrexed). In general, the treatment of stage III disease is individual and affected by the expansion of malignant tissue in the lung as well as comorbidities. In the case of an unresectable stage IIIA bronchial carcinoma, the standard therapy is combined chemoradiotherapy. In the case of stage IIIB, the patient is offered the same treatment as in stage IIIA. Further options are radio- or chemotherapy solely. Radiation therapy is also the main therapy in the case of an invasion of the mediastinum, the heart, great vessels or the spine.

In stage IV disease, therapy is limited to providing best palliative care with radio(chemo)therapy, targeted drugs or smaller surgical interventions such as bronchoscopic resection of tumor tissue constraining the airways or placement of stents and pleural drainage catheters. An exception in stage IV disease is the TNM stage T4 N0 M0 (no lymph node involvement or metastasis). In this case, a surgical removal with neo-adjuvant or adjuvant concomitant chemoradiotherapy can be taken into consideration.

An alternative option (especially in advanced stages) is a targeted therapy, which focuses on the inhibition of mutated, active genetic structures, such as tyrosine kinase inhibitors (e.g. erlotinib, gefitinib) in the case of changes in the EGF-receptor. Nevertheless, a targeted therapy is only possible in the presence of certain mutations.

The prognosis of the bronchial carcinoma is rather poor compared to other tumor entities. It is the most frequent tumorous cause of death. Less than 20 % of all lung cancer patients are still alive five years after diagnosis [24]. 30-40 % of all NSCLC cases are stage IV, and 60 % of SCLC are stage IV at diagnosis [23, 87]. Prognostic factors are the extension of the tumor tissue defined by the tumor staging, together with age, gender (women have a higher five-year-survival), immune response (a decreased lymphocyte number is associated with a worse prognosis) and histological subtype [73]. Clinically, the small cell lung carcinoma is more aggressive. It is characterized by a faster cell doubling time, an earlier dissemination and a

bigger number of dispersed metastases, but quite small multiple areas of metastatic tissue. With radiochemotherapy, a complete recovery is possible for 5 % of the patients with limited disease. By contrast, a five-year survival of up to 60 % for NSCLC patients with complete surgical resection of stage IA disease can be achieved [104].

1.1.5 Immune Checkpoint Inhibitors in the Therapy of Lung Cancer

The immune system has a major part in tumor combat and control. Nevertheless, conventional therapy methods were unable to achieve a sustainable long-term anti-tumor immune response. Therefore, the extension of molecularly targeted agents to the treatment of NSCLC was a major breakthrough. This progress is based on the findings that malign cells can circumvent immune defense by expressing the checkpoint molecule programmed death ligand 1 (PD-L1, B7-H1), serving as a specific ligand to the surface molecule programmed cell death protein 1 (PD-1) on surveilling lymphocytes and other immune cells [60, 122]. By forming a complex, these two proteins act as an immune checkpoint and can activate or damp the cellular adaptive immune response [18]. Like this, natural defense mechanisms can be knocked out by tumor cells.

The molecules of the immune checkpoints have become the target structures of a new therapeutic approach using monoclonal antibodies such as Nirvolumab, Pembrolizumab and Durvalumab. They block the interaction between the checkpoint molecules PD-1 on immune cells and PD-L1 on cancer cells. Recent studies represent a prolonged period of immunological activity under therapy with immune checkpoint inhibitors [18, 68, 113]. Immunohistochemical analysis of tumor tissue showed a massive invasion with $CD8^+$ lymphocytes [18]. In the peripheral blood, a redistribution of lymphocytes could be observed with an initial short drop in T cells. In the long term, the number of T cells increased and remained elevated for about one month.

In 2017, the New England Journal of Medicine published the PACIFIC study which demonstrated a longer median progression-free survival of stage III NSCLC patients (16,8 vs. 5,6 months with placebo) after the addition of the PDl-1 inhibitor Durvalumab to radio-

chemotherapy. In addition, the median overall survival could be improved (23.2 vs. 14.6 months) and the rate of brain metastases reduced [4].

So far, checkpoint inhibitors have been examined successfully and are taking final steps in clinical testing. Adverse reactions were less frequent compared to common drugs used for chemotherapy. They included mostly fatigue, immune-related endocrinopathies, pneumonitis, nephritis, rash and colon and liver toxicities [45, 123].

But despite the promising results, there is a relevant number of patients who do not benefit from blocking immune checkpoint inhibitors. A recent study on lung cancer and squamous carcinoma of the head and neck revealed that therapies with PD-1 blockade are most successful in tumors with many mutational aberrations [79, 111]. Shevtsov et al. achieved a delay in tumor growth and an improved overall survival in a syngeneic glioblastoma and xenograft lung cancer mouse model by combining the transfer of *ex vivo* activated NK cells and PD-1 inhibition [113]. Further, long-term tumor control was observed in a patient with stage IIIb NSCLC after radiochemotherapy combined with mHsp70-targeting NK cell transfer and second-line PD-1 inhibition [68]. Again, enhanced immunological activity with significantly elevated activated NK cells, elevated $CD8^+/CD4^+$ ratios and significantly reduced Tregs could be observed in the peripheral blood.

Overall, combined immunological treatment approaches are well tolerated and have great potential to control advanced tumors by complementing each other.

1.2 Role of Hsp70 and Osteopontin as Tumor Biomarkers of Lung Cancer

Tumor biomarkers are molecules or responses of the body which are specific of tumorous processes. Biomarkers can be particles which may be released by tumor cells and are physiologically not detectable or overexpressed by cancer cells. The impact of biomarkers is constantly growing in clinical routine as they can be acquired easily in a non-invasive way. Two of these biomarkers with a great potential are the heat-shock protein 70 (Hsp70) and osteopontin, which both are measurable in the blood of healthy individuals and overexpressed in tumor patients. The expression of Hsp70 is induced by cell stress, such as hypoxia or radio(chemo)therapy. An elevation of Hsp70 levels or the presence of hypoxic conditions have

been shown to affect therapy outcome adversely [54, 96]. Hsp70 further plays an important role in the interaction with the immune system. Osteopontin equally correlates with hypoxia and is indicative of the overall survival [99, 101]. Altogether, both biomarkers seem to have outstanding characteristics which might be beneficial for tumor therapy. For this reason, the investigations on Hsp70 regarding its function as a biomarker of vital tumor tissue were extended in consideration of immunological aspects, dynamics during therapy and a potential correlation with osteopontin.

1.2.1 Hsp70 Levels in Healthy Individuals and Tumor Patients

The Hsp70, also known as HSPA1A, Hsp70-1, Hsp72 or HspA1 [64], is present in different compartments of all eukaryotic cells. As a molecular chaperone, it interferes in cellular networks such as transcriptional, membrane, organelle and signalling processes [115]. It further maintains cellular homeostasis by refolding misfolded proteins. Under stress conditions, mitogen-activated protein kinase/extracellular signal-regulated kinase (MAPK/ERK) together with stress-activated protein kinase (SAPK) signalling cascades that stimulate heat shock factors (HSFs) are responsible for the induction of Hsp70 [1, 33, 88].

Elevated levels of Hsp70 in the blood can be observed in patients with inflammatory diseases like hepatitis or COPD for example [40]. Nevertheless, it is exceptional that the levels in cells of various cancer subtypes, such as head and neck, lung, colorectal, pancreas, glioblastoma cells or cells of haematological malignancies [52, 105] are constitutively higher. The expression of Hsp70 is additionally enforced by the exposure to cell stress in the tumor microenvironment, such as nutrient and oxygen deprivation, acidosis or free radicals, which create further mutant dysfunctional proteins.

Different to healthy cells, cancer cells contain Hsp70 not only in the cytosol, but also on their plasma membrane. Regarding its localization on the cell surface, Hsp70 interacts with specific components of the lipid bilayer, such as globoyltriaosylceramid [41] under physiological circumstances and phosphatidylserine (PS) [6, 7] in case of stress like radio-(chemo)therapy.

As Hsp70 and phosphatidylserine are colocalized in the lipid membrane, it is likely that during early apoptosis Hsp70 is inserted into the surface membrane by a flipping mechanism of

Hsp70 together with PS. Hsp70 is transported with endosomal and lysosomal vesicles [70] and not via a classical ER-Golgi transport pathway.

In addition, tumor cells with a membrane Hsp70-positive phenotype actively secrete exosome-like vesicles with a diameter of 50-100 nm. In general, exosomes can be detected in various bodily fluids like serum and plasma, milk, urine or broncho-alveolar lavages [108]. The reason for this is that except of tumor cells, many different cells like hematopoietic cells, neuronal cells, adipocytes, fibroblasts or intestinal epithelial cells can produce exosomes in a physiological way [2, 108]. Formed by a double inversion of the plasma membrane, the protein amount together with the orientation of proteins in the exosomal membrane mimick that of the cell from which they originate [66]. *In vitro* experiments revealed that lipid vesicles with Hsp70 in the plasma membrane also express high amounts of Hsp70 in their lumen [38]. Likewise, the protein composition inside exosomes is comparable to that of the cytosol.

Consequentially, Hsp70 membrane positive tumor cells release exosomes which exhibit Hsp70 on their surface [38] and additionally have high amounts of Hsp70 in their lumen. As a result, the Hsp70 phenotype of tumor cells can be deducted from the amount of Hsp70 that exosomes comprise [82].

In general, an overexpression of Hsp70 in tumors is associated with a more aggressive tumor phenotype. Elevated levels are associated with lymph node metastases in breast cancer [67] and with vascular invasion in gastric cancers [20]. Murakami et al. additionally have shown an increased radio-resistance of Hsp70-positive tumor cells [96].

On the other hand, it has been demonstrated that Hsp70 has the potential to induce immune response. The tumor biomarker serves as a recognition structure particularly for NK cells. Moreover, not only the biomarker itself, but also the N-terminal 14-mer peptide TKDNNLLGRFELSG (TKD, aa 450–463) which respresents the epitope of the monoclonal antibody cmHsp70.1 is able to enhance proliferative and cytolytic activity of NK cells in combination with low dose IL-2 (TKD/IL-2) [91]. This alternate recognition structure binds both free as well as membrane-bound Hsp70. The results of *in vitro* stimulation have shown that, after an incubation with Hsp70 protein or Hsp70 peptide plus IL-2, the density of activation markers CD94/NKG2C, NKG2D as well as the cytolytic activity against Hsp70 membrane-positive tumor cells were enhanced. The lysis of membrane Hsp70 positive tumor cells is predominantly mediated by the pro-apoptotic enzyme granzyme B, while perforin is only

moderately increased [47, 49] (Figure 6). Granzyme B has the capacity to enter tumor cells via membrane bound Hsp70.

In summary, constitutive high Hsp70 levels are characteristic of a malignant transformation and indicate a more aggressive tumor phenotype, but on the other hand membrane bound Hsp70 serves as a recognition structure for NK cells and thereby can lead to a stimulation of the innate immune system.

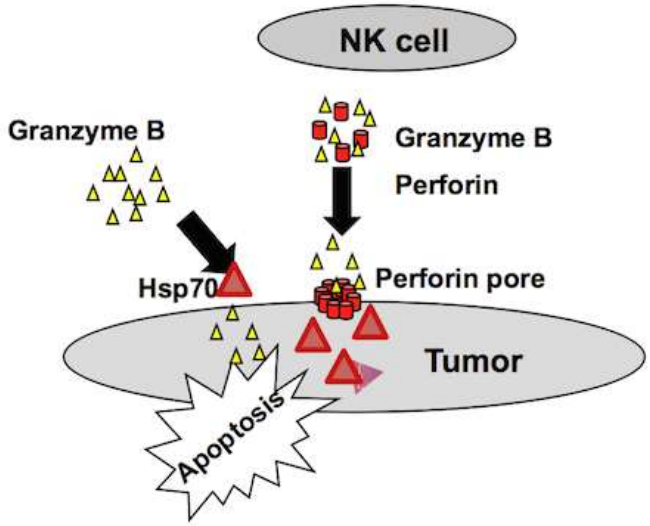

[93]

Figure 6:
Schematic representation of the granzyme B mediated lysis of membrane Hsp70 positive tumor cells by NK cells (Multhoff et al., 2012).
After binding of NK cells expressing the activation marker CD94/NKG2C and NKG2D, granzyme B (yellow triangles) is released either alone or accompanied by perforin (red cubes). The uptake of granzyme B into the tumor cell takes place by direct endocytosis via membrane-bound Hsp70 (red triangle). In the presence of perforin, there is a co-transport of perforin and granzyme B via perforin pore formation. Subsequently, the apoptosis of membrane Hsp70 positive tumor cells is induced.

1.2.2 Physiological Function of Osteopontin and its prognostic Value in Carcinogenesis

Similar to Hsp70, osteopontin (OPN) or bone sialoprotein I (BSP-1 or BNSP) is a physiologically present protein which is mostly expressed in the bone by (pre)osteoblasts and osteocytes. Located in extracellular structures, it serves as an organic component of bones. Apart from osseous structures, osteopontin can be synthesized by a large range of other tissue types like fibroblasts [8], endothelial and dendritic cells, macrophages [97], as well as smooth [56] and skeletal muscle [124]. Calcitriol (1,25-dihydroxy-vitamin D_3) increases the OPN transcription due to an incorporation of a specific vitamin D response element (VDRE) into its gene promoter [22, 107]. There are still further mediators of OPN expression like molecules which emerge in an inflammatory environment [50], such as tumor necrosis factor α (TNFα), interleukin-1β (IL-1β) or angiotensin II, but also physical situations of stress like hypoxia or

hyperglycemia. The main function of osteopontin is bone remodeling and biomineralization. According to recent findings, it is involved in anchoring osteoclasts to the bone matrix [109]. Stimulated by cytokines, this protein interacts with the immune system by blocking the synthesis of the TH2 cytokine IL-10. It further increases the production of immunoglobulins in B cells [135] and contributes to the activation of macrophages. The latter process has been demonstrated in a study that exhibited the ability of OPN-positive tumors to initiate macrophage activation in contrast to OPN-deficient tumors [30]. Equally to Hsp70, OPN is overexpressed in many different tumor types including lung, colorectal, stomach, breast, ovarian cancer and the melanoma. Chambers et al. could show that OPN RNA and protein were enhanced in most NSCLC tumor cells compared to physiological tissue, but OPN was primarily detected in tumor-infiltrating macrophages and necrotic areas [21]. A significant correlation between OPN-immuno-positivity of the tumor tissue and overall survival has been found [21]. Osteopontin is of particular interest in the oncological field due to its association with tumor hypoxia. In NSCLC, an inverse correlation between OPN plasma levels and intra-tumoral pO_2, measured with polarographic needle electrodes, has been detected [71]. Elevated plasma levels are associated with poor prognosis in several tumor types [28, 58]. In patients with head-and-neck cancer who received radiotherapy, the pre-therapeutic OPN plasma levels were used as an indicator of tumor hypoxia and to distinguish patients who most likely will profit from a treatment with the hypoxic radiosensitizer nimorazole [72, 102]. After chemo- [58] and surgical [14] therapy of lung cancer, OPN plasma levels diminished following resection of NSCLC.

1.2.3 Comparison of Hsp70 with the Hypoxia Induced Tumor Biomarker OPN

Both biomarkers, Hsp70 and OPN are physiologically present in many different cell types where they fulfil different functions. Under physiological conditions, Hsp70 is predominantly located in the cytosol where it maintains protein homeostasis. Osteopontin by contrast acts as a component of the extracellular bone matrix by anchoring osteoclasts, but it is also present in various other tissues and interacts with the immune system in healthy individuals. Both biomarkers have been found to be overexpressed in a large variety of tumor entities. Whilst Hsp70 is localized in the cytosol, on the plasma membrane and in secreted exosomes, OPN in

the tumor microenvironment is a result of an increased release of tumor and non-malignant cells, such as immune cells, fibroblasts or endothelial cells [3]. The release of OPN in tumor cells has been found to be based on an upregulated transcription due to promoter polymorphisms and dysregulated signaling pathways [76]. The released OPN can activate cells in the tumor microenvironment via autocrine and paracrine mechanisms (Figure 7) [3].

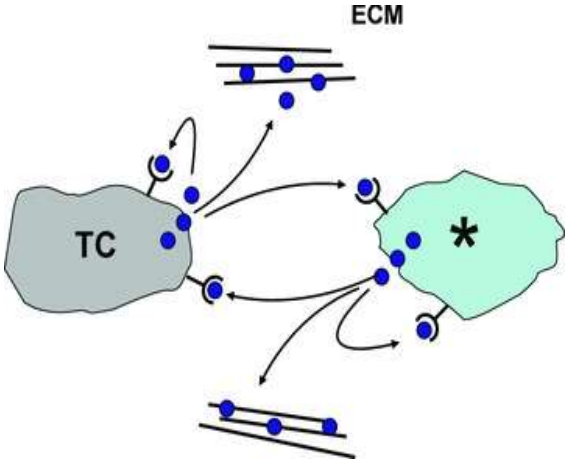

Figure 7: The presence of OPN in the tumor microenvironment (Anborgh et al., 2010). *OPN (solid circles) is secreted by tumor cells (TC) and non-tumor cells (*) including immune cells, fibroblasts, endothelial cells, etc. in the tumor microenvironment. The released OPN affects either the secreting cell itself in an autocrine manner or different cells with an integrin or CD 44 family cell surface receptor via paracrine mechanisms. The secreted OPN may not only have influence on the surrounding cells but can also be absorbed by the extracellular matrix.* an [3]

Increased Hsp70 and OPN levels in the plasma represent an aggressive tumor phenotype and a poor overall survival. The expression of Hsp70 is also stimulated by hypoxia. OPN by contrast serves as a predictor of tumor hypoxia as it correlates with intra-tumoral pO_2, which acts as a prognostic marker in NSCLC. A co-detection of the markers OPN, VEGF and CA IX augments the prognostic value of hypoxia and radio-resistance [99]. Tumor hypoxia is one of the major risks for radio-resistance and leads to insufficient therapy outcome of lung cancer patients after radiotherapy [10, 54, 129]. Poor intra-tumoral oxygenation evokes neo-angiogenesis and creates an aggressive, resistant and rapidly progressing tumor phenotype [128]. As a result, OPN seems to serve as a reliable tumor biomarker in the evaluation of tumor hypoxia. Due to the aforementioned overlaps between Hsp70 and OPN, the following research aims to investigate a possible correlation between these two markers and their potential function as a prognostic maker for clinical outcome.

1.3 The Impact of the Immune System on Tumor Development

The likelihood of developing malignant processes is affected by various factors. These involve the exposition to carcinogenic risk factors such as radiation, nitrosamines, polycyclic aromatic hydrocarbons or just an unfavourable genetic predisposition which is characterised by mutations in DNA regions of oncogenes. Different endogenous mechanisms control the transformation of normal tissues into malignant cells. Apart from tumor suppressing proteins like p53 or the Retinoblastoma protein (pRb) which act at the DNA level, the immune system represents another essential part in the combat against tumor cells. Therefore, the immune system and its functions in fighting cancer will be presented in the following chapter.

1.3.1 The Structure and Components of the Innate and Adaptive Immune System

The innate response is particularly attracted by pattern recognition receptors which are conserved among a broad group of microorganisms. This immune defense is unspecific in the manner of a generic reaction to pathogens [95]. It is a short-acting response against foreign antigens and the dominant system in most organisms. Innate immune cells include basophils, dendritic cells, eosinophils, Langerhans cells, mast cells, monocytes and macrophages, neutrophils and natural killer cells (NK cells) (Figure 9). In the context of Hsp70 recognition, especially NK cells are involved. Generally, they provide rapid responses against tumor cells and pathogen (bacterial, viral) infected cells and are independent from antigen presenting MHC (major histocompatibility complex) proteins or antibodies, resulting in a rapid immune reaction. They are activated by the proinflammatory cytokines such as IL-2, IL-12, IL-15, IL-15/IL-15RA complex and IL-1. Different from other immune cells, a subtype of NK cells detects and destroys harmful cells that lack an MHC class I expression (“missing self”) [133]. NK cells secrete cytotoxic granules containing perforin and granzymes which are taken up by target cells which in turn induce apoptotic death [74]. NK cytotoxicity is further mediated by members of the tumor necrosis factor (TNF) receptor superfamily like Fas/CD95, TRAIL receptors and TNFR1 [134, 138]. Additionally, NK cells have the capacity to secrete various cytokines and chemokines. Apart from interferon-y (IFN-y) which is crucial for the priming of a T helper 1 (Th1)-based T-cell responses [81, 85], the chemokines GM-CSF (granulocyte-

macrophage colony stimulating factor), MIP-1α (macrophage inflammatory protein-1α) and RANTES (regulated upon activation, normal T cell expressed and secreted) [12] derived from NK cells can contribute to the modulation of the immune response. A large variety of receptors are expressed on the surface of NK cells which mediate NK cell activation or suppression. The Natural Cytotoxicity Receptors including NKp30, NKp44 and NKp46 are important representatives of NK mediators and deliver signals to NK cells to secrete inflammatory cytokines and kill target cells. The CD94/NKG2C/A heterodimeric C-type lectin receptors on NK cells and a subset of $CD8^+$ T-lymphocytes [15, 26] have dual functions, transmitting activating or inhibitory signals [15].

Different from the innate immune system, cells of the adaptive or acquired immune system are responsible for an MHC mediated immune response and develop an immunological memory that recognizes pathogenic surface structures after exposition and leads to a faster elimination of “non-self” antigens. T lymphocytes originate from a common multipotent hematopoietic stem cell. T progenitor cells migrate from the bone marrow to the thymus where they undergo a selection to differentiate into mature T lymphocytes. Cells that are targeting endogenous “self” antigens are eliminated to accomplish peripheral tolerance whereas cells directed against “non-self” antigens mediate protective immunity. A minor subset of T lymphocytes develop into regulatory T cells (Tregs) that are capable of immune modulation. They are immunosuppressive and generally dampen the activity of effector T cells. Generally, lymphocytes are mostly found in lymphatic tissue like lymph nodes, the spleen or in the mucosa of the gastrointestinal system, but also in the blood circulation.

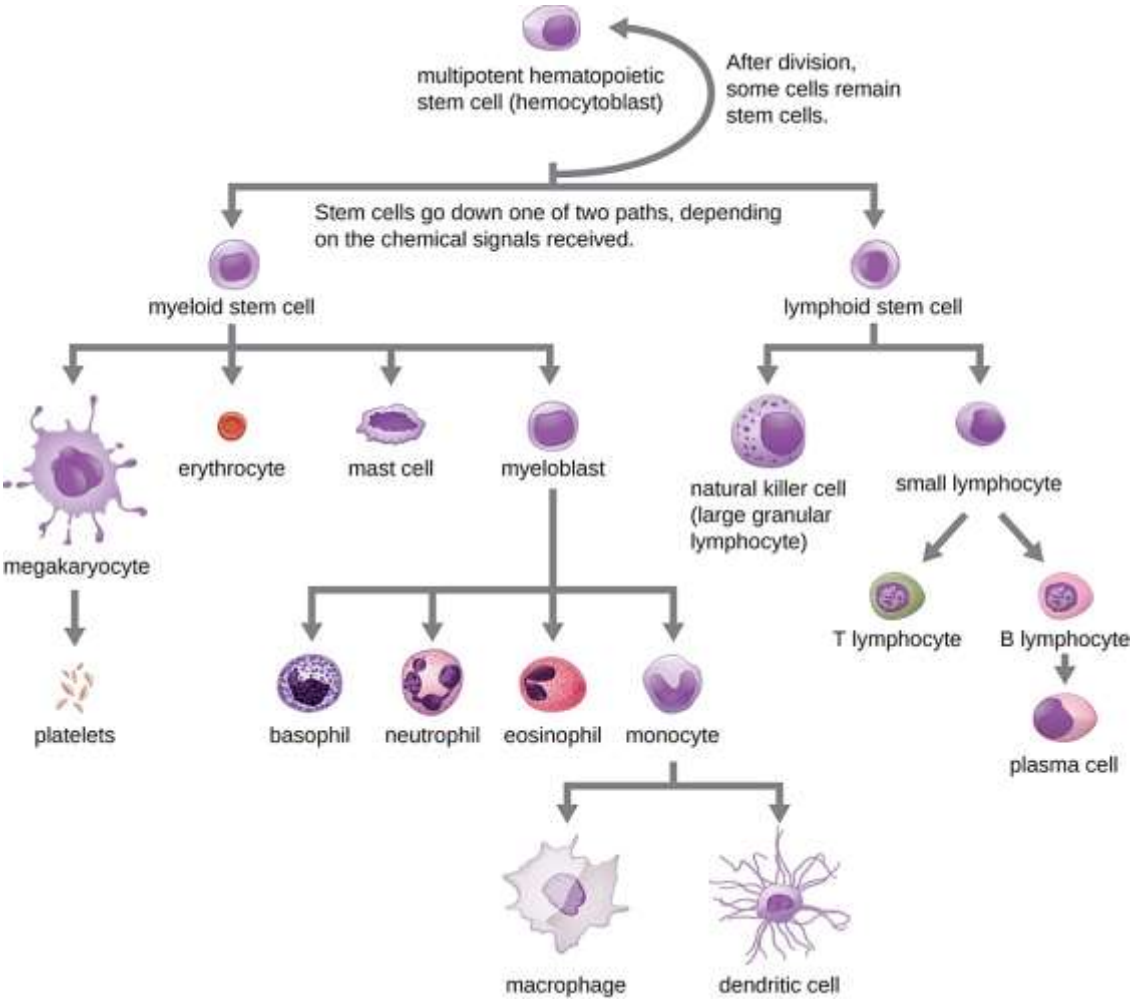

Figure 8: Evolution and composition of the immune system. *All cells derive from a multipotent hematopoietic stem cell which can pass into myeloid or lymphoid stem cells. Lymphoid stem cells can change into natural killer cells or a precursor of T- and B- cells.* [140]

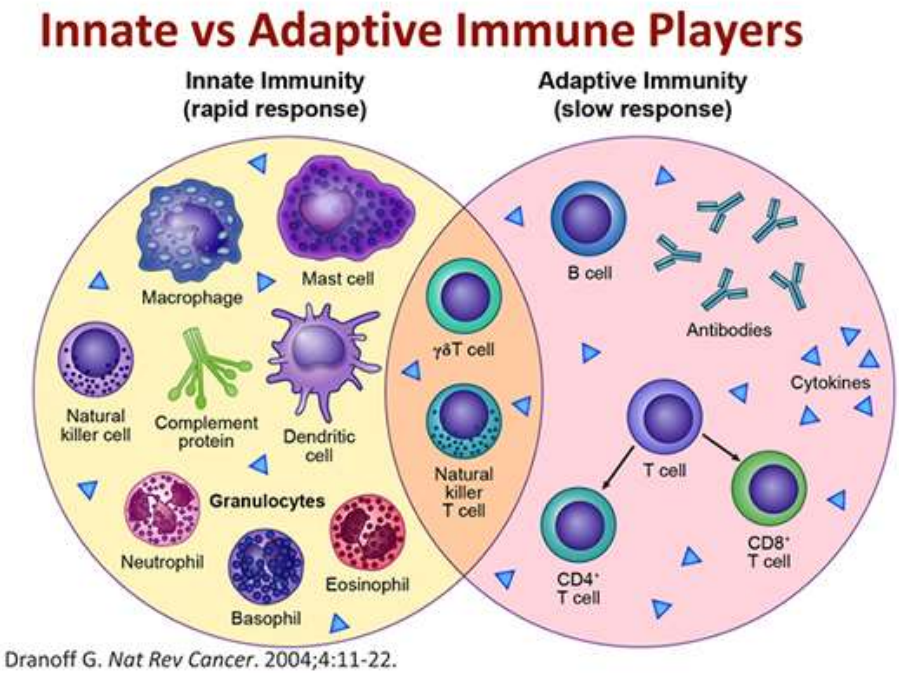

Figure 9: *Representative image of the components of the immune system and the interaction between cells of the innate and adaptive immune system.* [32]

Investigating tumor immunology, the 14-mer amino acid sequence (aa450–463) TKDNNLLGRFELSG (TKD) of Hsp70 emerged as a tumor-selective recognition structure for NK cells which are part of the innate immune system [136]. Therefore, a clinical phase I trial [69] was initiated to induce a requested positive effect in tumor patients by an increase of the interaction of this special peptide with NK cells.

1.3.2 The Role of Tumor Immunotherapy

In the therapy of cancer, the impact of tumor immunotherapy is constantly growing, especially as it is a treatment with less side effects compared to standard chemo- or radiotherapy, enforcing the endogenous fight against the tumor cells in a more natural way. Immunotherapy was elected as the “breakthrough of the year” for cancer treatment by the journal “Science” in 2013 [29]. New therapeutic approaches are enabled by the increase of knowledge in the detection of tumor-associated antigens which serve as tumor-specific targets for a specialized

therapy and by the development of immune checkpoint inhibitor therapies for which the Nobelprize was awarded in 2018.

Tumor immunotherapies can be categorized as active, passive or combined.

Active immunotherapy induces the immune system to fight tumor cells by recognizing tumor associated antigens which help to launch the recognition of tumor cells by the native immune cells.

Passive Immunotherapy involves the use of monoclonal antibodies, cytokines and lymphocytes. Antibodies can be adapted to antigens on the tumor surface very specifically which results in a wide range of treatment options for different tumors.

1.3.3 Introduction to targeted NK cell based adaptive Immunotherapy for the Treatment of Patients with NSCLC after Radio(chemo)therapy

Since NK but not T cells have been found to play a major role in killing membrane Hsp70-positive tumor cells [91] after activation with a 14-mer peptide (TKDNNLLGRFELSG, aa 450-463) combined with low dose IL-2 (TKD/IL-2), a phase I clinical trial with patients suffering from metastasized colorectal cancer and NSCLC had been set up to test safety and tolerability of ex vivo TKD/IL-2 stimulated, autologous NK cells [69]. As explained earlier, the 14-mer peptide is an extension of the epitope of the antibody cmHsp70.1. Different from previous monoclonal antibodies, cmHsp70.1 has the capability to detect both membrane bound and free Hsp70 [91, 118]. *In vitro* experiments revealed that an incubation of NK cells with Hsp70 or the 14-mer peptide combined with IL-2 could increase the surface density of CD94 together with the cytolytic activity against Hsp70 positive tumor cells [47, 49] and lead to an upregulated granzyme B production [69].

A mouse model with immunodeficient SCID/beige mice bearing Hsp70 positive colon carcinoma cells illustrated the success of the immunotherapy. A single injection of activated NK cells could provoke a significant reduction of the tumor weight in the mice [89].

When finally treating patients with confirmed metastatic colorectal cancer (N=11) and NSCLC (N=1) who had not responded to standard therapies with intravenous injections of *ex vivo* pre-activated NK cells in the range of 0.1 up to 1.5 x 10^9 cells in up to six cycles using complete leukapheresis products, no severe toxic side effects could be observed [69]. The amount of

CD94 on NK cells of the tumor patients, who had been treated with radio- and/or chemotherapy before, increased. After the fourth reinfusion cycle, the cytolytic activity of peripheral blood lymphocytes was enhanced significantly.

Based on these findings in the proof-of-concept study, a phase II randomized clinical study funded by BMBF–Innovative therapies was initiated to test the efficiency of autologous in vitro stimulated NK-cells regarding the reduction of tumor cells in humans [116]. The preparation and cultivation of the lymphocytes is currently done in the GMP laboratory of TUMCells. The regulatories of the study were accepted in 2015 and the results of this dissertation are based on the blood of patients which was collected within the frame of this clinical trial.

Figure 10:

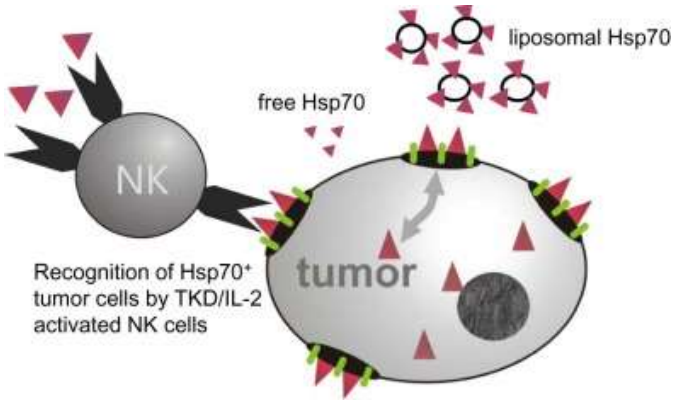

Representative image of the recognition of membrane Hsp70 positive tumor cells by autologous NK cells after ex vivo stimulation with Hsp70-peptide TKD combined with low dose IL-2 (large red triangles). *Due to the stimulation, activation markers (black symbols on NK cell) like CD94, NKG2C or NKG2D are overexpressed on NK cells. The transport of Hsp70 from the cell inner of the tumor to the plasma membrane takes place via a non-ER/golgi transport pathway. The small circles with the red triangles demonstrate the active release of Hsp70 in vesicles by Hsp70 membrane positive tumor cells. Free Hsp70 (small red triangles) originates from dying cells.* [92]

1.4 Aim of the Dissertation

Since lung cancer is among the three most frequent tumor entities [141] with poor overall survival, combined therapeutic options were tested, consisting of a standard radio(chemo)therapy followed by Hsp70-targeting, autologous NK cells to stimulate the body´s own defense mechanisms against cancer. With the targeted NK cell based adaptive immunotherapy, the aim was improving the progression-free and overall survival of these patients.

This work aims to expand knowledge about the interaction between immune cells and the tumor-target Hsp70 and osteopontin in the circulation. Hsp70 serum levels were studied

comparatively in lung cancer and healthy human individuals. The values of lung cancer patients were also assessed during the course of disease and associated with modulations in the immune phenotype. In addition, Hsp70 and osteopontin were contrasted concerning their function as tumor biomarkers and their relevance in tumor therapy.

2 MATERIALS AND METHODS

2.1 Collection of Patient Databases

In the context of our research, two patient collectives were analyzed.

The blood of donors of the patient collective #1 were 43 patients who had a bronchial carcinoma. When fulfilling the criteria which are summarized in Table 3, the patients were admitted to the clinical phase II study that has been outlined priorly. Patients with lung metastases of a tumor with non-pulmonary origin were excluded.

The data of the patient collective #2, consisting of 55 NSCLC patients, are based on a collaboration with the Martin Luther University Hospital of Halle-Wittenberg. Initially, the blood was used for a pilot study to investigate potential plasma hypoxia markers in the radiotherapy of non-small cell lung cancer in the working group of Prof. Dr. D. Vordermark at the Martin-Luther University Hospital [99]. Further on, the Hsp70 status of these patients was determined at the Klinikum Rechts der Isar and connected to the data which has been gathered in relation to the hypoxia marker osteopontin.

Table 3

Selection criteria of the phase II clinical trial: targeted NK cell based adoptive immunotherapy for the treatment of patients with non-small cell lung cancer (NSCLC) after radiochemotherapy. The assortment of patients for the phase II trial was essential to create the patient collective #1 on which the subsequent results are based on. [116]

Inclusion criteria	**Exclusion criteria**
First diagnose of histologically and/or cytologically proven and unresectable NSCLC with clinical stage III A and III B	Prior treatment with any other investigational drug within 4 weeks prior to first dose of study medication
Completion of radiochemotherapy no longer than 8 weeks ago	Any severe heart disease or any severe concomitant disease (ECOG status > 2) NSCLC patients (stage IIIA/B) eligible for initial surgery with a confirmed consent of an interdisciplinary tumor board
Progression free according to RECIST 1.1 criteria at the first assessment after completion of radiochemotherapy	Patients that show ALK positivity or an activating mutation of the EGFR-TK domain (assessment of ALK or EGFR status not mandatory)
Confirmed presence of Hsp70 on the patient`s tumor	Patients with locally advanced or metastatic NSCLC other than predominantly squamous cell histology
Female or male, age 18 to 75 years ECOG status ≤ 2	

Neutrophil count ≥ 1.5 x 10^9 /l after completion of radiochemotherapy	Any disease (including psychotic disorders, drug abuse, active infection, uncontrolled hypertension, unstable angina, congestive heart failure, myocardial infarction within the previous year, serious cardiac arrhythmia requiring medication, hepatic, renal or metabolic disease), metabolic dysfunction, physical examination finding, or clinical laboratory finding likely (in the investigator`s opinion) to affect the evaluation of the study or place the patient at risk whilst on treatment
White blood cell (WBC) ≥ 2.5 x 10^9 /l after completion of radiochemotherapy Hemoglobin ≥ 8 g /l after completion of radiochemotherapy	Any serious infection or sepsis
Platelet count ≥ 100 x 10^9 /l after completion of radiochemotherapy	Any active autoimmune disease
Normal renal function (creatinine < 150% ULN)	Any immunodeficiency syndrome
Normal liver function (bilirubin < 150% ULN; G-GT, GPT and GOT < 250% ULN)	Surgery or immunotherapy within 4 weeks before study entry
Normal blood coagulation (PTT 25-40s)	Patients with a known hypersensitivity to any of the administered substances should be excluded from the clinical trial
Measurable disease according to immune related RECIST criteria	Patients with a known positive HIV test should be excluded from the clinical trial as well as patients with positive Hepatitis A, B, C tests (assessment not mandatory)
Female patients of childbearing potential must have negative pregnancy test performed during screening period (≤ 14 days before initiation of study dosing) Postmenopausal women must be amenorrhoeal for at least 12 months to be considered of non-childbearing potential. Female patients of reproductive potential must agree to employ an effective method of birth control throughout the study and for 6 months following discontinuation of study drug.	Receipt of immunosuppressive drugs including systemic corticosteroids within 3 weeks before study entry. Low dose corticosteroids as they are a common treatment option for patients suffering from COPD are not an exclusion criterium Radio- cytostatic- and immunotherapy in parallel or within 2 weeks prior study start
Written (signed) Informed Consent document indicating that the patient of all pertinent aspects of the trial prior to enrolment and to participate in the study	Women who are pregnant or breast feeding
Ability to comply with the study	Female patients of reproductive potential unwilling to practice a highly effective method of birth control
	History of noncompliance with medical regimes
	Patients unwilling to or unable to comply with the protocol

Patient Collectives

Between 2011 and 2015, blood samples (9 ml) were taken from patients with suspicion of or confirmed lung cancer on condition of informed consent. Among these, most of the diagnoses were squamous cell (n=25) and adeno carcinomas of the lung (n=18). Patient characteristics are described in Table 4a. The blood samples were mostly supplied by the Klinikum Rechts der

Isar. Support was provided by other hospitals like the Klinikum Bogenhausen, the Ludwig Maximilian´s university hospital in Munich, the Asklepios Fachklinik in Gauting, the university hospitals in Regensburg, Frankfurt and Erlangen.

Additionally, within the framework of a collaboration with Christian Ostheimer from the Hospital for Radiotherapy of the University Hospital in Halle, our work group received plasma samples of patients with NSCLC and SCLC which had been treated with radio-chemotherapy or chemo-therapy only.

Table 4: Patient databases

Table 4a: Patient collective #1. *Clinico-pathological characteristics of 43 patients with NSCLC (median age 64 years, range 23 to 95 years) who received a treatment at the Klinikum rechts der Isar, TU München, Munich, Germany.*

Gender	Female	11
	Male	32
Histology	Squamous cell	25
	Adeno	18
UICC stage	Ia	1
	Ib	1
	IIa	0
	IIb	0
	IIIa	13
	IIIb	13
	IV	15

Table 4b: Patient collective #2. *Clinico-pathological characteristics of 55 patients with NSCLC (median age 63 years, range 47 to 86 years) who received a treatment at the Martin-Luther University Hospital, Halle-Wittenberg.*

Gender	Female	8
	Male	47
Histology	Squamous cell	28
	Adeno	24
	Large cell	1
	Other	1
	no histology	1

UICC stage	Ia	1
	Ib	0
	IIa	2
	IIb	0
	IIIa	18
	IIIb	34
	IV	0

Blood was collected in two EDTA KE tubes and one serum separator tube (S-Monovette, Sarstedt, Nümbrecht, Germany) and mixed by gently inverting the tube. For plasma separation, EDTA blood was centrifuged at 1,500 g for 15 min. For serum collection, blood clotted for 15 min at room temperature and serum was separated by centrifugation at 750 g for 10 min.

Serum and plasma were stored in 150 µl aliquots at -80°C. 1.4 ml of EDTA blood was used for FACS analysis and the remaining blood in the anticoagulant tube served for lymphocyte separation with Ficoll. The cells were frozen at -80°C and then stored in liquid nitrogen for further experiments.

Approval of the study was obtained by the Ethics Committees of the universities that are involved in the study (ethical review committees of the TUM medical faculty and Martin-Luther-University Halle-Wittenberg, approval numbers: 2428/09, EudraCT Nr. 2008-002130-30) and all procedures were in accordance with the Helsinki Declaration of 1975 as revised in 2008.

Table 5:

Summary of all samples which derive from the blood of the patient and control groups

Material	**Source**	**Material derives from**
Serum	Control group	Healthy donors
1,4 ml EDTA whole blood	Control group	Healthy donors
1,4 ml EDTA whole blood	Hospitals being involved in the phase II trial	Patients with pulmonary diseases
Serum	Hospitals being involved in the phase II lung study	Patients with pulmonary diseases
Plasma	University Hospital Halle	Patients with NSCLC and SCLC

2.2 Detection of Hsp70 in the Blood with the lipHsp70 ELISA and immunohistochemical Staining

With the help of former commercial ELISAs, it had only been possible to detect the free unbound form of Hsp70 which excluded the quantification of Hsp70 that is integrated in the tumor cell membrane. In order to determine the amount of Hsp70 in the blood more precisely, our research group developed the novel lipHsp70 ELISA [152]. In general, an ELISA (enzyme-linked immunosorbent assay) is a laboratory technique to identify molecular substances with the help of antibodies and color changes. Antigens of the material for analyzing are applied on a surface and covered with an antibody which is specific for the antigen. At least one antibody is used for an ELISA. A second antibody which binds to the first one can be added, carrying an enzyme which provokes a detectable signal such as a color change when adding a certain substrate. The intensity of the visible signal helps to quantify the antigen in the sample. Subsequently, the procedures of the novel lipHsp70 ELISA are going to be described.

2 µg/ml rabbit polyclonal antibody (Davids, Biotechnologie, Regensburg, Germany) directed against human recombinant Hsp70 was applied on 96-well MaxiSorp Nunc-Immuno plates (Thermo, Rochester, NY) in sodium carbonate buffer (0.1 M sodium carbonate, 0.1 M sodium hydrogen carbonate, pH 9.6). After incubation overnight, the plates were washed three times with phosphate buffered saline (PBS, Life Technologies, Carlsbad, CA, USA) with 0.05% Tween-20 (Calbiochem, Merck, Darmstadt, Germany) and then blocked with 2% milk powder (Carl Roth, Karlsruhe, Germany) in PBS for 1.5 h at 27°C. Following a further washing step, serum samples diluted 1:5 in CrossDown Buffer (Applichem, Chicago, IL, USA) were added to the wells for 2 h at 27°C. The wells were washed again and coated with 4 µg/ml of the biotinylated mouse monoclonal antibody cmHsp70.1 (multimmune, Munich, Germany) in 2% milk powder in PBS for 2 h at 27°C. After this, the wells were washed again before application of 0.2 µg/ml horseradish peroxidase-conjugated streptavidin (Pierce, Thermo, Rockford, IL, USA) in 1% bovine serum albumin (Sigma-Aldrich, St. Louis, MO, USA) for 1 h at 27°C. By adding 50 µl sulfuric acid per well, the reaction was stopped. Binding was determined after application of substrate reagent (R&D Systems, Minneapolis, MN, USA) for 30 min at 27°C and absorbance was read at 450 nm, corrected by absorbance at 570 nm, in a Microplate Reader (BioTek,

Winooski, VT, USA). Each ELISA test contained an Hsp70 eight-point standard using 0-50 ng/ml recombinant Hsp70 diluted in CrossDown Buffer.

Immunohistochemical staining was done by Stefan Stangl (AG Multhoff) who kindly provided the images for Figure 13. The immunohistochemical staining is presented in order to confirm the localization of Hsp70 in the tumor cell membrane but not in the surrounding tissue. Formalin-fixed and paraffin-embedded specimen of lung tumors (*n* = 9) were used for immunohistochemical staining. They were cut into sections, dewaxed and hydrated, heated for 30 min in a microwave oven in 600 ml DAKO retrieval buffer, then washed for 5 min in H2O. After this, the specimens were washed with T-PBS buffer twice. 10% rabbit serum in PBS containing 1% BSA were applied for one hour. Immunohistochemistry was performed with streptavidine–biotin complex (StreptABC) using mouse mAb cmHsp70.1 (multimmune, Munich Germany) at a dilution of 1:200 overnight 2 h at 4°C.

Table 6:

Antibodies, chemicals, plastic material and devices of the lipHsp70 ELISA

A) Antibodies and proteins

Description	Concentration	Producer
Mouse monoclonal antibody cmHsp70.1	4 µg/ml	Multimmune, Munich, Germany
Rabbit polyclonal antibody	2 µg/ml	Davids, biotechnology, Regensburg, Germany

B) Chemicals

Description	Concentration	Producer
Albumine, bovine serum, BSA	1 %	Sigma-Aldrich, St. Louis, MO, USA
CrossDown Buffer		Applichem, Chicago, IL, USA
Horseradish peroxidase-conjugated streptavidin	0.2 µg/ml	Pierce, Thermo, Rockford, IL, USA
Milk powder	2 %	Carl Roth, Karlsruhe, Germany
Phosphate buffered saline (PBS)	0.05 %; 0,05 % Tween®20 in PBS; pH=7.2-7.4	Life Technologies, Carlsbad, CA, USA)

Sodium carbonate buffer	0.1 M sodium carbonate, 0.1 M sodium hydrogen carbonate, pH 9.6	Merck, Darmstadt, Germany
substrate reagent		R&D Systems, Minneapolis, MN, USA
Sulfuric acid	5,6ml 100 % H_2SO_4 in 100ml sterile water	Sigma, MO, USA
Tween 20	0,05 %	Calbiochem, Merck, Darmstadt, Germany

C) Plastic material

96-well MaxiSorp Nunc-Immuno plates	Thermo, Rochester, NY
Disposable gloves	Sempermed, Vienna, A
Disposable pipette 1ml/2ml/5ml/10ml/25ml/50ml	Sarstedt, Nürnbrecht, D
Disposable pipette tips 10µl/200µl/300µl/1000µl	Eppendorf AG, Hamburg, D
Falcontubes 15ml	TPP
Falcontubes 50ml	Sarstedt, Nümbrecht, D
Fluid reservoirs 200ml	Roth, Karlsruhe, D
Reaction vessel 1.5ml/2ml	Eppendorf AG, Hamburg, D
SealPlate	Roth, Karlsruhe, D

D) Devices

Microplate Reader	BioTek, Winooski, VT, USA
Incubator	Heraeus, Hanau, D
Pipette 10ml/20ml/100ml/1000ml	Eppendorf, Hamburg, D
8-channel pipette	Roth, Karlsruhe, D
Table centrifuge	Heraeus, Hanau, D

2.3 Detection of OPN Levels

OPN levels were quantified with the “Human Osteopontin Assay” ELISA (IBL Ltd., Japan) and optical density was measured blinded in duplicates. The OPN concentration was provided with the standard curve which was supplied by the kit and OPN plasma concentration was recorded in ng/ml (±1 SD). Age- and/or gender-related associations could be found for neither of the two biomarkers. OPN detection had been performed and the results kindly provided by the research group of Prof. Dr. med. Dirk Vordermark (Martin-Luther university Halle-Wittenberg) for further research.

2.4 Analysis of the Immune Phenotype with FACS

An efficient immune system is essential for long-term tumor control and in the prevention of distant metastasis (74). For this reason, differences in the immune composition of healthy human donors (n=10) and NSCLC patients (patient collective #1; n=43; Table 1A) were investigated using EDTA blood at diagnosis and multi-color FACS (fluorescence activated cell sorting) analysis (FACS Calibur flow cytometer, BD Biosciences). Flow cytometry is a biotechnological method utilizing laser to count and differentiate between cell subtypes after suspending them in fluids (e.g. fluorescence marked antibodies) and analyzing them with an electronic detection device. FACS allows to differentiate between physical and chemical traits of many hundreds of small particles in few seconds.

To determine the amount as well as the receptor density of the different lymphocyte subpopulations in the tumor patients, FACS analysis was immediately done with 1.4 ml EDTA blood after receiving the sample.

The blood was transferred into 14 test tubes with 100 µl each to add fluorescent-marked antibodies as a next step. The panel of fluorescence-labeled antibodies and antibody combinations which were used for the study are summarized in Table 7.

At the end of an incubation time of 15 min without exposition to light, the tubes were washed with 2 ml 10% FCS in PBS for 5 min at 500 g at room temperature. In order to eliminate erythrocytes, the blood cells were incubated with a lysing buffer (1:9 dilution of BD Lysing Solution Cat. 3490202 with millipore H2O) for ten minutes at room temperature in the dark, following a further washing step with FACS buffer under remaining conditions. Finally, the pellets of tube one to eleven were resuspended with 500 µl FACS buffer and the phenotype of 5 x 10^4 cells was determined by flow cytometry within an hour. In the meantime, special staining for the characterization of regulatory T-cells was in preparation. The cells in the three remaining tubes twelve to fourteen were treated with a special buffer A (1:10 dilution of component A with H2O), then washed two times with FACS-buffer and permeabilized with buffer C (1:50 dilution of buffer A with component B) for 30 min without light exposition. Following two washing steps with FACS buffer, a PE-conjugated antibody matching the Treg transcription factor FoxP3 (Forkhead box P3) or an isotype IgG1-antibody serving as a negative control were added for another 30 min of incubation period in the dark. Before measurement

of 5 x 10^4 cells, the remaining cells were washed with FACS buffer two times and finally resuspended with 500 µl FACS buffer per tube.

Table 7:

List of antibodies and 14 antibody combinations which were used for FACS analysis of the lymphocyte subpopulations in NSCLC patients and healthy donors;

APC, allophycocyanin; BD, Becton Dickinson Biosciences; BC, Beckman Coulter; CD, cluster of differentiation; Ctrl, control; FITC, fluorescein isothiocyanate; PE, phycoerythrin

Specificity	Antibody	Clone	Company	Cat No.	Volume
Ctrl	IgG1-FITC	X40	BD	345815	5
	IgG1-PE	X40	BD	345816	5
	IgG1-PerCP	X40	BD	345817	5
	IgG1-APC	X40	Caltag/Invitrogen	MG 105	1
T/NK	CD94-FITC	HP-3D9	BD	555888	5
	CD56-PE	NCAM16.2	BD	345811	5
	CD3-PerCP	SK7	BD	345766	10
	CD45-APC	HI30	Caltag/Invitrogen	MHCD 4505	1
B/T/NK	CD56-FITC	NCAM16.2	BD	345811	5
	CD19-PE	HIB19	BD	555413	20
	CD3-PerCP	SK7	BD	345766	10
	CD45-APC	HI30	Caltag/Invitrogen	MHCD 4505	1
T/NK	CD56-FITC	NCAM16.2	BD	345811	5
	CD16-PE	3G8	BD	555407	10
	CD3-PerCP	SK7	BD	345766	10
	CD45-APC	HI30	Caltag/Invitrogen	MHCD 4505	1
T/NK	CD56-FITC	NCAM16.2	BD	555518	5
	NKG2D-PE	149810	R&D	FAB139P	10
	CD3-PerCP	SK7	BD	345766	10
	CD69-APC	L78	BD	340560	5
T/NK	CD56-FITC	NCAM16.2	BD	345811	5
	NKp30-PE	IM3709	BC	PN 3709	10
	CD3-PerCP	SK7	BD	345766	10
	CD69-APC	L78	BD	340560	5
T/NK	CD56-FITC	NCAM16.2	BD	345811	5
	NKp46-PE	IM3711	BC	PN 3711	10
	CD3-PerCP	SK7	BD	345766	10
	CD69-APC	L78	BD	340560	5
T/NK	CD94-FITC	HP-3D9	BD	555888	5
	NKG2D-PE	149810	R&D	FAB139P	10
	CD3-PerCP	SK7	BD	345766	10
	CD56-APC	B159	BD	555518	10
T/NK	CD94-FITC	HP-3D9	BD	555888	5

Specificity	Antibody	Clone	Company	Cat No.	Volume
	NKp30-PE	IM3709	BC	PN 3709	10
	CD3-PerCP	SK7	BD	345766	10
	CD56-APC	B159	BD	555518	10
T/NK	CD94-FITC	HP-3D9	BD	555888	5
	NKp46-PE	IM3711	BC	PN 3711	10
	CD3-PerCP	SK7	BD	345766	10
	CD56-APC	B159	BD	555518	10
CD4/CD8 T	CD4-FITC	RPA-T4	BD	555346	20
	CD8-PE	RPA-T8	BD	555366	20
	CD3-PerCP	SK7	BD	345766	10
	CD45-APC	HI30	Caltag/Invitrogen	MHCD 4505	1
Ctrl	IgG1-FITC	X40	BD	345815	5
	IgG1-PE	X40	BD	345816	5
	IgG1-PerCP	X40	BD	345817	5
	IgG1-APC	X40	Caltag/Invitrogen	MG 105	1
CD4 Treg	CD4-PE	RPA-T4	BD	555346	20
	FoxP3-FITC	259/C7	BD	560046	20
	CD3-PerCP	SK7	BD	345766	10
	CD25-APC	2A3	BD	340907	5
CD8 Treg	CD8-PE	RPA-T8	BD	555366	20
	FoxP3-FITC	259/C7	BD	560046	20
	CD3-PerCP	SK7	BD	345766	10
	CD25-APC	2A3	BD	340907	5

Table 8: Chemicals, plastic materials and devices used for FACS-analysis

A) Chemicals

Description	Concentration	Producer
Buffer A (BD Human FoxP3 Buffer A)		BD Biosciences, USA
Buffer C	1:50 diluted BD Human FoxP3 Buffer B in diluted Buffer A	
FACS Buffer	10%, FCS in PBS	
FoxP3-PE antibody		BD Biosciences, USA
Lysing Solution		BD Biosciences, USA

B) Plastic material

Blood tube, EDTA S-Monovette	Sarstedt, Nümbrecht, Germany
Disposable gloves	Sempermed, Vienna, Austria
Disposable pipette 1ml/2ml/5ml/10ml/25ml/50ml	Sarstedt, Nümbrecht, Germany

Disposable pipette tips 10µl/200µl/300µl/1000µl	Eppendorf AG, Hamburg, Germany
Test tubes	Sarstedt, Nümbrecht, Germany

C) Devices

FACS Calibur flow cytometer	BD Biosciences
Pipet Aid Pipetboy	Integra Biosciences, USA
Table centrifuge	Heraeus, Hanau, Germany

Miscellaneous materials and devices that are not mentioned were obtained by corresponding companies, such as Carl Roth GmbH (Karlsruhe, Germany), and were verified for the use of scientific work.

The devices were sterilized and maintained regularly.

2.5 Radio(chemo)therapy and volumetric Parameters of Patient Collective #2

The patients received a normofractionated three-dimensional RT (3D-RT, 5 fractions/week) which was CT based (66 Gy total dose, 2 Gy single dose; Siemens Primus, Germany). Before RT, a PET-scan (Philips Accel, USA) was done. Regarding chemotherapy, two courses with cisplatin (20 mg/m^2 body surface on day 1-5) and vinorelbine (25 mg/m^2 body surface on day 1) in treatment week one and five were established. GTV was defined as the primary tumor and involved nodes (pathologic confirmed, highly suspicious by CT and PET) and determined by a radiation oncologist at the university hospital in Halle with the help of CT and PET images. The medical imaging data was registered in the Oncentra Masterplan external beam planning software (Nucletron, USA) used for RT plan calculation.

2.6 Statistical Analysis

Statistical analysis was done using the IBM SPSS 20.0 software package for Windows (SPSS Inc., USA). Two-sided p-values ($p < 0.05$) determined statistical significance. Median Hsp70 plasma levels were used as cutoff values. Non-parametric tests (Mann-Whitney U test, Kruskal

Wallis H test) were used to determine statistically significant differences between Hsp70 levels of patients with high and low GTV and high and low CD94 expression, lymphocyte subpopulations of healthy donors, patients with squamous cell and adenocarcinoma as well as between the percentage of all lymphocytes of patients with high and low Hsp70 expression with and without response. Spearman´s Rank Correlation Coefficient helped to analyze a correlation between serum Hsp70 levels and GTV. Wilcoxon Rank-Sum Test was used to evaluate potential differences in Hsp70 serum levels in NSCLC patients before and after RCT. The Kruskal-Wallis test with a Dunn multiple comparison test helped to compare Hsp70 levels in the serum of two patient groups (squamous cell and adeno NSCLC) with a group of healthy donors. Differences in Hsp70 levels in patients with and without therapy response were investigated using Pearson's chi-squared test. Coherences between Hsp70 and OPN as a hypoxia-related marker were evaluated using Pearson's rank correlation coefficient and paired samples test assessed potential differences in plasma Hsp70 levels before and after RT. Survival analysis was performed with the Kaplan–Meier product limit method with the log-rank test. Local citizen registration offices helped to follow up the survival status of the patients. Overall survival (OS) was involved the start of radiotherapy until death or last seen in follow-up. The primary endpoint was therapy response which was devided into responding responding (complete or partial remission (decrease of 30% in the lesion with the largest diameter) after RT) vs. non-responding patients (progressive or stable disease after RT). The Cox proportional hazard regression model was used to calculate the relative risk and hazard ratio and its 95% confidence interval (CI) for univariate and multivariate analysis. Receiver operating characteristic (ROC) curves illustrate the performance of Hsp70 plasma levels as a binary classifier system in the prediction of therapy response after RT.

3 RESULTS

Tumor patients have elevated Hsp70 levels in their blood [52, 105] as tumor cells secrete exosomes actively [80], carry this molecule in the cytosol and expose it on their lipid membrane [38]. Hsp70 levels can also be detected in healthy humans. Physiologically, Hsp70 levels originate from apoptotic or necrotic cells. Until recently, commercial ELISAs were able to detect only free but not lipid-bound Hsp70 in aqueous solutions. Therefore, our research group developed a new ELISA using the monoclonal cmHsp70.1 antibody as a detection reagent [152] to determine lipid bound Hsp70 in the blood of patients.

The cmHsp70.1 antibody is able to capture both, free and lipid bound Hsp70, on tumor cells *in vitro* and *in vivo* (Figure 11). Consequently, the quantification of the overall Hsp70 with the lipHsp70 ELISA is more precise and detects higher concentrations compared to values determined by commercial Hsp70 ELISA kits [152].

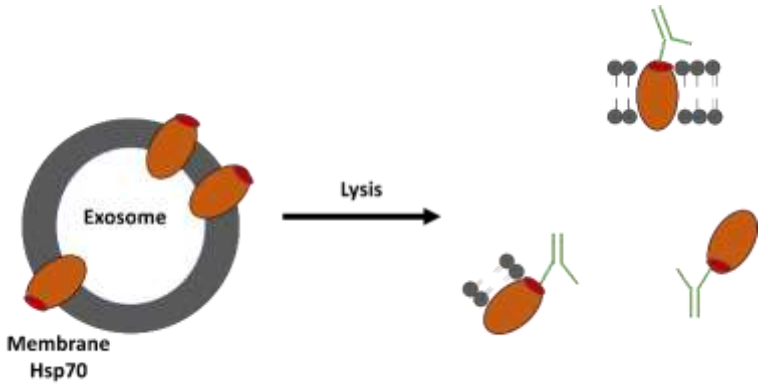

Figure 11:
Lipid-association of Hsp70 in exosomes and in the plasma membrane of living tumor cells. *An incomplete dissolution of lipid vesicles such as exosomes with detergents used in ELISA tests can induce the formation of Hsp70-lipid complexes.*

[152]

An Hsp70 overexpression could be confirmed in our present analysis with serum samples of 25 squamous cell and 18 adeno NSCLC patients (patient collective #1), using a control group of 126 age- and gender-matched healthy donors (Figure 12A). Squamous cell and adeno NSCLC patients (NSCLC; n=43) had significantly higher serum Hsp70 levels at diagnosis ($p \leq 0.001$)

compared to the control group (healthy; n=126). The cut-off value to differentiate between healthy and pathological levels was 7.7 ng/ml [152].

Using the healthy control group as a reference, the present research did not reveal any significant difference between the mean or median serum Hsp70 levels of squamous cell and adeno NSCLC (16.69 ± 2.7 ng/ml and 14.51 ± 2.49; median 12.15 vs. 12.20 ng/ml; p=0.825) (Figure 12B). It was remarkable that serum levels of both tumor types showed significant differences ($p \leq 0.001$) compared to the mean of healthy controls (7.0 ng/ml) as shown in Figure 12B.

Figure 12:

Hsp70 serum levels (nanogram per milliliter) of healthy human individuals contrasted with levels of NSCLC patients at diagnosis.

A)

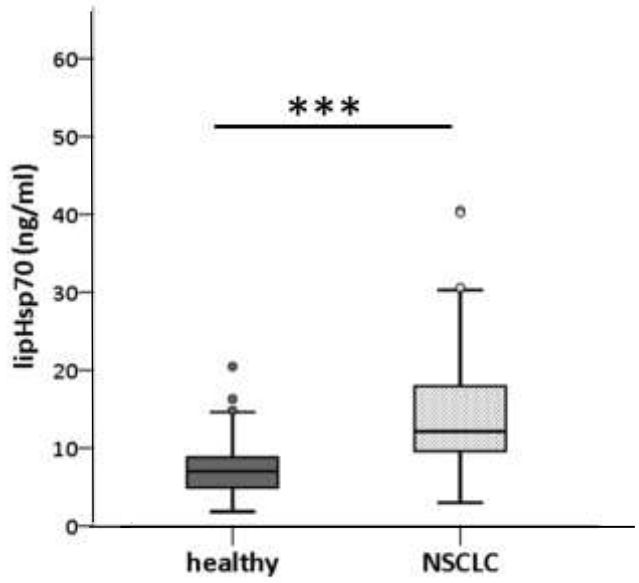

Serum Hsp70 levels of healthy donors (healthy; n *= 126; median Hsp70 level: 7.03 ng/ml, 95th percentile: 13.84 ng/ml) and patients with (NSCLC;* n *= 43; median Hsp70 level: 12.15 ng/ml, 95th percentile = 40.20 ng/ml) (patient collective #1) at diagnosis measured with the lipHsp70 ELISA; ***p < 0.001 (Mann–Whitney U-Test).*

B)

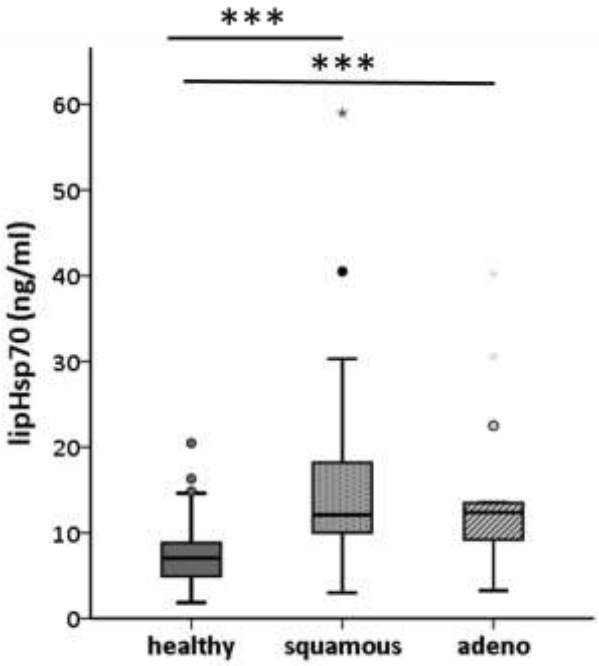

Serum Hsp70 levels of healthy donors (healthy; n = *126) and patients with squamous cell (squamous;* n = *25; median Hsp70 level: 12.10 ng/ml; 95th percentile: 40.50 ng/ml) and adeno (adeno;* n = *18; median Hsp70 level: 12.38 ng/ml; 95th percentile: 40.20 ng/ml) NSCLC (patient collective #1) at diagnosis measured with the lipHsp70 ELISA;* ***p < *0.001 (Kruskal–Wallis test with Dunn's multiple comparison test).*

To determine Hsp70 not only in the peripheral blood but also in tumor tissues, 9 tumor sections of squamous and adeno NSCLCs of patient collective #1 (three in stage III and six in stage IV) were analyzed. Representative results of NSCLC patients with squamous cell and adeno carcinomas are shown in Figure 13. Hsp70 staining was predominant in the tumor cells of all tumor sections, as opposed to the surrounding tissue.

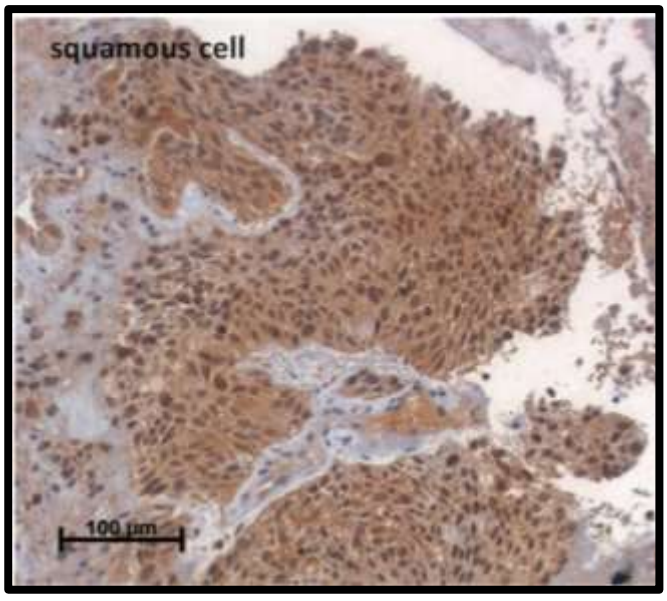

Figure 13:

Representative immunohistochemical images of a squamous cell and adeno NSCLC section stained with cmHsp70.1 antibody*; 20× magnification (patient collective #1). The upper graph shows a squamous cell NSCLC and the lower graph an adeno NSCLC section. Only the tumor tissue but not the surrounding tissue shows an Hsp70 staining.*

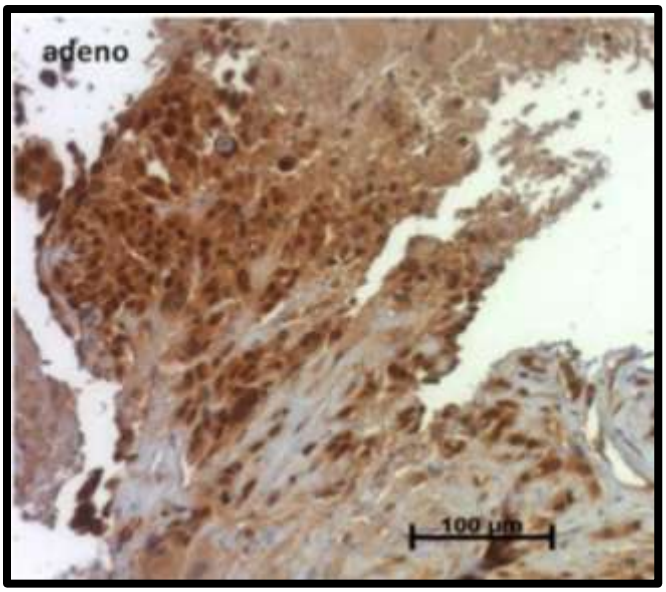

3.1 Significant Correlation of Hsp70 in the Blood with the GTV

The major part of Hsp70 in the blood circulation is bound to lipid-vesicles (exosomes), being actively secreted and localized in the cytosol and on the surface of exosomes and viable tumor cells [38, 132]. As a result, a potential correlation of Hsp70 in the blood with the gross tumor volume (GTV) in 55 NSCLC patients (patient collective #2; Table 4b) was investigated. Hsp70 levels were quantified with the lipHsp70 ELISA and the GTV was detected by PET-imaging before start of the therapy. The average tumor size was 219.9 ± 32.3 ml and the mean Hsp70 level was 11.2 ± 1.7 ng/ml which was increased compared to the cut-off value of healthy donors (7.7 ng/ml). A statistically significant correlation ($p=0.03$) between Hsp70 in the blood and the GTV using Spearman´s Rank Correlation Coefficient was detected. Additionally, the patient group was subdivided into a group with low (≤143.6 ml) and high (>143.6 ml) median GTV according to the median GTV of 143.6 ml. Figure 14 demonstrates that patients with higher Hsp70 levels had a significantly higher tumor volume than patients of the group with less Hsp70 ($p<0.05$).

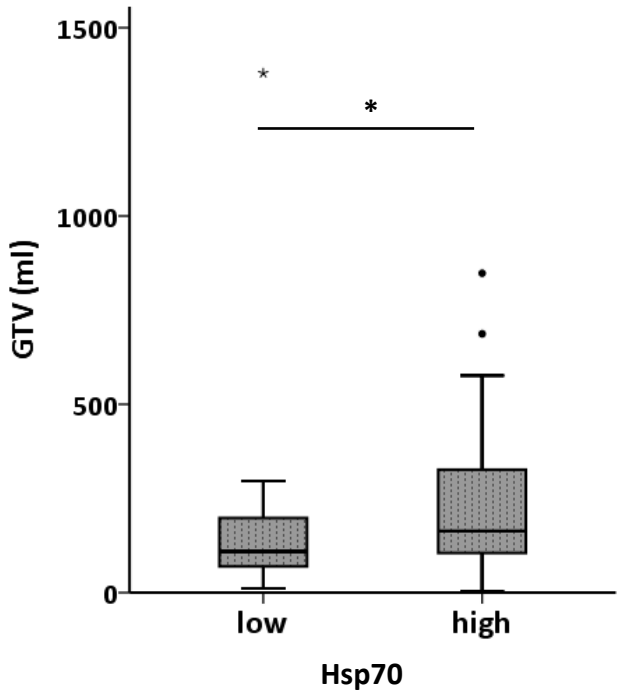

Figure 14:

Hsp70 serum levels in association with the gross tumor volume (GTV) in NSCLC patients.
*NSCLC patients (*n *= 55; patient collective #2) were divided into patients with low GTV (≤143.6 ml; median GTV: 109.40 ml; 95th percentile: 296.30 ml) and high GTV (>143.6 ml; median GTV: 163.50 ml; 95th percentile: 688.00 ml) depending on their median Hsp70 levels;* *p *< 0.05 (Mann–Whitney* U*-test).*

3.2 Differences of the Immune Phenotype between NSCLC Patients and Healthy Donors

The conditions which contribute to the formation of tumor cells are complex and multifactorial. It is well accepted that the immune system takes over a major part in the control of carcinogenesis and metastatic spread [34]. The composition of immune cells and immunological processes are unique in every individual, they have an enormous potential of adaptability and depend on life-long exposition to antigens. As a result, the immune phenotype determined with multi-color FACS analysis of lymphocyte subpopulations in the EDTA blood of healthy donors (n=10) and NSCLC patients of patient collective #1 (n=43) was compared before therapy start. The fluorescence-labeled antibodies used in the study are represented in Table 7.

A representative image of the gating strategy for the determination of lymphocyte subsets is illustrated in Figure 15. Gate R1 represents the lymphocytes, whereas gate R2 illustrates the population of granulocytes. The $CD14^+$ monocytes is localized between the gates R1 and R2.

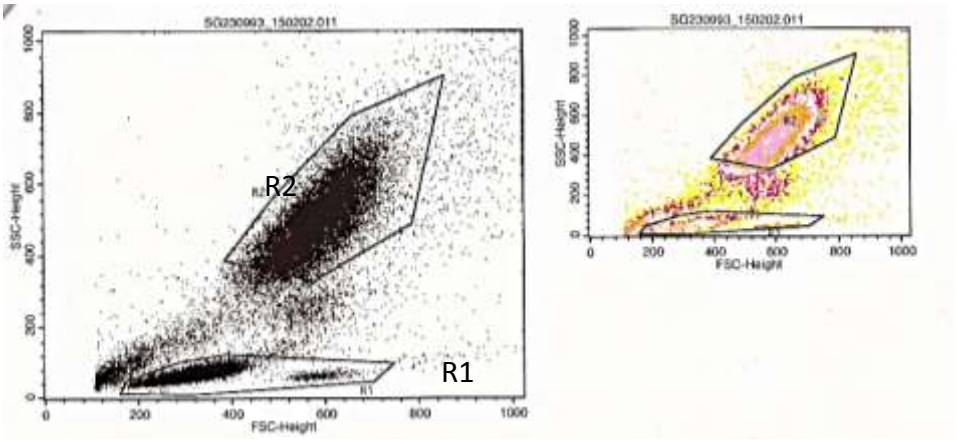

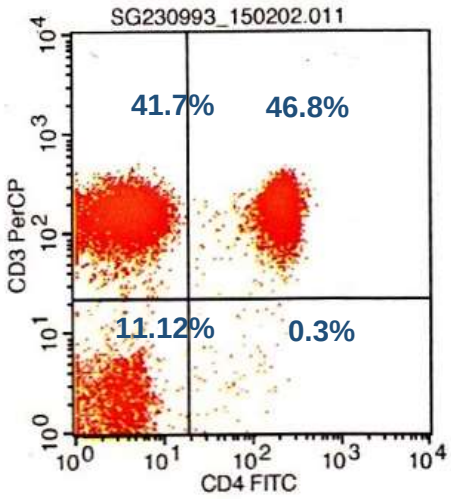

Figure 15:

Quantification of relative amounts of lymphocytes (%) in healthy human individuals and NSCLC patients. *Detection of peripheral blood lymphocytes (PBL) in healthy human individuals (n = 10) and patients with squamous cell (n = 25) and adeno (n = 18) NSCLC at diagnosis (patient collective #1); **p < 0.01, ***p < 0.001 (Mann–Whitney U-test). gate R1 depicts the population of PBL which is analyzed by FACS, R2 comprises the population of granulocytes.*

Patients with squamous cell (n=25) and adeno (n=18) carcinoma of the lung showed significantly lower lymphocyte numbers (p=0.001 vs p=0.008, Mann–Whitney U-test) compared to healthy donors, although the percentage of lymphocytes within the NSCLC subtypes was similar (22.4 ± 1.6% for squamous cell and 21.8 ± 2.4% for adenocarcinoma patients vs. 34.5 ± 1.77% in healthy controls) (Figure 16A).

Regarding $CD19^+$ B cells, patients with squamous cell carcinoma exhibited significantly lower amounts than the healthy control groups (p = 0.001) and adenocarcinoma patients (p = 0.02, Mann–Whitney U-test) (Figure 16B). A comparison of different $CD3^+$ T cell subpopulations, such as $CD4^+$, $CD8^+$, $CD4^+/CD25^+$ regulatory, $NKG2D^+$, and $CD94^+$ T cells revealed no major differences in patients with adeno lung carcinomas compared to healthy controls (p = 0.038), apart from a significant increase in the subpopulation of $CD3^+/CD56^+$ NKT cells (Figure 16C). The activation marker CD69 appeared to be slightly elevated on $CD3^+$ T cells of patients with

squamous cell (p = 0.81) and adenocarcinoma (p = 0.197) patients compared to healthy controls (Figure 16C).

Different from the T cell populations, $CD3^-$ NK cells presented alterations regarding the activation marker CD69 and the C-type lectin receptor CD94. The concentration of $CD3^-/CD56^+/CD69^+$ (p = 0.016) and $CD3^-/CD56^+/CD94^+$ (p = 0.028) NK cells was significantly elevated in squamous cell carcinoma patients compared to healthy controls (Figure 16D). Additionally, squamous cell NSCLC had elevated ratios of $CD3^-/CD56^+$ NK cells and $CD3^-/NKG2D^+$ NK cells, but the difference was not significant (p = 0.053) (Figure 16D).

Figure 16: Representation of the immune phenotype of squamous cell and adeno NSCLC patients and healthy donors, as determined by FACS analysis.

A)

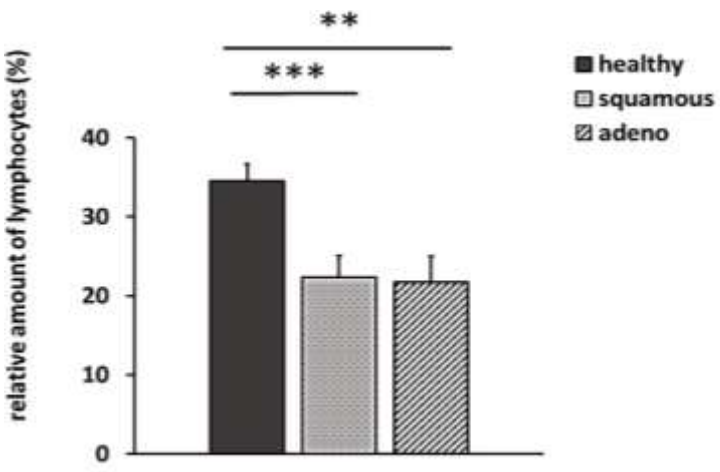

*Comparison of the amount of peripheral blood lymphocytes (PBL) in healthy human individuals (n = 10) and patients with squamous cell (n = 25) and adeno (n = 18) NSCLC at diagnosis (patient collective #1); **p < 0.01, ***p < 0.001 (Mann–Whitney U-test).*

B)

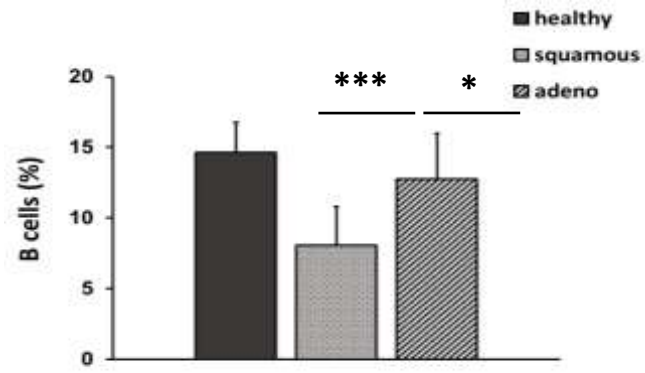

*Proportion of B cells in the blood of healthy donors (n = 10), squamous cell (n = 25) and adeno (n = 18) NSCLC patients (patient collective #1); *p < 0.05, ***p = 0.001 (Mann–Whitney U-test).*

C)

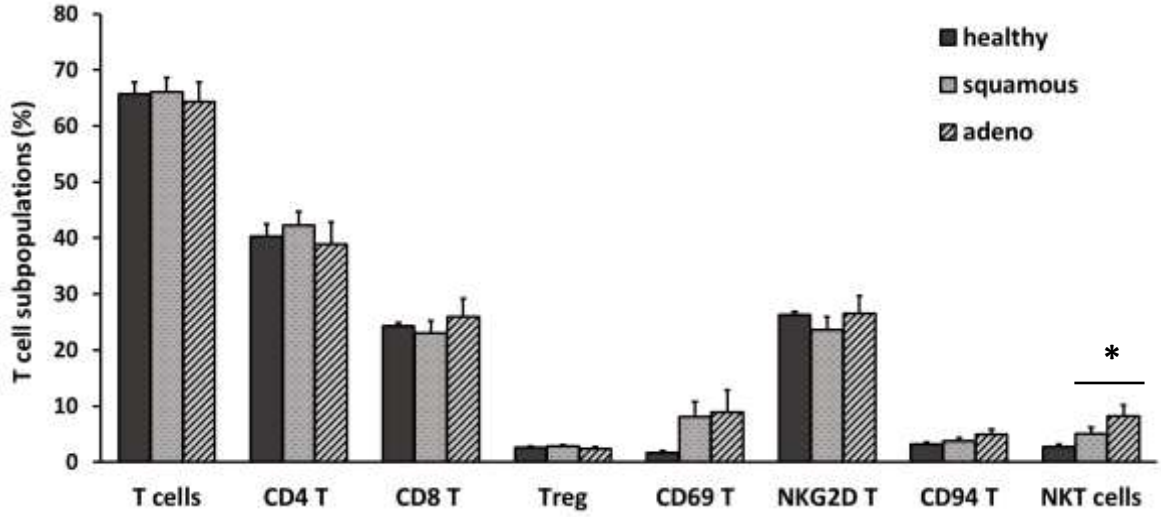

*Relative amount of T cell subpopulations in the blood of healthy donors (n = 10), squamous cell (n = 25) and adeno (n = 18) NSCLC patients (patient collective #1); *p < 0.05 (Mann–Whitney U-test).*

D)

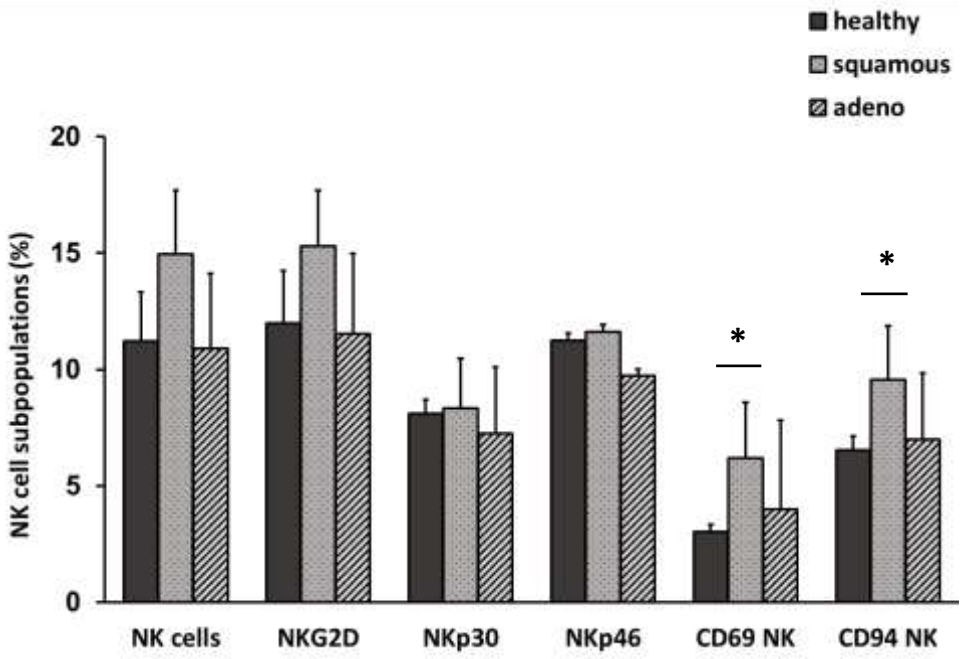

*Relative amount of NK cell subpopulations in the blood of healthy individuals (n = 10), squamous cell (n = 25) and adeno (n = 18) NSCLC patients (patient collective #1); *p < 0.05 (Mann–Whitney U-test).*

3.3 Correlation of Hsp70 Serum Levels with Lymphocyte Subpopulations in NSCLC Patients

The analysis of the immune phenotype revealed significantly elevated ratios of $CD3^-/CD94^+$ NK cells in squamous cell NSCLC (Figure 16D). As it could be shown that the C-type lectin receptor CD94 plays a key role in the recognition of Hsp70 on the tumor cell membrane by NK cells, I further investigated a potential correlation of Hsp70 with the percentage of $CD3^-/CD94^+$ NK cells. Patients with squamous cell (n = 25) and adenocarcinoma (n = 18) were divided into groups with high (≥8.5% in squamous cell and ≥6.5% in adenocarcinoma, percentage of all lymphocytes) and low (<8.5% in squamous cell and <6.5% in adenocarcinoma, percentage of all lymphocytes) median percentages of $CD3^-/CD94^+$ NK cells. Squamous cell NSCLC patients with a high $CD3^-/CD94^+$ NK cell ratio showed significantly lower serum Hsp70 levels than the corresponding group with a low ratio of $CD3^-/CD94^+$ NK cells ($p = 0.048$) (Figure 17B). The co-expression of $CD94^+$ and $CD69^+$ on the NK cell population documents the activity of these NK cells. Patients with high percentages of $CD94^+/CD69^+$ NK cells had low Hsp70 serum levels and a smaller GTV. It seems probable that these NK cells can control the growth of mHsp70-positive tumor cells. Patients with adenocarcinoma by contrast did not have a significant correlation between $CD3^-/CD94^+$ NK cells and serum Hsp70 levels ($p = 0.908$) (Figure 17A).
These results might be a hint that the NSCLC of the squamous cell subtype has a higher immunogenicity than the adeno NSCLC.

Figure 17:

CD94 immune phenotype in association with Hsp70 serum levels in squamous cell and adeno NSCLC patients.

Adeno carcinoma of the lung

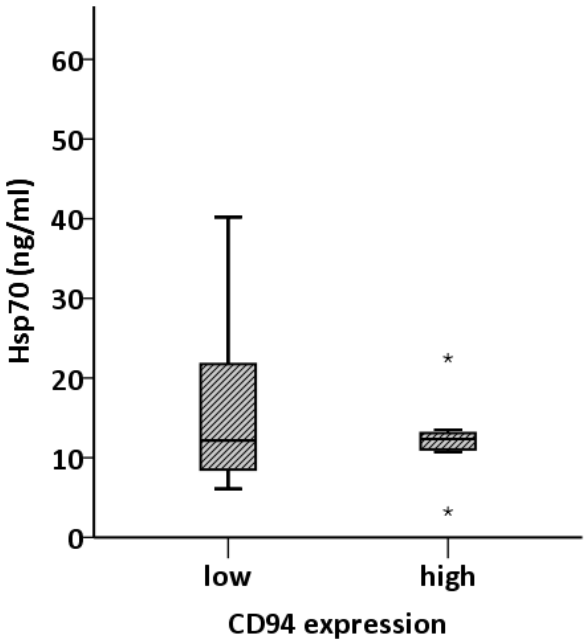

*CD94 expression and serum Hsp70 levels in adeno NSCLC patients (*n = *18) (patient collective #1). Division of adeno NSCLC patients into a group with low (≤6.5% CD3⁻/CD94⁺ NK cells; median Hsp70 level: 12.15 ng/ml; 95th percentile: 40.20 ng/ml) and high (>6.5% CD3⁻/CD94⁺ NK cells; median Hsp70 level: 12.35 ng/ml; 95th percentile: 22.50 ng/ml) percentage of CD3⁻/CD94⁺ NK cells;* p > *0.05 (Mann–Whitney* U-*test).*

Squamous cell carcinoma of the lung

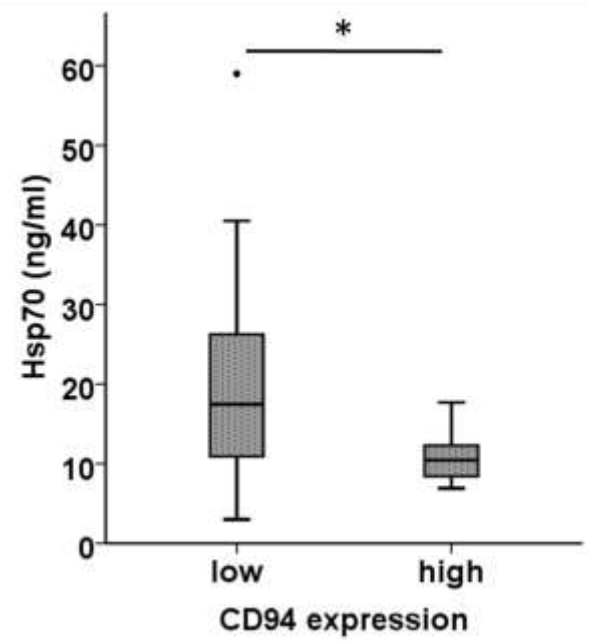

Association of CD94 expression and serum Hsp70 levels in squamous cell NSCLC patients (n = 25) (patient collective #1). Division of patients with squamous cell NSCLC into a group with low (≤8.5% CD3−/CD94+ NK cells; median Hsp70 level: 17.45 ng/ml; 95th percentile: 59.00 ng/ml) and high (>8.5% CD3−/CD94+ NK cells; median Hsp70 level: 10.45 ng/ml; 95th percentile: 17.70 ng/ml) percentage of CD3−/CD94+ NK cells; p* < 0.05 (Mann–Whitney U-test).

3.4 Impact of Radio(chemo)therapy on Hsp70 Blood Levels and its Correlation with Therapy Response

During the first part of my research work, a significant correlation of Hsp70 levels with the GTV in NSCLC patients was detected. This result confirms that the origin of the elevated serum and plasma Hsp70 are predominantly exosome-secreting vital tumor cells that carry Hsp70 in their lipid membrane.

Our investigations concerning lymphocyte compositions in NSCLC patients revealed higher percentages of activated $CD69^+$ and $CD94^+$ positive NK cell subpopulations in SCC NSCLC patients compared to healthy donors and high ratios of $CD94^+$ positive NK cells were associated with lower Hsp70 levels.

Apart from its interaction with the immune system, a potential correlation of Hsp70 with the biomarker osteopontin was investigated. Elevated levels of the latter molecule are an indicator of hypoxia and poor overall survival [99]. Hypoxic conditions affect therapy response adversely and constitute cell stress which stimulates the expression of Hsp70. Earlier on, our work group was able to demonstrate an enhanced hypoxia mediated radio-resistance of malign cells [96]. A further significant correlation was detected between high OPN levels and reduced lung function and weight loss [99].

In relation to radio(chemo)therapy, pre- and post-therapeutic Hsp70 levels were compared to figure out if the therapy had any impact on peripheral Hsp70 in the blood. Moreover, although enhanced osteopontin is associated with a worse survival time, there was no correlation with the therapy response. Therefore, I explored if Hsp70 had a predictive function in this particular field.

3.4.1 Correlation of Pre-Therapeutic (T1) OPN Levels with Hsp70 Plasma Levels in Patients with NSCLC

Results were obtained in a patient collective of 44 NSCLC patients (6 females, 38 males) without metastasis (M0). Table 9A represents the clinico-pathological characteristics of all 44 patients, Table 9B compares the characteristics of responding and non-responding patients. With respect to tumor volume ($p = 0.086$), age ($p = 0.114$), gender ($p = 0.306$), histology

(p = 0.158), and UICC stage (p = 0.175), no statistically significant differences were determined in non-responding and responding patients.

Table 9: Clinicopathological characteristics of 44 patients of collective #2

		Counts	
Gender	Female	6	14%
	Male	38	86%
Histological type	Squamous cell carcinoma	23	52%
	Adeno ca	19	43%
	Other	2	5%
UICC stage	I–II	2	5%
	IIIa	16	36%
	IIIb	26	59%

9A)

*Description of all non-small-cell lung cancer patients (*n = *44) at M0 (Martin Luther University Hospital, Halle-Wittenberg).*

9B) *Description of non-responding and responding non-small-cell lung cancer patients without metastases (M0) (Martin Luther University Hospital, Halle-Wittenberg).*

		Non-responder Counts		Responder Counts	
Gender	Female	0		6	17.6%
	Male	10	100%	28	82.4%
Histological type	Squamous cell ca	7	70%	16	47%
	Adeno ca	2	20%	17	50%
	Other	1	10%	1	3%
UICC stage	I–II	1	10%	1	2.9%
	IIIa	4	40%	12	35.3%
	IIIb	5	50%	21	61.8%

The two biomarkers OPN and Hsp70 were measured in the plasma of all patients (Table 9A) before therapy start (T1, before RT). It has been demonstrated that high pre-therapeutic OPN plasma levels (above median, *n* = 22) significantly correlated with inferior OS compared to low

(below median, *n* = 22) levels (13 [5–66] vs. 23 [5–61]; *p* < 0.05) in larger NSCLC patient groups with and without metastatic spread [99]. A positive correlation according to the Pearson´s correlation coefficient between the two biomarkers OPN and Hsp70 (*r* = 0.422, *p* = 0.005) was found at T1 (Table 10). Furthermore, the patient collective was divided into patients with high and low Hsp70 expression according to the median Hsp70 value of 9.30 ng/ml within the patient collective. According to the Mann–Whitney U test (Figure 18), patients whose Hsp70 values were above the median of 9.30 ng/ml showed a significantly higher OPN expression compared to those with median Hsp70 values below 9.30 ng/ml (*n* = 43, *p* = 0.021).

	OPN T1 (ng/ml)	lipHsp70 T1
N (missing)	44 (0)	43 (1)
Mean	872.14	12.13
SEM	71.63	2.02
Median	752.45	9.30
SD	475.11	13.26
Maximum	2441.00	67.50
Minimum	299.30	0.20
Paired samples test (OS)	p<0.05	

Table 10:

Comparison of pre-therapeutic (T1) osteopontin (OPN) and heat shock protein 70 (Hsp70) plasma levels in non-small-cell lung cancer patients (M0; n = *44) in relation to overall survival.*

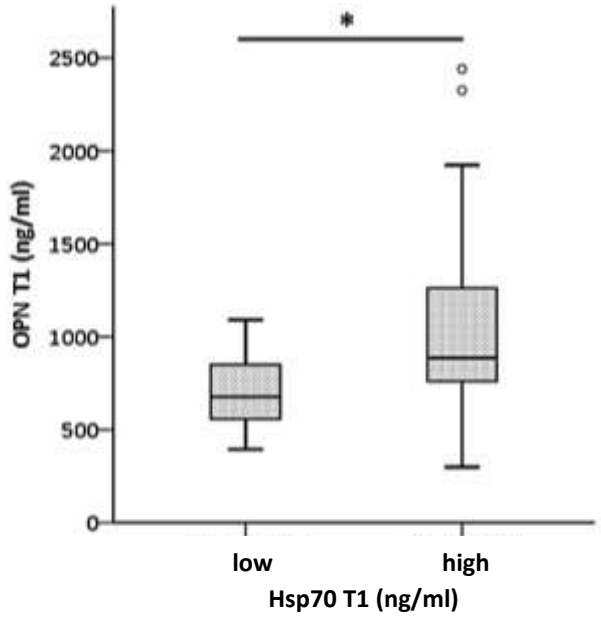

Figure 18:

Pre-therapeutic (T1) osteopontin (OPN) levels in non-small-cell lung cancer patients (M0) in dependence of high and low median heat shock protein 70 (Hsp70) plasma levels. *The patient cohort (*n = *43) was divided into two subgroups with median Hsp70 plasma levels below (low) or above 9.30 ng/ml (high) according to the median Hsp70 plasma level of 9.30 ng/ml; Mann–Whitney* U *test,* p = *0.021.*

3.4.2 Drop of Hsp70 Plasma Levels after RT in Patients with NSCLC

Apart from the comparison with the biomarker osteopontin, the impact of RT on Hsp70 plasma levels was investigated. First investigations regarding this subject have been performed earlier in a small patient subgroup consisting of 6 patients. Their blood was drawn before start and shortly after termination of therapy. Throughout this time period, Hsp70 levels remained significantly upregulated in comparison with those of healthy human individuals. Nevertheless, a small drop which failed to achieve statistical significance (p=0.463; Wilcoxon Rank-Sum Test) in this small patient group could be observed after completion of therapy (Figure 19).

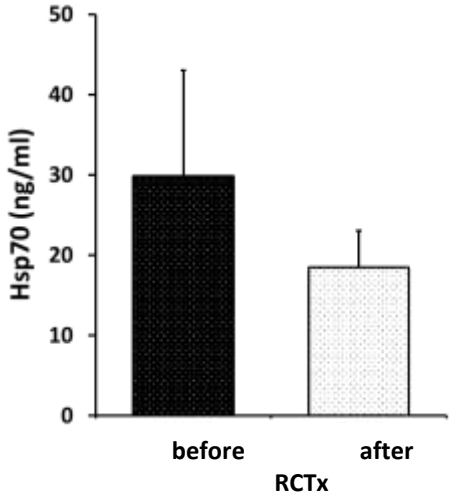

Figure 19:

*Dynamics of serum Hsp70 levels of NSCLC patients (*n = *6; patient collective #1) at diagnosis (before) and directly after RCT (after).*

Repeating these investigations in a larger patient collective #2, I contrasted pre- (T1) and post- (T2) therapeutic Hsp70 plasma levels of 26 patients from whom blood was received before and after therapy. Table 11 demonstrates a significant drop from 10.35 ng/ml before RT to 6.05 ng/ml after RT (paired samples test, $p = 0.016$) in median Hsp70 levels. According to the Pearson's correlation coefficient, a significant positive correlation was determined ($r = 0.659$, $p < 0.0001$).

	Hsp70 T1 (ng/ml)	Hsp70 T2 (ng/ml)
N	26	26
Mean	14.94	9.02
SEM	3.02	1.81
Median	10.35	6.05
SD	15.41	9.24
Maximum	67.50	46.20
Minimum	0.20	0.80
Paired samples test	$p = 0.016$	

Table 11: *Dynamics of heat shock protein 70 (Hsp70) plasma levels before (T1) and 4–6 weeks after (T2) radio(chemo)therapy in patients with NSCLC (M0).*

A similar drop in peripheral Hsp70 after RT could be observed by mean Hsp70 levels (T1 vs. T2: 14.94 ng/ml vs. 9.02 ng/ml). Nevertheless, Hsp70 levels were still significantly upregulated before (T1) as well as after (T2) RT ($p<0.05$) compared to the levels of a control group of 114 healthy donors (7.8 ng/ml) [152].

3.4.3 Prediction of Clinical Response to RT by High Post-Therapeutic Hsp70 Plasma Levels

First investigations with a small group of NSCLC patients showed a drop in Hsp70 levels after RT (Figure 19), although the levels were still elevated compared to those of healthy donors. I repeated this experiment with a larger patient collective and investigated if Hsp70 levels did reflect the therapy response. I could confirm that responding patients had a significantly improved OS in contrast to non-responding patients (23 vs. 9 months, $p = 0.026$, log-rank Mantel Cox) who had an increased risk of death ($r = 2.11$, *CI* [0.94–4.57], $p = 0.58$). A comparison of Hsp70 plasma levels before (T1) and 4–6 weeks after RT (T2) in non-responding ($n = 7$, 9.76 ng/ml vs. 4.03 ng/ml) and responding patients ($n = 19$, 16.85 ng/ml vs. 10.87 ng/ml) demonstrated that in both patient subgroups, mean and median Hsp70 plasma levels declined after RT (Figure 20). The median post-therapeutic plasma Hsp70 levels at T2 (median 8.6 ng/ml, range 0.8–46.2) of patients with therapy response were significantly higher in comparison with those without response (median 2.8, range 1.5–12.2) (Mann–Whitney U test, $p = 0.013$) (Figure 21). The mean Hsp70 values revealed similar results with

respect to both time-points in responding (11.10 ng/ml at T1 vs. 8.60 ng/ml at T2) and non-responding (5.30 ng/ml at T1 vs. 2.80 ng/ml at T2) patients (paired samples test $p = 0.034$).

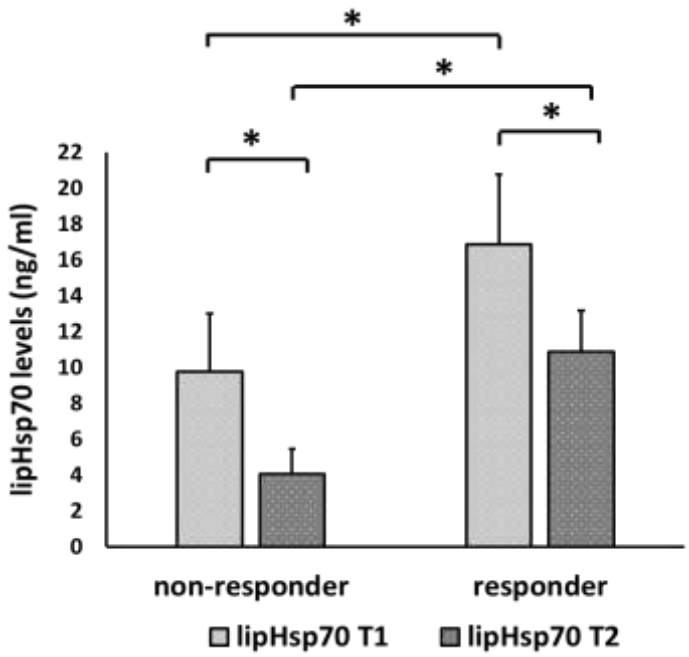

Figure 20:

Comparison of mean pre- (T1) and post- (T2) therapeutic heat shock protein 70 (Hsp70) plasma levels in non-responding and responding non-small-cell lung cancer patients (M0). Non-responder: 7, responder: 19. Mann–Whitney U *test,* *p < *0.05.*

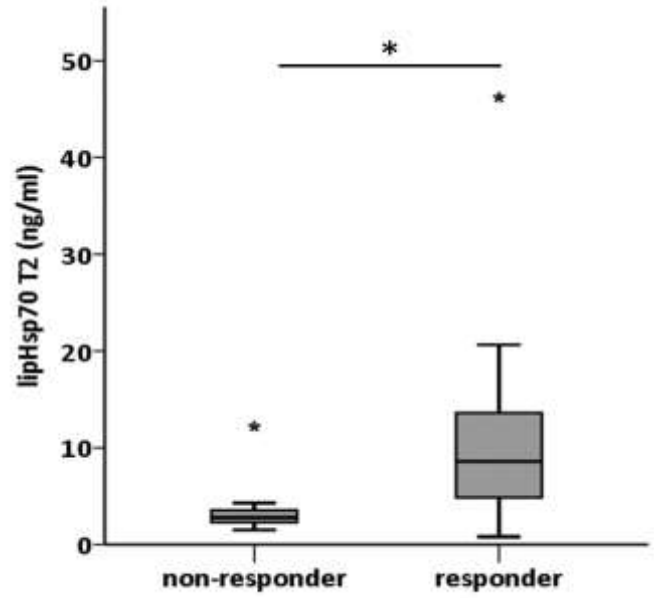

Figure 21:

Comparison of median post (T2) therapeutic heat shock protein 70 (Hsp70) plasma levels in NSCLC patients (M0) with different therapy response. Non-responder: 7, responder: 19. Mann–Whitney U *test, asterisks above the box plots indicate outliers;* *p = *0.013.*

Additionally, the patient cohort was subdivided into a group with Hsp70 plasma levels above and below the median plasma Hsp70 of 5.0 ng/ml at T2. The patients above the threshold showed significantly higher response rates than those below the threshold (92.9 vs. 50%,

Pearson Chi-Square $p = 0.02$) (Table 12). In line with these findings, I studied the potential of post-therapeutic Hsp70 levels to predict therapy response. A ROC curve analysis was created (Figure 22) which could affirm a significant predictive function ($p = 0.014$) of plasma Hsp70 levels for therapy response with an area under the curve (AUC) of 0.82. The optimal cutoff value to differentiate between positive and negative therapy response was a value of ≤4.35 ng/ml with a sensitivity of 0.895 and a false positive rate of 0.143. The same analysis was conducted with plasma Hsp70 before therapy start (T1) but failed to be statistically significant.

Therapy response (T2)	**Median Hsp70 above 5 ng/ml**	**Median Hsp70 below 5 ng/ml**
N	14	12
Non-responder	1 (7%)	6 (50%)
Responder	13 (93%)	6 (50%)
Pearson chi-square	$p = 0.02$	

Table 12:
Posttherapeutic (T2) heat shock protein 70 (Hsp70) plasma levels in dependence of the therapy response in NSCLC patients (M0).

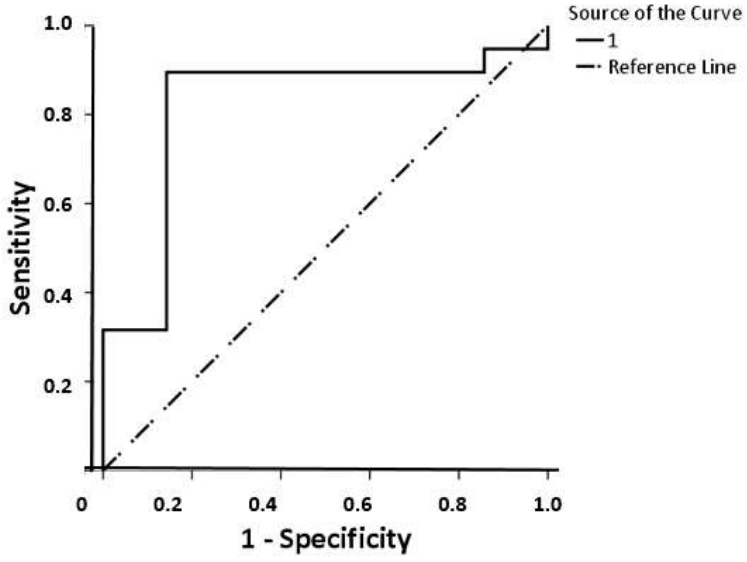

Figure 22:
Prediction of therapy response using a receiver operating characteristic (ROC) curve analysis of heat shock protein 70 (Hsp70) plasma levels of non-small-cell lung cancer (NSCLC) patients (M0). Area under the curve = 0.82, p *= 0.014. The optimal cutoff value for the identification of responders and non-responders was an Hsp70 plasma level of 4.35 ng/ml with a sensitivity of 0.895 and a false positive rate of 0.143.*

4 DISCUSSION

4.1 Role of Hsp70 in Tumor Detection and Prognosis

Frequently, lung cancer is diagnosed in a late tumor stage. The reason for this is that patients with lung cancer suffer from unspecific symptoms like coughing, dyspnea or fever that are most frequently seen in inflammatory diseases of the lung, such as chronic obstructive pulmonary disease (COPD) or pneumonia. The consequence of a diagnosis in a late stage is a reduced access to curative-intent treatment as the tumor has progressed. Furthermore, COPD patients who mostly share a history of smoking have a higher risk of developing lung cancer. As a result, there is an urgent need to explore novel tumor biomarkers to differentiate between malignant and benign diseases. One of these biomarkers is the major stress-inducible Hsp70. Unlike normal cells, tumor cells exhibit higher cytosolic Hsp70 levels, frequently present Hsp70 on their cell surface and actively release it in lipid vesicles as exosomes [53, 75, 105]. Exosomal Hsp70 contributes to enhanced Hsp70 levels which are easily detectable in the blood using the novel lipHsp70 ELISA [152]. A concentration of approximately 7.7 ng/ml is detectable in the blood of healthy individuals (N=145) and therefore is considered as a cut-off value which separates tumor patients from healthy donors. Physiologically the molecular chaperone Hsp70 is residing in the cytosol of cells. Therefore, the presence of Hsp70 in the blood circulation of healthy individuals is most likely a consequence of cell death. A high cytosolic density of Hsp70 is responsible for the protection of cancer cells from apoptotic cell death, an increased therapy resistance, it supports tumor cell proliferation and migration and creates a cancer phenotype with enhanced aggressiveness. Elevated Hsp70 levels have not only been found in lung tumors, but also in hematological malignancies, breast, prostate, colon, brain, and lung cancer [52, 105]. Hence, Hsp70 is suitable as a tumor biomarker for a large variety of different tumor entities. This research showed significantly elevated levels of Hsp70 in the blood of squamous cell and adeno NSCLC patients compared to a group of healthy volunteers. Nevertheless, Hsp70 is not only enhanced in the blood of tumor patients like patients with hepatocellular carcinoma, but also in patients who have inflammatory diseases like chronic hepatitis or liver cirrhosis [40]. It was noticeable though that tumor

patients still had the highest Hsp70 levels compared to patients with chronic inflammation. In line with these findings, another study demonstrated that NSCLC patients have more Hsp70 in the blood than COPD patients [139]. The fact that cancer can arise from diseases with chronic inflammation and that this transition goes along with an increase in exosomal Hsp70, makes this marker valuable to monitor malignant transformation by the lipHsp70 ELISA. Since blood samples are easy accessibility with minimal invasive methods, the detection of the tumor-specific biomarker Hsp70 seems to be suitable to differentiate between inflammatory and malignant diseases of various tissue types.

4.2 Hsp70 as a Biomarker of Vital Tumor Mass

Since Hsp70 is present on the surface of tumor cells and is actively released in exosomes, elevated Hsp70 levels in the blood represent the activity of the vital tumor mass. In tumor patients, the major part of circulating Hsp70 originates from exosomes. The remnant Hsp70 originates from membrane-positive tumor cells which have been released into the blood circulation, from dying tumor cells and from the physiological base line levels which are even present in healthy individuals, set free by apoptotic and necrotic cells. Along this line, I investigated if there was a potential connection between the peripheral Hsp70 measured in the blood and the size of the tumor tissue which had been measured by PET-imaging in NSCLC patients (n=55; collective #2). A direct correlation between serum Hsp70 and the GTV could be determined (Figure 14). Lower Hsp70 levels were associated with a smaller GTV, and higher levels were accompanied by a larger viable tumor mass. Furthermore, the statistical Spearman´s Rank Order Correlation analysis could show a significant correlation between serum Hsp70 levels and PET-based tumor volume. Also Kokowski et al. could show that a decrease in tumor size was accompanied by a drop in Hsp70 concentrations [68].

More investigations on a potential correlation of Hsp70 with the UICC stage need to be performed in larger patient cohorts with a more balanced distribution of different UICC stages. Moreover, Zimmermann et al. [139] were able to show an association of Hsp27 and Hsp70 serum levels with clinical stages in NSCLC and Bauer et al. [9] argue that both HSPs are beneficial in the risk stratification of UICC stage I/II colon cancer. Future studies will deal with

the combined acquisition and evaluation of serial GTV and serum Hsp70 registrations at various time points before, during and after RT. Apart from this, it is still not clear if the Hsp70 membrane expression within one tumor or in tumors of different patients is homogenous. More knowledge about the processes of Hsp70 secretion might help to analyze the correlation of Hsp70 levels and viable tumor mass.

To confirm that tumor tissue is Hsp70 positive different from the surrounding healthy tissue, immunohistochemistry was performed. Figure 13 demonstrates a clear separation of tumor and normal tissue based on the Hsp70 positivity. In patients with squamous cell carcinoma of the head and neck it also has been shown that a high Hsp70 expression was associated with high serum Hsp70 levels [44]. Yet it remains unknown which circumstances might affect the quantity of actively released Hsp70 positive vesicles by malignant cells. More research is still pending concerning the Hsp70 secretion behavior of tumor cells, just as well as concerning the exact functions of Hsp70 secretion in vesicles. Salamuta S. Mambula for example described a reinsertion of released Hsp70 into the cell membrane of prostate carcinoma cells after [78]. This phenomenon might have an influence on peripheral blood Hsp70 levels on the one hand, and on the other hand increase the Hsp70 membrane positivity and therefore also radio-resistance [96], tumor progression [62] and aggressivity of initially Hsp70 negative tumor tissue.

4.3 Interpretation of immunological Phenotypes and Differences in NSCLC Patients in relation to Hsp70 Levels

Besides all the negative facets of elevated Hsp70 levels in the blood, Hsp70 can serve as a target structure for the innate immune system [17, 42, 43], particularly for pre-activated NK cells. The reaction of immune cells to different antigens is highly individual and based on the genetic constitution along with lifelong exposition to exogenous particles. Due to its control function in the detection of “non-self” antigens, the immune system has a major role in the formation and spread of malignantly transformed cells. Different tumor immune escape mechanisms [13] are responsible for the fact that natural systems of defense can be evaded and tumor patients are immunosuppressed in respect of immunological tumor recognition. Based on these findings, particular differences between patients with NSCLC of different

histology and healthy volunteers could be detected and therefore confirmed that the immune system plays an important role in the tumor control. Regarding the relative number of lymphocytes in the peripheral blood, healthy controls had significantly higher percentages of lymphocytes compared to squamous cell and adenocarcinoma patients (Figure 16A). As it is known that membrane Hsp70 is a recognition structure for Hsp70 pre-activated NK cells [17], a potential influence of systemic Hsp70 on the cell subtype composition of peripheral blood lymphocytes (PBL) was studied. Flow cytometric analysis of the blood of patients with squamous cell carcinoma showed decreased percentages of B cells (Figure 16B), but elevated percentages of activated NK cell subpopulations in patients with squamous cell NSCLC, unlike in patients with adeno NSCLC (Figure 16D). Significantly increased percentages of $CD69^+/CD94^+$ NK cells were found in squamous cell carcinoma patients compared to the healthy donors and adenocarcinoma patients. In the second patient collective, high serum Hsp70 levels could be correlated with a larger tumor volume. High serum Hsp70 levels were associated with a lower percentage of $CD94^+/CD69^+$ activated NK cells in squamous cell NSCLC (Figure 16D). As lower serum Hsp70 is associated with a smaller GTV (Figure 14) and a higher percentage of $CD94^+/CD69^+$ activated NK cells (Figure 17), it is assumable that $CD94^+/CD69^+$ activated NK cells are essential in the control of tumor growth and dispersal of Hsp70-positive tumor cells. Kokowski et al. could likewise demonstrate that among NK cells with further activation markers, $CD94^+$ NK cells were significantly elevated in a stage IIIb NSCLC patient with long-term tumor control who had received a combined therapy with radiochemotherapy, NK cell transfer and PD-1 inhibition [68]. Also Gross et al. have shown that an increased density of CD94/NKG2 and CD56 enables NK cells to kill mHsp70-positive tumor cells [47, 49].

The two major functions of Hsp70 are opponent and associated with the subcellular localization of this protein. Being exposed on the outer membrane, lipid-bound Hsp70 acts as a recognition structure for activated NK cells, whereas intracellular together with membrane-bound Hsp70 can mediate protection from apoptotic cell death and therefore is responsible for enhanced therapy resistance [96]. Tumor cells with an enhanced aggressiveness might be able to circumvent immunological recognition and secrete larger amounts of Hsp70 as a result. Therefore, I conclude that high Hsp70 levels combined with a larger GTV might be accompanied by a functional loss of activated C-type lectin-positive NK cells. A positive correlation between $CD94^+/ CD69^+$ NK cells and serum Hsp70 levels could only be detected in

squamous cell NSCLC, but not in adenocarcinomas of the lung. This corresponds with the fact that adenocarcinomas are considered to have a decreased immunogenicity. Our results further match with previous findings which demonstrate an increase of the cell surface density of the C-type lectin receptor CD94 on NK cells following stimulation with Hsp70-peptide TKD (aa450–463) and low-dose IL-2 [69]. This receptor additionally interacts with non-classical HLA-E molecules [19] and it fulfills either an activating or inhibitory function depending on the NKG2C or NKG2A co-receptor [77]. Hsp70 membrane-positive SCCHN (squamous cell carcinoma of the head and neck) patients, too, exhibited an up-regulation of the CD94 and NKG2D density on NK cells, even 2 years after surgery and radiation therapy.

An augmented expression of the receptor CD69 on NK cells indicates enhanced cytotoxic activity, proliferation, TNF-α production and the induction of further activation markers, such as CD25 and ICAM-1 [16]. The density of both the receptors CD69 and CD94 was only enhanced in the blood of squamous cell carcinoma patients but not of adeno NSCLC patients according to our present research. Equally, a significant correlation of the CD94 expression with serum Hsp70 was only detectable in squamous cell NSCLC patients which is presented in Figure 17. These results reconfirm that patients with squamous carcinoma are more receptive to immunological recognition and expression control of Hsp70.

In general, NSCLC of the adeno-subtype are highly heterogenous depending on their gene expression patterns (Figure 23) which can have an influence on tumor aggressiveness and immune-escape. Because of this, the outcome in overall survival can differ between the different subgroups [37].

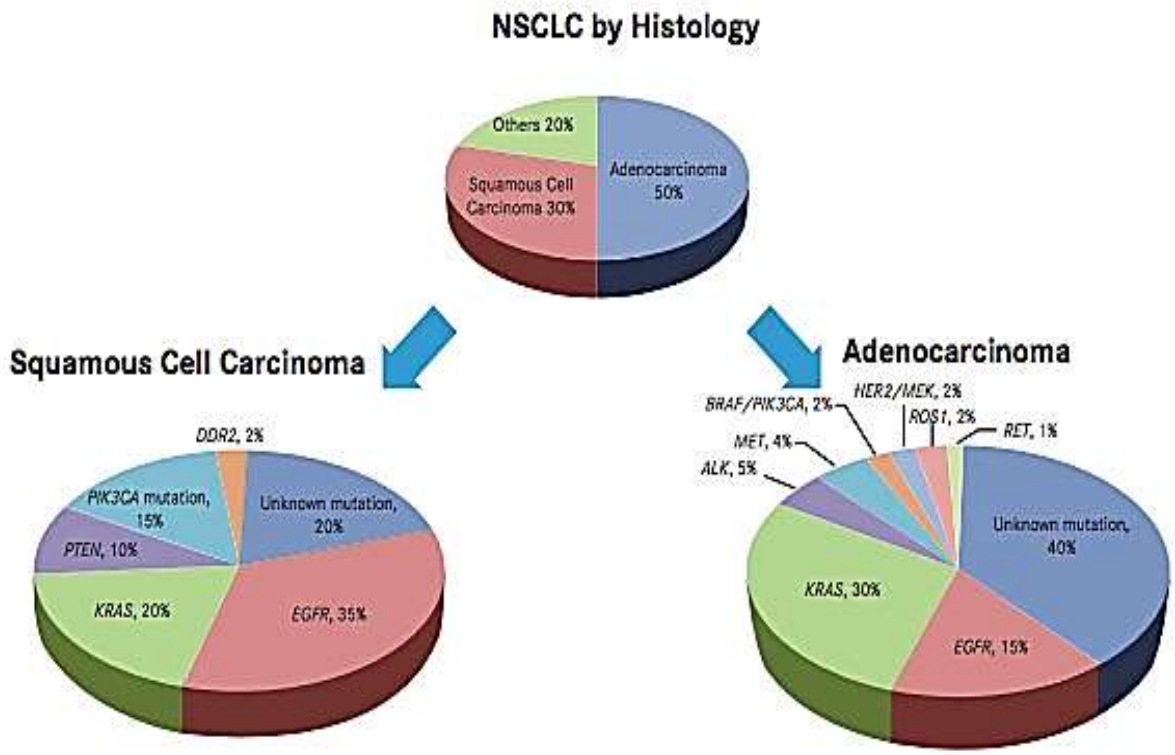

Figure 23: Percentage distribution of NSCLC subtypes and mutation analysis in the squamous cell and adeno carcinoma*; although both subtypes of lung cancer partially show similar mutations, the diversity of mutations in the gene pool of the adenocarcinoma is larger* [150]

A reinforcement of the body´s own defense mechanisms would be an ideal way in the combat against tumor cells. Regarding physiological immune processes, especially NK cells of patients with squamous cell carcinoma not only detect "missing self" on malignant cells [61], but can be stimulated with circulating Hsp70 and recognize membrane Hsp70 on the tumor cell surface [90]. Because of the lower radio-sensitivity of adeno carcinomas, this effect might be a good supplement to increase the success of therapy in this NSCLC subtype.

But tumor detection and combat are not the only functions of NK cells. The interaction and stimulation of the adaptive immune system is equally important. Experimental mouse models demonstrate that the initiation of $CD8^+$ cytotoxic T cell activity is based on IFN-γ which is secreted by NK cells in the elimination of tumor cells [31, 65]. The cytokines IFN-γ and TNF further activate macrophages and dendritic cells which belong to the innate immune system. Vice versa, an 11-year follow-up epidemiologic survey demonstrated that a lack in activated NK cells increases the risk of developing cancer [57]. A reduced immunological activity can be the result of tumor immune escape, for example in the case of tumor cells with a broad range

of genetic mutations, such as certain adeno carcinoma subtypes. In the case of immune escape against tumor cells [35, 51, 120, 137], new therapeutic approaches have to be explored and improved, such as a reactivation of the patient´s immune defense by inhibiting tumor-induced immune checkpoints that circumvent the induction of immune response against tumor cells [4, 27, 55]. This seems especially promising in lung cancer subtypes with high mutational load [4]. Benson et al. demonstrated that different from NK cells of healthy persons, NK cells in multiple myeloma express the immune checkpoint molecule PD-1 which dampens immunological defense by forming a complex with the PD-L1 on malignant cells [11]. A therapy with the anti-PD-1 antibody Pidilizumab could enhance NK cell toxicity towards the tumor. Using immune checkpoint inhibitors, long-term tumor control and an advanced overall survival in lung cancer patients were observed in further studies [4, 68]. Therefore, the combination of PD-1 inhibition with the transfer of ex vivo-stimulated NK cells might synergistically enforce the cytolytic activity of NK cells and is the matter of current research [68, 113].

Finally, our findings imply that among all immune cells, NK cells play a central role in the surveillance and combat against tumor cells. The immunological defense can be re-inforced in the presence of the stress molecule Hsp70 and pro-inflammatory cytokines, such as IL-2. Long-term outcomes in respect of a correlation between immunological phenotypes, the presence of immune cell activation markers and the overall survival of tumor patients are still pending. Future research will also have to deal with the prognostic value of activated cells and their correlation with Hsp70 with a special focus on survival time, and recent studies concerning this matter seemed could achieve promising results [68, 113].

4.4 Relevance of Hsp70 in Therapy Monitoring

In the field of cancer management, tumor biomarkers are also essential to monitor therapy response and tumor progression in order to optimize a patient´s treatment. Especially because of changes in tumor biology and in the sensitivity to a certain therapy, there is an urgent need for biomarkers which can serially give information about the current status of tumor response to R(C)T or other medications. In most cases, drugs that are used for chemo-therapy are toxic

and have a broad range of side effects on healthy cells, clinically leading to nausea, vomiting or hair loss for example. With the help of tumor biomarkers, it is possible to adapt tumor therapy more precise and shorten the toxic therapy cycles to a minimum.

Relating to the tumor biomarker Hsp70, it could be shown that high pre-therapeutic levels of Hsp70 positively correlate with the gross tumor volume and can additionally lead to increased radio-resistance. High intracellular Hsp70 levels imply protection against stress-inducible programmed cell death by hampering apoptotic pathways (123). In contrast, previous findings demonstrated that Hsp70 is a highly immunogenic molecule and stimulates NK cell mediated immune response [39, 48, 69, 116] which is crucial in tumor control. Because of its dual functions and the tumor-specific overexpression of this molecule, I had a look at the dynamics of Hsp70 levels and compared it to the tumor biomarker osteopontin.

4.4.1 Post-Therapeutic Hsp70 Plasma Levels as a Biomarker of Therapy Response

Prior experiments demonstrated that enhanced cytosolic Hsp70 in tumor cells can mediate resistance against RT by compensating RT-induced cell stress [96]. Therefore, I investigated how Hsp70 levels were changed by radiochemotherapy and if the dynamics were coherent with a favorable therapy effect. Therapy response was defined as a complete remission (disappearance of all target lesions) and partial remission (decrease of 30% in the lesion with the largest diameter).

Comparing Hsp70 levels at different time points, there was a drop from pre- to post-therapeutic Hsp70. Responding patients had significantly higher Hsp70 levels than non-responders after therapy. Nevertheless, Hsp70 levels were elevated compared to healthy donors at both time points.

As demonstrated, high pre-therapeutic Hsp70 levels are associated with a higher tumor volume (Figure 14). I attribute these findings to vital tumor cells actively secreting exosomes and therefore contributing to an enhanced circulation of Hsp70 in the blood stream. Radio(chemo)therapy evokes a major change in tumor biology and also in healthy cells with a high mitotic activity. Some chemotherapy drugs have a direct effect on DNA by inserting

artificial molecules or agglutinating the DNA strands for example. Radiotherapy harms cancer cells by exposing them to high energy radiation. This leads to ionization processes that can directly impair cellular components or damage tissue via the formation of free radicals. The aim of radio(chemo)therapy is to provoke a mainly organized cell death by the induction of apoptosis and necrosis. Subsequently, there is a huge depletion and release of cellular danger associated molecular patterns (DAMPs), including Hsp70. The lipHsp70 ELISA detects particularly the membrane bound form of Hsp70 which is integrated in the tumorous cell membrane but cannot be found in the membrane of healthy cells. As higher post-therapeutic levels in patients with therapy response could be observed, I assume that there is a larger tumor cell decay in responders. The release of Hsp70 in the form of impaired tumor cell components might then stimulate immunological activity, comparable to the effects of vaccination.

In some cases, tumor cells withstand therapy even though the gross tumor volume has been reduced. It is still unclear how the exosomal secretion behavior of the remaining tumor cells after radio(chemo)therapy is affected.

As radiotherapy induces cell decay, thereby affecting Hsp70 release decisively and lowering tumor cell activity, I quantified post-therapeutic Hsp70 levels and investigated whether it is possible to predict therapy outcome on the basis of serum Hsp70. A ROC analysis which was created for this purpose turned out to have an AUC of 0.82 ($p = 0.014$) which reflects a high capability of Hsp70 in the prediction of therapy response. Identical analysis with pre-therapeutic Hsp70 plasma levels showed a similar trend, but the results missed statistical significance. Nevertheless, further research on pre- and post-therapeutic Hsp70 with measurements at serial time-points and its correlation with clinical response in larger patient cohorts are necessary to gather more detailed knowledge about the exact dynamics and the prognostic relevance of circulating Hsp70.

4.4.2 Role of Hypoxia in the Context of Tumor Metabolism and its Influence on Hsp70 and OPN Expression

Various factors can have an influence on prognosis and overall survival. Apart from immunological defense, the tumor microenvironment after therapy affects different parameters and thus a patient´s overall survival decisively.

The presence of hypoxic stress for example has a negative influence on prognosis and therapy response to radiotherapy. Schilling et al. demonstrated that an exposition to hypoxic stress decreased the membrane expression of Hsp70 and the major histocompatibility class I chain-related proteins A and B (MICA/B) on H1339 and MDA-MB-231-cells [112]. Since Hsp70 and MICA/B serve as potent ligands for NK cells, hypoxia consequently leads to reduced immunological recognition and NK cell-mediated lysis. Further on, knockdown experiments of the molecule HIF-1α which promotes tumor cell survival and impairs membrane Hsp70 expression indicated that there might additionally be an inhibition of transport to the membrane under hypoxia which is still unknown and protects tumor cells from NK cell-mediated lysis [112].

Usually, hypoxic conditions are a result of a limited oxygen supply in the case of an enlargement of solid tumor tissue which increases interstitial transport distances and lowers hydrostatic pressure gradients between blood vessels and the interstitium [94]. To compensate an adequate delivery of oxygen and nutrients, new microvessels are formed reactively in solid tumor tissue. Nevertheless, the morphology of these adjuvant microvessels differs from the structure of vessels in healthy tissue [125]. The poor quality of the vascular wall can contribute to aggravated transport conditions for oxygen and also for the delivery of antitumor immune therapies via blood circulation.
Consequently, the tumor metabolism is characterized by hypoxia, a shortage of nutrients, elevated lactate levels as well as adenosine and acidosis [94, 125, 127]. Hypoxia further leads to several effects on the tumor that have a negative influence on the prognosis such as genetic instability and heterogeneity, therapy resistance, tumor progression and continuous angiogenesis [83, 126, 130]. Moreover, hypoxic conditions can result in an activation and extension of stromal cell populations which have an immune-suppressive character and therefore interfere with tumor immunotherapy [131].

A shortage in oxygen supply additionally results in an overexpression of OPN which is a physiologically present molecule. Normally, it contributes to the process of bone remodeling [25]. It is remarkable though that tumor patients have shown an overexpression [110] which has turned out to be an indicator of increased tumor aggression. In NSCLC, the height of OPN plasma levels correlated significantly with the hypoxic extent in the microenvironment [71]. Ostheimer et al. detected that high pre-therapeutic OPN levels and rising levels after RT pass into poor survival in NSCLC after radical radiotherapy [99, 101]. The statistical significance of these findings could be improved when combined with the biomarkers VEGF and CAIX [99].
Apart from OPN overexpression, hypoxic stress enforces the secretion of exosomes [63] by tumor cells which carry high amounts of Hsp70. Due to the overexpression of both biomarkers in a hypoxic environment, I compared the prognostic and predictive value of Hsp70 levels with OPN in the patient collectives #1 and #2. In both groups, Hsp70 and OPN showed a significant positive correlation at diagnosis. As previously demonstrated with a larger, more heterogenous NSCLC patient collective [100], high OPN concentrations at T1 were associated with decreased OS on significant levels in non-metastasized NSCLC patients. Although a direct significant correlation between Hsp70 and the overall survival was not detectable, I speculate that the correlation between OPN and Hsp70 might be a hint that in a larger more balanced patient cohort, Hsp70 might likewise be an indicator of overall survival. Finally, the expression of both markers shows great potential for an individual therapy monitoring, but nevertheless represents a highly aggressive tumor phenotype with a worse outcome.

5 CONCLUSION

Hsp70 is a molecule which is overexpressed in the cytosol and gets released into the blood of patients with various tumor types [20, 67, 69]. Different from normal cells, Hsp70 is integrated in the lipid membrane of tumor cells which have the capability to secrete Hsp70-positive exosomes actively [2, 66, 108]. Therefore, the stress protein Hsp70 serves as a biomarker for the detection of tumor metabolism. Apart from malignant processes, it is additionally elevated in diseases with chronic inflammation, such as COPD or liver cirrhosis. However, the serum levels of tumor patients surpass those of patients with inflammatory diseases. Hsp70 will take on greater importance especially in tumor types that lack symptoms or are covered by unspecific symptoms. This is frequently the case in tumors of the lung, of which the NSCLC is the most common type. Our investigations revealed that the gross tumor volume in the NSCLC is positively correlated with Hsp70 levels in the blood circulation. Consequentially, Hsp70 might serve as a biomarker of viable tumor mass and therefore mirrors the overall tumor burden. Changes in tumor volume during radiotherapy in NSCLC patients have potential prognostic and predictive value [36, 59] and might also be reflected by the dynamics of Hsp70 during therapy. Nevertheless, a certain interval of radiotherapy-induced inflammation and cell death must be considered with care in future studies.

As a result of its high immunogenic character, the presence of Hsp70 can affect the prognosis in a beneficial way on the one hand, although its expression is in association with increased aggressiveness on the other hand. Since Hsp70 is known to serve as a target structure of NK cells, the exact lymphocyte compositions in the blood of NSCLC patients with different histological subtype were analyzed. NSCLC patients had decreased lymphocyte counts compared to the healthy control group which is indicative of a suppression in immunological activity. Elevated percentages of $CD69^+/CD94^+$ NK cells were found in squamous cell, but not in adeno NSCLC. This might display a higher immunogenicity of the squamous cell NSCLC compared to the adeno carcinoma which is already known for its vast range of gene expression patterns [150]. As lower Hsp70 levels were associated with a smaller GTV as well as a higher percentage of $CD69^+/CD94^+$ positive NK cells, activated NK cells might be able to control and oppose mHsp70-positive malignant cells especially in squamous cell NSCLC patients.

Nevertheless, if tumor escape mechanisms interfere with NK cell activation, tumor cells cannot be killed. Here, combined therapies with ex vivo activated NK cell transfer and immune checkpoint inhibition have shown to be successful by synergistically enhancing the cytolytic activity of NK cells and prolonging tumor control and overall survival in lung cancer patients [68].

Besides its negative facets, Hsp70 expression can affect prognosis in a beneficial manner by inducing immune response. But since many tumor patients are immunosuppressed, exhibiting reduced counts of lymphocytes for example, radiotherapy is still an important basis of disease control. The requested effect of radiotherapy is the impairment and eradication of tumor cell activity and therefore, radiotherapy is stress for tumor cells and affects the expression and the release of Hsp70. An overexpression of Hsp70 is associated with higher aggressiveness, similarly to osteopontin which also serves as a tumor biomarker and is enhanced in the case of a hypoxic tumor microenvironment, equally to Hsp70. Ostheimer et al. have shown that osteopontin overexpression represents a poor survival [99]. Since both biomarkers are stimulated under similar conditions, I searched for a potential correlation between them. Before therapy at the timepoint T1, I found that high Hsp70 levels were accompanied by higher osteopontin levels. I further examined the dynamics of Hsp70 levels during the run of radiotherapy in NSCLC patients and investigated if they were indicative of therapy response. Generally, the point in time of the determination of Hsp70 levels has to be considered. Pre-therapeutic Hsp70 (T1) is most likely to be an indicator of viable tumor mass as it is released by tumor cells whereas a post-therapeutic overexpression is rather a consequence of cell decay which includes the death of malign cells. Although pre- and post-therapeutic Hsp70 levels were enhanced compared to physiological levels, a drop in Hsp70 4-6 weeks after therapy in both responding and non-responding patients could be observed. A subdivision of the patient group according to their Hsp70 levels demonstrated that patients with higher post-therapeutic Hsp70 expression showed significantly higher response rates than those below the threshold. A ROC curve analysis which was performed to estimate the prognostic function of Hsp70 concerning therapy response revealed a significant predictive function for post-therapeutic Hsp70 levels. The comparison of the two biomarkers Hsp70 and OPN revealed different functions of the two molecules. Whereas elevated OPN levels significantly correlate with decreased OS, reduced lung function and weight loss [99], Hsp70 can be used for the detection of especially asymptomatic tumors and the differentiation from inflammatory

diseases which malign cells can originate from, it reflects the height of the Hsp70 positive tumor burden and post-therapeutic levels predict therapy outcome. The co-detection of both biomarkers in the run of radiotherapy joins prognostic (OPN) and predictive (Hsp70) information for therapy response which can result in a more rapid therapy adaptation to improve clinical outcome of tumor patients. Further research concerning Hsp70 and its correlation with overall survival in larger patient cohorts will have to be performed as present investigations using patient collectives with a limited patient number revealed a trend but failed to be significant. It is still a matter of debate how cytosolic Hsp70 is transported to the plasma membrane, how exactly they are anchored in the plasma membrane and if lipid-bound Hsp70 takes over chaperoning functions for adjacent proteins like receptors residing in lipid rafts.

Due to its high immunogenicity and interaction with NK cells, Hsp70 additionally has a great potential in the development of new therapeutic approaches that deal with tumor immune therapy. The present research including the current targeted NK cell based adaptive immunotherapy for the treatment of NSCLC patients initiated a phase II clinical trial with the aim to prolong overall survival in patients with advanced NSCLC after radiochemotherapy and constitute the basis of future combined immunological therapy approaches.

6 ACKNOWLEDGEMENTS

Diese Dissertation ist das Resultat umfangreicher Forschungsarbeiten und der Bereitschaft, getane Arbeit wieder zu verwerfen und von Neuem zu beginnen. Auf dem langen Weg wurde ich durch sehr viele Menschen begleitet, denen ich hiermit gerne danken würde, auch den namentlich nicht erwähnten.

Ein ganz besonderer Dank gilt Frau Prof. Multhoff. Durch ihr Vertrauen erhielt ich einen prägenden Einblick in die Grundlagenforschung und experimentelle Arbeits- und Denkweisen. Sie war zu jeder Zeit auch in Phasen von Rückschlägen für mich als Mentorin mit sowohl fachlichen Ratschlägen als auch emotionaler Unterstützung präsent. Ihre Zuverlässigkeit, positive Art und Stärke sind außergewöhnlich und waren stets eine große Stütze für mich.

Als unerfahrene Medizinstudentin wurde ich herzlich in der AG Multhoff empfangen, eingearbeitet und zu Forschungsarbeit motiviert. Die Unterstützung durch das Team trug entscheidend dazu bei, dass ich meine experimentelle Forschungsarbeit parallel zum Studium vollenden konnte. Ich möchte mich deshalb herzlich für den respektvollen Umgang und die gute Zusammenarbeit bedanken.

Ein weiterer Dank gilt Herrn Prof. Dr. med. Vordermark und Dr. med. Ostheimer für die gute Kooperation zwischen den Universitätskliniken der TU München und Halle an der Saale. Insbesondere durch die intensive Betreuung durch Dr. Ostheimer und den Datenaustausch zwischen den Arbeitsgruppen konnten unsere Forschungsarbeiten entscheidend ausgeweitet werden.

Danke an meine liebenswerte und willensstarke Mutter, die uns alleine großzog. Ihre Entschlossenheit und ihr Fleiß dienten mir als Vorbild, meinen jetzigen Standpunkt zu erreichen.
Danke an diejenigen, die mich seit vielen Jahren in schwierigen Situationen immer wieder auffingen und mir neue Kraft gaben.

Mein größter Dank gilt den Patienten, die sich in einem sehr belastenden Lebensabschnitt dazu bereit erklärten, an der Studie teilzunehmen. Ich wünsche ihnen viel Stärke, Durchhaltevermögen und möglicherweise auch etwas Hoffnung durch unsere Forschungsarbeiten.

Nicht zuletzt stellt diese Arbeit für mich ein Andenken an meinen lieben Großvater dar, der in jungen Jahren an Lungenkrebs verstarb und den ich deshalb nicht mehr kennenlernen durfte.

7 REFERENCES

7.1 Bibliography

1. Adler V, Schaffer A, Kim J, Dolan L, Ronai Z (1995) UV irradiation and heat shock mediate JNK activation via alternate pathways. J Biol Chem 270:26071–26077

2. Anand PK (2010) Exosomal membrane molecules are potent immune response modulators. Commun Integr Biol 3:405–408. doi: 10.4161/cib.3.5.12474

3. Anborgh PH, Mutrie JC, Tuck AB, Chambers AF (2010) Role of the metastasis-promoting protein osteopontin in the tumour microenvironment. J Cell Mol Med 14:2037–2044. doi: 10.1111/j.1582-4934.2010.01115.x

4. Antonia SJ, Villegas A, Daniel D, Vicente D, Murakami S, Hui R, Kurata T, Chiappori A, Lee KH, de Wit M, Cho BC, Bourhaba M, Quantin X, Tokito T, Mekhail T, Planchard D, Kim Y-C, Karapetis CS, Hiret S, Ostoros G, Kubota K, Gray JE, Paz-Ares L, de Castro Carpeño J, Faivre-Finn C, Reck M, Vansteenkiste J, Spigel DR, Wadsworth C, Melillo G, Taboada M, Dennis PA, Özgüroğlu M (2018) Overall Survival with Durvalumab after Chemoradiotherapy in Stage III NSCLC. New England Journal of Medicine 379:2342–2350. doi: 10.1056/NEJMoa1809697

5. Arastéh K, Baenkler H-W (2009) Duale Reihe Innere Medizin. Georg Thieme Verlag, p 410

6. Arispe N, Doh M, De Maio A (2002) Lipid interaction differentiates the constitutive and stress-induced heat shock proteins Hsc70 and Hsp70. Cell Stress Chaperones 7:330–338

7. Arispe N, Doh M, Simakova O, Kurganov B, De Maio A (2004) Hsc70 and Hsp70 interact with phosphatidylserine on the surface of PC12 cells resulting in a decrease of viability. FASEB J 18:1636–1645. doi: 10.1096/fj.04-2088com

8. Ashizawa N, Graf K, Do YS, Nunohiro T, Giachelli CM, Meehan WP, Tuan TL, Hsueh WA (1996) Osteopontin is produced by rat cardiac fibroblasts and mediates A(II)-induced DNA synthesis and collagen gel contraction. J Clin Invest 98:2218–2227

9. Bauer K, Nitsche U, Slotta-Huspenina J, Drecoll E, von Weyhern CH, Rosenberg R, Höfler H, Langer R (2012) High HSP27 and HSP70 expression levels are independent adverse prognostic factors in primary resected colon cancer. Cell Oncol (Dordr) 35:197–205. doi: 10.1007/s13402-012-0079-3

10. Bayer C, Vaupel P (2012) Acute versus chronic hypoxia in tumors: Controversial data concerning time frames and biological consequences. Strahlenther Onkol 188:616–627. doi: 10.1007/s00066-012-0085-4

11. Benson DM, Bakan CE, Mishra A, Hofmeister CC, Efebera Y, Becknell B, Baiocchi RA, Zhang J, Yu J, Smith MK, Greenfield CN, Porcu P, Devine SM, Rotem-Yehudar R, Lozanski G, Byrd JC, Caligiuri MA (2010) The PD-1/PD-L1 axis modulates the natural killer cell versus multiple myeloma effect: a therapeutic target for CT-011, a novel monoclonal anti–PD-1 antibody. Blood 116:2286–2294. doi: 10.1182/blood-2010-02-271874

12. Biron CA, Nguyen KB, Pien GC, Cousens LP, Salazar-Mather TP (1999) Natural killer cells in antiviral defense: function and regulation by innate cytokines. Annu Rev Immunol 17:189–220. doi: 10.1146/annurev.immunol.17.1.189

13. Blankenstein T, Coulie PG, Gilboa E, Jaffee EM (2012) The determinants of tumour immunogenicity. Nat Rev Cancer 12:307–313. doi: 10.1038/nrc3246

14. Blasberg JD, Pass HI, Goparaju CM, Flores RM, Lee S, Donington JS (2010) Reduction of Elevated Plasma Osteopontin Levels With Resection of Non–Small-Cell Lung Cancer. J Clin Oncol 28:936–941. doi: 10.1200/JCO.2009.25.5711

15. Borrego F, Masilamani M, Marusina AI, Tang X, Coligan JE (2006) The CD94/NKG2 family of receptors: from molecules and cells to clinical relevance. Immunol Res 35:263–278. doi: 10.1385/IR:35:3:263

16. BORREGO F, ROBERTSON MJ, RITZ J, PEÑA J, SOLANA R (1999) CD69 is a stimulatory receptor for natural killer cell and its cytotoxic effect is blocked by CD94 inhibitory receptor. Immunology 97:159–165. doi: 10.1046/j.1365-2567.1999.00738.x

17. Botzler C, Li G, Issels RD, Multhoff G (1998) Definition of extracellular localized epitopes of Hsp70 involved in an NK immune response. Cell Stress Chaperones 3:6–11

18. Brahmer JR, Pardoll DM (2013) Immune checkpoint inhibitors: making immunotherapy a reality for the treatment of lung cancer. Cancer Immunol Res 1:85–91. doi: 10.1158/2326-6066.CIR-13-0078

19. Braud VM, Allan DS, O'Callaghan CA, Söderström K, D'Andrea A, Ogg GS, Lazetic S, Young NT, Bell JI, Phillips JH, Lanier LL, McMichael AJ (1998) HLA-E binds to natural killer cell receptors CD94/NKG2A, B and C. Nature 391:795–799. doi: 10.1038/35869

20. Canöz Ö, Belenli O, Patiroglu TE (2002) General features of gastric carcinomas and comparison of HSP70 and NK cell immunoreactivity with prognostic factors. Pathol Oncol Res 8:262–269. doi: 10.1007/BF03036742

21. Chambers AF, Wilson SM, Kerkvliet N, O'Malley FP, Harris JF, Casson AG (1996) Osteopontin expression in lung cancer. Lung Cancer 15:311–323

22. Chang PL, Prince CW (1991) 1 alpha,25-dihydroxyvitamin D3 stimulates synthesis and secretion of nonphosphorylated osteopontin (secreted phosphoprotein 1) in mouse JB6 epidermal cells. Cancer Res 51:2144–2150

23. Chen Z, Fillmore CM, Hammerman PS, Kim CF, Wong K-K (2014) Non-small-cell lung cancers: a heterogeneous set of diseases. Nat Rev Cancer 14:535–546. doi: 10.1038/nrc3775

24. Cheng T-YD, Cramb SM, Baade PD, Youlden DR, Nwogu C, Reid ME (2016) The International Epidemiology of Lung Cancer: Latest Trends, Disparities, and Tumor Characteristics. J Thorac Oncol 11:1653–1671. doi: 10.1016/j.jtho.2016.05.021

25. Choi ST, Kim JH, Kang E-J, Lee S-W, Park M-C, Park Y-B, Lee S-K (2008) Osteopontin might be involved in bone remodelling rather than in inflammation in ankylosing spondylitis. Rheumatology 47:1775–1779. doi: 10.1093/rheumatology/ken385

26. Colonna M, Moretta A, Vély F, Vivier E (2000) A high-resolution view of NK-cell receptors: structure and function. Immunol Today 21:428–431

27. Cooling LL, Sherbeck J, Mowers JC, Hugan SL (2017) Development of red blood cell autoantibodies following treatment with checkpoint inhibitors: a new class of anti-neoplastic, immunotherapeutic agents associated with immune dysregulation. Immunohematology 33:15–21

28. Coppola D, Szabo M, Boulware D, Muraca P, Alsarraj M, Chambers AF, Yeatman TJ (2004) Correlation of osteopontin protein expression and pathological stage across a wide variety of tumor histologies. Clin Cancer Res 10:184–190

29. Couzin-Frankel J (2013) Cancer Immunotherapy. Science 342:1432–1433. doi: 10.1126/science.342.6165.1432

30. Crawford HC, Matrisian LM, Liaw L (1998) Distinct Roles of Osteopontin in Host Defense Activity and Tumor Survival during Squamous Cell Carcinoma Progression in Vivo. Cancer Res 58:5206–5215

31. Diefenbach A, Jensen ER, Jamieson AM, Raulet DH (2001) Rae1 and H60 ligands of the NKG2D receptor stimulate tumour immunity. Nature 413:165–171. doi: 10.1038/35093109

32. Dranoff G (2004) Cytokines in cancer pathogenesis and cancer therapy. Nature Reviews Cancer 4:11–22. doi: 10.1038/nrc1252

33. Dubois MF, Bensaude O (1993) MAP kinase activation during heat shock in quiescent and exponentially growing mammalian cells. FEBS Lett 324:191–195

34. Dunn GP, Old LJ, Schreiber RD (2004) The Immunobiology of Cancer Immunosurveillance and Immunoediting. Immunity 21:137–148. doi: 10.1016/j.immuni.2004.07.017

35. Folberg R, Rummelt V, Parys-Van Ginderdeuren R, Hwang T, Woolson RF, Pe'er J, Gruman LM (1993) The prognostic value of tumor blood vessel morphology in primary uveal melanoma. Ophthalmology 100:1389–1398

36. Fox J, Ford E, Redmond K, Zhou J, Wong J, Song DY (2009) Quantification of tumor volume changes during radiotherapy for non-small-cell lung cancer. Int J Radiat Oncol Biol Phys 74:341–348. doi: 10.1016/j.ijrobp.2008.07.063

37. Garber ME, Troyanskaya OG, Schluens K, Petersen S, Thaesler Z, Pacyna-Gengelbach M, van de Rijn M, Rosen GD, Perou CM, Whyte RI, Altman RB, Brown PO, Botstein D, Petersen I (2001) Diversity of gene expression in adenocarcinoma of the lung. Proc Natl Acad Sci U S A 98:13784–13789. doi: 10.1073/pnas.241500798

38. Gastpar R, Gehrmann M, Bausero MA, Asea A, Gross C, Schroeder JA, Multhoff G (2005) Heat shock protein 70 surface-positive tumor exosomes stimulate migratory and cytolytic activity of natural killer cells. Cancer Res 65:5238–5247. doi: 10.1158/0008-5472.CAN-04-3804

39. Gastpar R, Gross C, Rossbacher L, Ellwart J, Riegger J, Multhoff G (2004) The cell surface-localized heat shock protein 70 epitope TKD induces migration and cytolytic activity selectively in human NK cells. J Immunol 172:972–980

40. Gehrmann M, Cervello M, Montalto G, Cappello F, Gulino A, Knape C, Specht HM, Multhoff G (2014) Heat shock protein 70 serum levels differ significantly in patients with chronic hepatitis, liver cirrhosis, and hepatocellular carcinoma. Front Immunol 5:307. doi: 10.3389/fimmu.2014.00307

41. Gehrmann M, Liebisch G, Schmitz G, Anderson R, Steinem C, De Maio A, Pockley G, Multhoff G (2008) Tumor-Specific Hsp70 Plasma Membrane Localization Is Enabled by the Glycosphingolipid Gb3. PLoS ONE 3. doi: 10.1371/journal.pone.0001925

42. Gehrmann M, Marienhagen J, Eichholtz-Wirth H, Fritz E, Ellwart J, Jäättelä M, Zilch T, Multhoff G (2005) Dual function of membrane-bound heat shock protein 70 (Hsp70), Bag-4, and Hsp40: protection against radiation-induced effects and target structure for natural killer cells. Cell Death Differ 12:38–51. doi: 10.1038/sj.cdd.4401510

43. Gehrmann M, Schmetzer H, Eissner G, Haferlach T, Hiddemann W, Multhoff G (2003) Membrane-bound heat shock protein 70 (Hsp70) in acute myeloid leukemia: a tumor specific recognition structure for the cytolytic activity of autologous NK cells. Haematologica 88:474–476

44. Gehrmann M, Specht HM, Bayer C, Brandstetter M, Chizzali B, Duma M, Breuninger S, Hube K, Lehnerer S, van Phi V, Sage E, Schmid TE, Sedelmayr M, Schilling D, Sievert W, Stangl S, Multhoff G (2014) Hsp70--a biomarker for tumor detection and monitoring of outcome of radiation therapy in patients with squamous cell carcinoma of the head and neck. Radiat Oncol 9:131. doi: 10.1186/1748-717X-9-131

45. Gettinger SN, Horn L, Gandhi L, Spigel DR, Antonia SJ, Rizvi NA, Powderly JD, Heist RS, Carvajal RD, Jackman DM, Sequist LV, Smith DC, Leming P, Carbone DP, Pinder-Schenck MC, Topalian SL, Hodi FS, Sosman JA, Sznol M, McDermott DF, Pardoll DM, Sankar V, Ahlers CM, Salvati M, Wigginton JM, Hellmann MD, Kollia GD, Gupta AK, Brahmer JR (2015) Overall Survival and Long-Term Safety of Nivolumab (Anti-Programmed Death 1 Antibody, BMS-936558, ONO-4538) in Patients With Previously Treated Advanced Non-Small-Cell Lung Cancer. J Clin Oncol 33:2004–2012. doi: 10.1200/JCO.2014.58.3708

46. Gress DM, Edge SB, Greene FL, Washington MK, Asare EA, Brierley JD, Byrd DR, Compton CC, Jessup JM, Winchester DP, Amin MB, Gershenwald JE (2017) Principles of

Cancer Staging. In: Amin MB, Edge SB, Greene FL, Byrd DR, Brookland RK, Washington MK, Gershenwald JE, Compton CC, Hess KR, Sullivan DC, Jessup JM, Brierley JD, Gaspar LE, Schilsky RL, Balch CM, Winchester DP, Asare EA, Madera M, Gress DM, Meyer LR (eds) AJCC Cancer Staging Manual. Springer International Publishing, Cham, pp 3–30

47. Gross C, Hansch D, Gastpar R, Multhoff G (2003) Interaction of heat shock protein 70 peptide with NK cells involves the NK receptor CD94. Biol Chem 384:267–279. doi: 10.1515/BC.2003.030

48. Gross C, Koelch W, DeMaio A, Arispe N, Multhoff G (2003) Cell surface-bound heat shock protein 70 (Hsp70) mediates perforin-independent apoptosis by specific binding and uptake of granzyme B. J Biol Chem 278:41173–41181. doi: 10.1074/jbc.M302644200

49. Gross C, Schmidt-Wolf IGH, Nagaraj S, Gastpar R, Ellwart J, Kunz-Schughart LA, Multhoff G (2003) Heat shock protein 70-reactivity is associated with increased cell surface density of CD94/CD56 on primary natural killer cells. Cell Stress Chaperones 8:348–360

50. Guo H, Cai CQ, Schroeder RA, Kuo PC (2001) Osteopontin Is a Negative Feedback Regulator of Nitric Oxide Synthesis in Murine Macrophages. The Journal of Immunology 166:1079–1086. doi: 10.4049/jimmunol.166.2.1079

51. Hanahan D, Weinberg RA (2011) Hallmarks of cancer: the next generation. Cell 144:646–674. doi: 10.1016/j.cell.2011.02.013

52. Hantschel M, Pfister K, Jordan A, Scholz R, Andreesen R, Schmitz G, Schmetzer H, Hiddemann W, Multhoff G (2000) Hsp70 plasma membrane expression on primary tumor biopsy material and bone marrow of leukemic patients. Cell Stress Chaperones 5:438–442

53. Hartl FU (1996) Molecular chaperones in cellular protein folding. Nature 381:571–579. doi: 10.1038/381571a0

54. Höckel M, Vaupel P (2001) Biological consequences of tumor hypoxia. Semin Oncol 28:36–41

55. Iafolla MAJ, Juergens RA (2017) Update on Programmed Death-1 and Programmed Death-Ligand 1 Inhibition in the Treatment of Advanced or Metastatic Non-Small Cell Lung Cancer. Front Oncol 7:67. doi: 10.3389/fonc.2017.00067

56. Ikeda T, Shirasawa T, Esaki Y, Yoshiki S, Hirokawa K (1993) Osteopontin mRNA is expressed by smooth muscle-derived foam cells in human atherosclerotic lesions of the aorta. J Clin Invest 92:2814–2820

57. Imai K, Matsuyama S, Miyake S, Suga K, Nakachi K (2000) Natural cytotoxic activity of peripheral-blood lymphocytes and cancer incidence: an 11-year follow-up study of a general population. Lancet 356:1795–1799. doi: 10.1016/S0140-6736(00)03231-1

58. Isa S-I, Kawaguchi T, Teramukai S, Minato K, Ohsaki Y, Shibata K, Yonei T, Hayashibara K, Fukushima M, Kawahara M, Furuse K, Mack PC (2009) Serum osteopontin levels are highly

prognostic for survival in advanced non-small cell lung cancer: results from JMTO LC 0004. J Thorac Oncol 4:1104–1110. doi: 10.1097/JTO.0b013e3181ae2844

59. Jian Z Wang NAM (2010) Sequential magnetic resonance imaging of cervical cancer: the predictive value of absolute tumor volume and regression ratio measured before, during, and after radiation therapy. Cancer 116:5093–101

60. Jiang Y, Li Y, Zhu B (2015) T-cell exhaustion in the tumor microenvironment. Cell Death Dis 6:e1792. doi: 10.1038/cddis.2015.162

61. Johansson MH, Bieberich C, Jay G, Kärre K, Höglund P (1997) Natural Killer Cell Tolerance in Mice with Mosaic Expression of Major Histocompatibility Complex Class I Transgene. J Exp Med 186:353–364

62. Juhasz K, Lipp A-M, Nimmervoll B, Sonnleitner A, Hesse J, Haselgruebler T, Balogi Z (2013) The complex function of hsp70 in metastatic cancer. Cancers (Basel) 6:42–66. doi: 10.3390/cancers6010042

63. Jung KO, Youn H, Lee C-H, Kang KW, Chung J-K (2016) Visualization of exosome-mediated miR-210 transfer from hypoxic tumor cells. Oncotarget 8:9899–9910. doi: 10.18632/oncotarget.14247

64. Kampinga HH, Hageman J, Vos MJ, Kubota H, Tanguay RM, Bruford EA, Cheetham ME, Chen B, Hightower LE (2009) Guidelines for the nomenclature of the human heat shock proteins. Cell Stress Chaperones 14:105–111. doi: 10.1007/s12192-008-0068-7

65. Kelly JM, Darcy PK, Markby JL, Godfrey DI, Takeda K, Yagita H, Smyth MJ (2002) Induction of tumor-specific T cell memory by NK cell-mediated tumor rejection. Nat Immunol 3:83–90. doi: 10.1038/ni746

66. Kharaziha P, Ceder S, Li Q, Panaretakis T (2012) Tumor cell-derived exosomes: a message in a bottle. Biochim Biophys Acta 1826:103–111. doi: 10.1016/j.bbcan.2012.03.006

67. Kluger HM, Chelouche Lev D, Kluger Y, McCarthy MM, Kiriakova G, Camp RL, Rimm DL, Price JE (2005) Using a xenograft model of human breast cancer metastasis to find genes associated with clinically aggressive disease. Cancer Res 65:5578–5587. doi: 10.1158/0008-5472.CAN-05-0108

68. Kokowski K, Stangl S, Seier S, Hildebrandt M, Vaupel P, Multhoff G (2019) Radiochemotherapy combined with NK cell transfer followed by second-line PD-1 inhibition in a patient with NSCLC stage IIIb inducing long-term tumor control: a case study. Strahlenther Onkol 195:352–361. doi: 10.1007/s00066-019-01434-9

69. Krause SW, Gastpar R, Andreesen R, Gross C, Ullrich H, Thonigs G, Pfister K, Multhoff G (2004) Treatment of colon and lung cancer patients with ex vivo heat shock protein 70-peptide-activated, autologous natural killer cells: a clinical phase i trial. Clin Cancer Res 10:3699–3707. doi: 10.1158/1078-0432.CCR-03-0683

70. Lancaster GI, Febbraio MA (2005) Exosome-dependent trafficking of HSP70: a novel secretory pathway for cellular stress proteins. J Biol Chem 280:23349–23355. doi: 10.1074/jbc.M502017200

71. Le Q-T, Chen E, Salim A, Cao H, Kong CS, Whyte R, Donington J, Cannon W, Wakelee H, Tibshirani R, Mitchell JD, Richardson D, O'Byrne KJ, Koong AC, Giaccia AJ (2006) An evaluation of tumor oxygenation and gene expression in patients with early stage non-small cell lung cancers. Clin Cancer Res 12:1507–1514. doi: 10.1158/1078-0432.CCR-05-2049

72. Le Q-T, Kong C, Lavori PW, O'byrne K, Erler JT, Huang X, Chen Y, Cao H, Tibshirani R, Denko N, Giaccia AJ, Koong AC (2007) Expression and prognostic significance of a panel of tissue hypoxia markers in head-and-neck squamous cell carcinomas. Int J Radiat Oncol Biol Phys 69:167–175. doi: 10.1016/j.ijrobp.2007.01.071

73. Lee JS, Hong WK (1992) Prognostic Factors in Lung Cancer. New England Journal of Medicine 327:47–48. doi: 10.1056/NEJM199207023270110

74. Lieberman J (2003) The ABCs of granule-mediated cytotoxicity: new weapons in the arsenal. Nat Rev Immunol 3:361–370. doi: 10.1038/nri1083

75. Lindquist S, Craig EA (1988) The heat-shock proteins. Annu Rev Genet 22:631–677. doi: 10.1146/annurev.ge.22.120188.003215

76. Liu J, He C, Yuan Q, Wang Z, Xing C, Yuan Y (2015) Association between promoter polymorphisms of OPN gene and cancer risk: a meta-analysis. Onco Targets Ther 9:87–97. doi: 10.2147/OTT.S94606

77. López-Botet M, Pérez-Villar JJ, Carretero M, Rodríguez A, Melero I, Bellón T, Llano M, Navarro F (1997) Structure and function of the CD94 C-type lectin receptor complex involved in recognition of HLA class I molecules. Immunol Rev 155:165–174

78. Mambula SS, Calderwood SK (2006) Heat Shock Protein 70 Is Secreted from Tumor Cells by a Nonclassical Pathway Involving Lysosomal Endosomes. The Journal of Immunology 177:7849–7857. doi: 10.4049/jimmunol.177.11.7849

79. Mandal R, Şenbabaoğlu Y, Desrichard A, Havel JJ, Dalin MG, Riaz N, Lee K-W, Ganly I, Hakimi AA, Chan TA, Morris LG (2016) The head and neck cancer immune landscape and its immunotherapeutic implications. JCI Insight 1:e89829. doi: 10.1172/jci.insight.89829

80. Marrinucci D, Bethel K, Luttgen M, Bruce RH, Nieva J, Kuhn P (2009) Circulating tumor cells from well-differentiated lung adenocarcinoma retain cytomorphologic features of primary tumor type. Arch Pathol Lab Med 133:1468–1471. doi: 10.1043/1543-2165-133.9.1468

81. Martín-Fontecha A, Thomsen LL, Brett S, Gerard C, Lipp M, Lanzavecchia A, Sallusto F (2004) Induced recruitment of NK cells to lymph nodes provides IFN-gamma for T(H)1 priming. Nat Immunol 5:1260–1265. doi: 10.1038/ni1138

82. Mathivanan S, Ji H, Simpson RJ (2010) Exosomes: extracellular organelles important in intercellular communication. J Proteomics 73:1907–1920. doi: 10.1016/j.jprot.2010.06.006

83. Mayer A, Vaupel P (2013) Hypoxia, lactate accumulation, and acidosis: siblings or accomplices driving tumor progression and resistance to therapy? Adv Exp Med Biol 789:203–209. doi: 10.1007/978-1-4614-7411-1_28

84. Mirsadraee S, Oswal D, Alizadeh Y, Caulo A, van Beek EJ (2012) The 7th lung cancer TNM classification and staging system: Review of the changes and implications. World J Radiol 4:128–134. doi: 10.4329/wjr.v4.i4.128

85. Mocikat R, Braumüller H, Gumy A, Egeter O, Ziegler H, Reusch U, Bubeck A, Louis J, Mailhammer R, Riethmüller G, Koszinowski U, Röcken M (2003) Natural killer cells activated by MHC class I(low) targets prime dendritic cells to induce protective CD8 T cell responses. Immunity 19:561–569

86. Moon Y, Lee KY, Sung SW, Park JK (2016) Differing histopathology and prognosis in pulmonary adenocarcinoma at central and peripheral locations. J Thorac Dis 8:169–177. doi: 10.3978/j.issn.2072-1439.2016.01.15

87. Morgensztern D, Ng SH, Gao F, Govindan R (2010) Trends in Stage Distribution for Patients with Non-small Cell Lung Cancer: A National Cancer Database Survey. Journal of Thoracic Oncology 5:29–33. doi: 10.1097/JTO.0b013e3181c5920c

88. Morimoto RI (1993) Cells in stress: transcriptional activation of heat shock genes. Science 259:1409–1410

89. Moser C, Schmidbauer C, Gürtler U, Gross C, Gehrmann M, Thonigs G, Pfister K, Multhoff G (2002) Inhibition of tumor growth in mice with severe combined immunodeficiency is mediated by heat shock protein 70 (Hsp70)-peptide-activated, CD94 positive natural killer cells. Cell Stress Chaperones 7:365–373. doi: 10.1379/1466-1268(2002)007<0365:IOTGIM>2.0.CO;2

90. Multhoff G, Botzler C, Jennen L, Schmidt J, Ellwart J, Issels R (1997) Heat shock protein 72 on tumor cells: a recognition structure for natural killer cells. J Immunol 158:4341–4350

91. Multhoff G, Pfister K, Gehrmann M, Hantschel M, Gross C, Hafner M, Hiddemann W (2001) A 14-mer Hsp70 peptide stimulates natural killer (NK) cell activity. Cell Stress Chaperones 6:337–344

92. Multhoff G, Pockley AG, Schmid TE, Schilling D (2015) The role of heat shock protein 70 (Hsp70) in radiation-induced immunomodulation. Cancer Lett 368:179–184. doi: 10.1016/j.canlet.2015.02.013

93. Multhoff G, Pockley AG, Streffer C, Gaipl US (2012) Dual role of heat shock proteins (HSPs) in anti-tumor immunity. Curr Mol Med 12:1174–1182

94. Multhoff G, Vaupel P (2012) Radiation-induced changes in microcirculation and interstitial fluid pressure affecting the delivery of macromolecules and nanotherapeutics to tumors. Front Oncol 2. doi: 10.3389/fonc.2012.00165

95. Muraille E (2016) The Unspecific Side of Acquired Immunity Against Infectious Disease: Causes and Consequences. Front Microbiol 6. doi: 10.3389/fmicb.2015.01525

96. Murakami N, Kühnel A, Schmid TE, Ilicic K, Stangl S, Braun IS, Gehrmann M, Molls M, Itami J, Multhoff G (2015) Role of membrane Hsp70 in radiation sensitivity of tumor cells. Radiat Oncol 10. doi: 10.1186/s13014-015-0461-1

97. Murry CE, Giachelli CM, Schwartz SM, Vracko R (1994) Macrophages express osteopontin during repair of myocardial necrosis. Am J Pathol 145:1450–1462

98. Oberije C, De Ruysscher D, Houben R, van de Heuvel M, Uyterlinde W, Deasy JO, Belderbos J, Dingemans A-MC, Rimner A, Din S, Lambin P (2015) A Validated Prediction Model for Overall Survival From Stage III Non-Small Cell Lung Cancer: Toward Survival Prediction for Individual Patients. Int J Radiat Oncol Biol Phys 92:935–944. doi: 10.1016/j.ijrobp.2015.02.048

99. Ostheimer C, Bache M, Güttler A, Kotzsch M, Vordermark D (2014) A pilot study on potential plasma hypoxia markers in the radiotherapy of non-small cell lung cancer. Osteopontin, carbonic anhydrase IX and vascular endothelial growth factor. Strahlenther Onkol 190:276–282. doi: 10.1007/s00066-013-0484-1

100. Ostheimer C, Bache M, Güttler A, Kotzsch M, Vordermark D (2014) A pilot study on potential plasma hypoxia markers in the radiotherapy of non-small cell lung cancer: Osteopontin, carbonic anhydrase IX and vascular endothelial growth factor. Strahlentherapie und Onkologie 190:276–282. doi: 10.1007/s00066-013-0484-1

101. Ostheimer C, Bache M, Güttler A, Reese T, Vordermark D (2014) Prognostic information of serial plasma osteopontin measurement in radiotherapy of non-small-cell lung cancer. BMC Cancer 14:858. doi: 10.1186/1471-2407-14-858

102. Overgaard J, Eriksen JG, Nordsmark M, Alsner J, Horsman MR, Danish Head and Neck Cancer Study Group (2005) Plasma osteopontin, hypoxia, and response to the hypoxia sensitiser nimorazole in radiotherapy of head and neck cancer: results from the DAHANCA 5 randomised double-blind placebo-controlled trial. Lancet Oncol 6:757–764. doi: 10.1016/S1470-2045(05)70292-8

103. Parkin DM, Bray F, Ferlay J, Pisani P (2001) Estimating the world cancer burden: Globocan 2000. Int J Cancer 94:153–156

104. Pfannschmidt J, Muley T, Hoffmann H, Bülzebruck H, Dienemann H (2006) [Prognosis after complete surgical resection for non-small cell lung cancer based on the staging classification]. Dtsch Med Wochenschr 131:2643–2648. doi: 10.1055/s-2006-956268

105. Pfister K, Radons J, Busch R, Tidball JG, Pfeifer M, Freitag L, Feldmann H-J, Milani V, Issels R, Multhoff G (2007) Patient survival by Hsp70 membrane phenotype: association with different routes of metastasis. Cancer 110:926–935. doi: 10.1002/cncr.22864

106. Prevention (US) C for DC and, Promotion (US) NC for CDP and H, Health (US) O on S and (2010) How Tobacco Smoke Causes Disease: The Biology and Behavioral Basis for Smoking-Attributable Disease. Centers for Disease Control and Prevention (US)

107. Prince CW, Butler WT (1987) 1,25-Dihydroxyvitamin D3 Regulates the Biosynthesis of Osteopontin, a Bone-Derived Cell Attachment Protein, in Clonal Osteoblast-Like Osteosarcoma Cells. Collagen and Related Research 7:305–313. doi: 10.1016/S0174-173X(87)80036-5

108. Record M, Subra C, Silvente-Poirot S, Poirot M (2011) Exosomes as intercellular signalosomes and pharmacological effectors. Biochem Pharmacol 81:1171–1182. doi: 10.1016/j.bcp.2011.02.011

109. Reinholt FP, Hultenby K, Oldberg A, Heinegård D (1990) Osteopontin--a possible anchor of osteoclasts to bone. PNAS 87:4473–4475. doi: 10.1073/pnas.87.12.4473

110. Rittling SR, Chambers AF (2004) Role of osteopontin in tumour progression. Br J Cancer 90:1877–1881. doi: 10.1038/sj.bjc.6601839

111. Rizvi NA, Hellmann MD, Snyder A, Kvistborg P, Makarov V, Havel JJ, Lee W, Yuan J, Wong P, Ho TS, Miller ML, Rekhtman N, Moreira AL, Ibrahim F, Bruggeman C, Gasmi B, Zappasodi R, Maeda Y, Sander C, Garon EB, Merghoub T, Wolchok JD, Schumacher TN, Chan TA (2015) Cancer immunology. Mutational landscape determines sensitivity to PD-1 blockade in non-small cell lung cancer. Science 348:124–128. doi: 10.1126/science.aaa1348

112. Schilling D, Tetzlaff F, Konrad S, Li W, Multhoff G (2015) A hypoxia-induced decrease of either MICA/B or Hsp70 on the membrane of tumor cells mediates immune escape from NK cells. Cell Stress and Chaperones 20:139–147. doi: 10.1007/s12192-014-0532-5

113. Shevtsov M, Pitkin E, Ischenko A, Stangl S, Khachatryan W, Galibin O, Edmond S, Lobinger D, Multhoff G (2019) Ex vivo Hsp70-Activated NK Cells in Combination With PD-1 Inhibition Significantly Increase Overall Survival in Preclinical Models of Glioblastoma and Lung Cancer. Front Immunol 10. doi: 10.3389/fimmu.2019.00454

114. Smolle E, Pichler M (2019) Non-Smoking-Associated Lung Cancer: A Distinct Entity in Terms of Tumor Biology, Patient Characteristics and Impact of Hereditary Cancer Predisposition. Cancers (Basel) 11. doi: 10.3390/cancers11020204

115. Soti C, Pál C, Papp B, Csermely P (2005) Molecular chaperones as regulatory elements of cellular networks. Curr Opin Cell Biol 17:210–215. doi: 10.1016/j.ceb.2005.02.012

116. Specht HM, Ahrens N, Blankenstein C, Duell T, Fietkau R, Gaipl US, Günther C, Gunther S, Habl G, Hautmann H, Hautmann M, Huber RM, Molls M, Offner R, Rödel C, Rödel F, Schütz M, Combs SE, Multhoff G (2015) Heat Shock Protein 70 (Hsp70) Peptide Activated Natural Killer (NK) Cells for the Treatment of Patients with Non-Small Cell Lung Cancer (NSCLC) after Radiochemotherapy (RCTx) – From Preclinical Studies to a Clinical Phase II Trial. Front Immunol 6. doi: 10.3389/fimmu.2015.00162

117. Spyratos D, Zarogoulidis P, Porpodis K, Tsakiridis K, Machairiotis N, Katsikogiannis N, Kougioumtzi I, Dryllis G, Kallianos A, Rapti A, Li C, Zarogoulidis K (2013) Occupational

exposure and lung cancer. J Thorac Dis 5:S440–S445. doi: 10.3978/j.issn.2072-1439.2013.07.09

118. Stangl S, Gehrmann M, Riegger J, Kuhs K, Riederer I, Sievert W, Hube K, Mocikat R, Dressel R, Kremmer E, Pockley AG, Friedrich L, Vigh L, Skerra A, Multhoff G (2011) Targeting membrane heat-shock protein 70 (Hsp70) on tumors by cmHsp70.1 antibody. Proc Natl Acad Sci USA 108:733–738. doi: 10.1073/pnas.1016065108

119. Subramanian J, Govindan R (2007) Lung Cancer in Never Smokers: A Review. JCO 25:561–570. doi: 10.1200/JCO.2006.06.8015

120. Sun B, Zhang S, Zhao X, Zhang W, Hao X (2004) Vasculogenic mimicry is associated with poor survival in patients with mesothelial sarcomas and alveolar rhabdomyosarcomas. Int J Oncol 25:1609–1614

121. Talhout R, Schulz T, Florek E, van Benthem J, Wester P, Opperhuizen A (2011) Hazardous Compounds in Tobacco Smoke. Int J Environ Res Public Health 8:613–628. doi: 10.3390/ijerph8020613

122. Taube JM, Klein A, Brahmer JR, Xu H, Pan X, Kim JH, Chen L, Pardoll DM, Topalian SL, Anders RA (2014) Association of PD-1, PD-1 ligands, and other features of the tumor immune microenvironment with response to anti-PD-1 therapy. Clin Cancer Res 20:5064–5074. doi: 10.1158/1078-0432.CCR-13-3271

123. Topalian SL, Hodi FS, Brahmer JR, Gettinger SN, Smith DC, McDermott DF, Powderly JD, Carvajal RD, Sosman JA, Atkins MB, Leming PD, Spigel DR, Antonia SJ, Horn L, Drake CG, Pardoll DM, Chen L, Sharfman WH, Anders RA, Taube JM, McMiller TL, Xu H, Korman AJ, Jure-Kunkel M, Agrawal S, McDonald D, Kollia GD, Gupta A, Wigginton JM, Sznol M (2012) Safety, activity, and immune correlates of anti-PD-1 antibody in cancer. N Engl J Med 366:2443–2454. doi: 10.1056/NEJMoa1200690

124. Uaesoontrachoon K, Yoo H-J, Tudor EM, Pike RN, Mackie EJ, Pagel CN (2008) Osteopontin and skeletal muscle myoblasts: Association with muscle regeneration and regulation of myoblast function in vitro. The International Journal of Biochemistry & Cell Biology 40:2303–2314. doi: 10.1016/j.biocel.2008.03.020

125. Vaupel P (2004) Tumor microenvironmental physiology and its implications for radiation oncology. Semin Radiat Oncol 14:198–206. doi: 10.1016/j.semradonc.2004.04.008

126. Vaupel P (2008) Hypoxia and aggressive tumor phenotype: implications for therapy and prognosis. Oncologist 13 Suppl 3:21–26. doi: 10.1634/theoncologist.13-S3-21

127. Vaupel P, Kallinowski F, Okunieff P (1989) Blood flow, oxygen and nutrient supply, and metabolic microenvironment of human tumors: a review. Cancer Res 49:6449–6465

128. Vaupel P, Kelleher DK, Höckel M (2001) Oxygen status of malignant tumors: pathogenesis of hypoxia and significance for tumor therapy. Semin Oncol 28:29–35

129. Vaupel P, Mayer A (2007) Hypoxia in cancer: significance and impact on clinical outcome. Cancer Metastasis Rev 26:225–239. doi: 10.1007/s10555-007-9055-1

130. Vaupel P, Mayer A, Höckel M (2004) Tumor hypoxia and malignant progression. Meth Enzymol 381:335–354. doi: 10.1016/S0076-6879(04)81023-1

131. Vaupel P, Multhoff G (2017) Accomplices of the Hypoxic Tumor Microenvironment Compromising Antitumor Immunity: Adenosine, Lactate, Acidosis, Vascular Endothelial Growth Factor, Potassium Ions, and Phosphatidylserine. Front Immunol 8. doi: 10.3389/fimmu.2017.01887

132. Vega VL, Rodríguez-Silva M, Frey T, Gehrmann M, Diaz JC, Steinem C, Multhoff G, Arispe N, De Maio A (2008) Hsp70 translocates into the plasma membrane after stress and is released into the extracellular environment in a membrane-associated form that activates macrophages. J Immunol 180:4299–4307

133. Vivier E, Raulet DH, Moretta A, Caligiuri MA, Zitvogel L, Lanier LL, Yokoyama WM, Ugolini S (2011) Innate or Adaptive Immunity? The Example of Natural Killer Cells. Science 331:44–49. doi: 10.1126/science.1198687

134. Voskoboinik I, Smyth MJ, Trapani JA (2006) Perforin-mediated target-cell death and immune homeostasis. Nat Rev Immunol 6:940–952. doi: 10.1038/nri1983

135. Wang KX, Denhardt DT (2008) Osteopontin: role in immune regulation and stress responses. Cytokine Growth Factor Rev 19:333–345. doi: 10.1016/j.cytogfr.2008.08.001

136. Wells AD, Malkovsky M, Wells AD, Malkovsky M (2000) Heat shock proteins, tumor immunogenicity and antigen presentation: an integrated view. Immunology Today 21:129–132. doi: 10.1016/S0167-5699(99)01558-3

137. Williamson SC, Metcalf RL, Trapani F, Mohan S, Antonello J, Abbott B, Leong HS, Chester CPE, Simms N, Polanski R, Nonaka D, Priest L, Fusi A, Carlsson F, Carlsson A, Hendrix MJC, Seftor REB, Seftor EA, Rothwell DG, Hughes A, Hicks J, Miller C, Kuhn P, Brady G, Simpson KL, Blackhall FH, Dive C (2016) Vasculogenic mimicry in small cell lung cancer. Nature Communications 7:13322. doi: 10.1038/ncomms13322

138. Zamai L, Ponti C, Mirandola P, Gobbi G, Papa S, Galeotti L, Cocco L, Vitale M (2007) NK cells and cancer. J Immunol 178:4011–4016

139. Zimmermann M, Nickl S, Lambers C, Hacker S, Mitterbauer A, Hoetzenecker K, Rozsas A, Ostoros G, Laszlo V, Hofbauer H, Renyi-Vamos F, Klepetko W, Dome B, Ankersmit HJ (2012) Discrimination of clinical stages in non-small cell lung cancer patients by serum HSP27 and HSP70: a multi-institutional case-control study. Clin Chim Acta 413:1115–1120. doi: 10.1016/j.cca.2012.03.008

140. (2016) 17.3: Cellular Defenses. In: Biology LibreTexts. https://bio.libretexts.org/TextMaps/Microbiology/Book%3A_Microbiology_(OpenStax)/17%3A_Innate_Nonspecific_Host_Defenses/17.3%3A_Cellular_Defenses. Accessed 9 Sep 2018

141. Worldwide cancer statistics | Cancer Research UK. http://www.cancerresearchuk.org/health-professional/cancer-statistics/worldwide-cancer#heading-Zero. Accessed 2 Aug 2015

142. Lung Cancer Signs & Symptoms | Common Symptoms of Lung Cancer. https://www.cancer.org/cancer/lung-cancer/detection-diagnosis-staging/signs-symptoms.html. Accessed 18 Feb 2020

143. What Is Non-Small Cell Lung Cancer? https://www.cancer.org/cancer/non-small-cell-lung-cancer/about/what-is-non-small-cell-lung-cancer.html. Accessed 30 Nov 2017

144. WHO | Cancer. In: WHO. http://www.who.int/mediacentre/factsheets/fs297/en/. Accessed 16 Sep 2015

145. Key Statistics for Lung Cancer. https://www.cancer.org/cancer/non-small-cell-lung-cancer/about/key-statistics.html. Accessed 14 Jan 2018

146. Krebs - Lungenkrebs. https://www.krebsdaten.de/Krebs/DE/Content/Krebsarten/Lungenkrebs/lungenkrebs_node.html. Accessed 31 Jan 2018

147. Lung Cancer 101 | Lungcancer.org. https://www.lungcancer.org/find_information/publications/163-lung_cancer_101/273-risks. Accessed 30 Nov 2017

148. Health Risks of Secondhand Smoke. https://www.cancer.org/cancer/cancer-causes/tobacco-and-cancer/secondhand-smoke.html. Accessed 7 Feb 2018

149. Lung Carcinoma - Pulmonary Disorders. In: Merck Manuals Professional Edition. http://www.merckmanuals.com/professional/pulmonary-disorders/tumors-of-the-lungs/lung-carcinoma. Accessed 17 Sep 2015

150. Evolving Paradigms in Squamous NSCLC: Introduction. In: Targeted Oncology. http://www.targetedonc.com/publications/evolving-paradigms/2015/squamous-nsclc/evolving-paradigms-in-squamous-nsclc-introduction. Accessed 15 Feb 2018

151. Stage 3 | Lung cancer | Cancer Research UK. http://www.cancerresearchuk.org/about-cancer/lung-cancer/stages-types-grades/stage-3. Accessed 11 Feb 2018

152. Quantitative Analysis of Liposomal Heat Shock Protein 70 (Hsp70) in the Blood of Tumor Patients Using a Novel LipHsp70 ELISA | Open Access | OMICS Publishing Group. http://www.omicsonline.org/open-access/quantitative-analysis-of-liposomal-heat-shock-protein-hsp-in-the-blood-of-tumor-patients-2155-9899-5-264.php?aid=38483. Accessed 2 Aug 2015

7.2 Register of Illustrations

7.3 Register of Tables

Hautmann H, Hautmann M, Huber RM, Molls M, Offner R, Rödel C, Rödel F, Schütz M, Combs SE, Multhoff G [Inclusion/exclusion criteria of the phase II clinical trial], 2015 *Front Immunol*, 6: doi:10.3389/fimmu.2015.00162

8 APPENDIX

8.1 Publications with first Authorship

frontiers in Immunology

ORIGINAL RESEARCH
published: 02 November 2015
doi: 10.3389/fimmu.2015.00556

Correlation of Hsp70 serum levels with gross tumor volume and composition of lymphocyte subpopulations in patients with squamous cell and adeno non-small cell lung cancer

*Sophie Gunther[1†], Christian Ostheimer[2†], Stefan Stangl[1], Hanno M. Specht[1], Petra Mozes[1], Moritz Jesinghaus[3], Dirk Vordermark[2], Stephanie E. Combs[1,4,5], Friedhelm Peltz[6], Max P. Jung[1] and Gabriele Multhoff[1,4,5]**

[1] Department of Radiation Oncology, Klinikum rechts der Isar, Technische Universität München (TUM), München, Germany, [2] Department of Radiation Oncology, Martin Luther University Halle-Wittenberg, Halle (Saale), Germany, [3] Department of Pathology, Klinikum rechts der Isar, Technische Universität München (TUM), München, Germany, [4] Department of Innovative Radiotherapy (iRT), Helmholtz Zentrum München, Oberschleißheim, Germany, [5] Department of Radiation Sciences (DRS), Helmholtz Zentrum München, Oberschleißheim, Germany, [6] Pulmonary Division, 1 Medizinische Klinik, Klinikum rechts der Isar, Technische Universität München (TUM), München, Germany

OPEN ACCESS

Edited by:
Francisco Borrego,
Cruces University Hospital, Spain

Reviewed by:
Catharina C. Gross,
University Hospital Münster, Germany
Franz Rödel,
Johann Wolfgang Goethe-University Frankfurt am Main, Germany

***Correspondence:**
Gabriele Multhoff
gabriele.multhoff@tum.de

[†]Sophie Gunther and Christian Ostheimer have contributed equally to this work.

Specialty section:
This article was submitted to NK Cell Biology, a section of the journal Frontiers in Immunology

Received: 15 September 2015
Accepted: 17 October 2015
Published: 02 November 2015

Citation:
Gunther S, Ostheimer C, Stangl S, Specht HM, Mozes P, Jesinghaus M, Vordermark D, Combs SE, Peltz F, Jung MP and Multhoff G (2015) Correlation of Hsp70 serum levels with gross tumor volume and composition of lymphocyte subpopulations in patients with squamous cell and adeno non-small cell lung cancer. Front. Immunol. 6:556. doi: 10.3389/fimmu.2015.00556

Heat-shock protein 70 (Hsp70) is frequently found on the plasma membrane of a large number of malignant tumors including non-small cell lung cancer (NSCLC) and gets released into the blood circulation in lipid vesicles. On the one hand, a membrane (m) Hsp70-positive phenotype correlates with a high aggressiveness of the tumor; on the other hand, mHsp70 serves as a target for natural killer (NK) cells that had been pre-stimulated with Hsp70-peptide TKD plus low-dose interleukin-2 (TKD/IL-2). Following activation, NK cells show an up-regulated expression of activatory C-type lectin receptors, such as CD94/NKG2C, NKG2D, and natural cytotoxicity receptors (NCRs; NKp44, NKp46, and NKp30) and thereby gain the capacity to kill mHsp70-positive tumor cells. With respect to these results, the efficacy of *ex vivo* TKD/IL-2 stimulated, autologous NK cells is currently tested in a proof-of-concept phase II clinical trial in patients with squamous cell NSCLC after radiochemotherapy (RCT) at the TUM. Inclusion criteria are histological proven, non-resectable NSCLC in stage IIIA/IIIB, clinical responses to RCT and a mHsp70-positive tumor phenotype. The mHsp70 status is determined in the serum of patients using the lipHsp70 ELISA test, which enables the quantification of liposomal and free Hsp70. Squamous cell and adeno NSCLC patients had significantly higher serum Hsp70 levels than healthy controls. A significant correlation of serum Hsp70 levels with the gross tumor volume was shown for adeno and squamous cell NSCLC. However, significantly elevated ratios of activated $CD69^+/CD94^+$ NK cells that are associated with low serum Hsp70 levels were observed only in patients with squamous cell lung cancer. These data might provide a first hint that squamous cell NSCLC is more immunogenic than adeno NSCLC.

Keywords: biomarker, tumor markers, biological, heat-shock protein 70, NSCLC, gross tumor volume, lymphocytes, immune responses

INTRODUCTION

According to recent statistics, lung cancer is still among the most frequent causes of cancer-related deaths and the second most common cancer in both men and women in Western societies (1). The numbers of new cases are further increasing especially in Asia and Africa (2). According to the GLOBOCAN report 2000 (3), the incidence of lung cancer worldwide is 1,238,900 with a mortality of 1,103,100 and a 5-year prevalence of 1,394,400. One reason for this high mortality is that patients with lung cancer are frequently diagnosed in advanced tumor stages since the symptoms, such as dyspnea, coughing, or chest pain, are quite unspecific for a long period of time (4). Even after radical surgery, chemo-, and/or radiotherapy using up-to-date therapeutic approaches could not improve the outcome of locally advanced tumor stages. The progression-free and overall survival of non-small cell lung cancer (NSCLC) patients in stage IIIA and IIB is often <16 months (5). Therefore, there is a high medical need to explore new treatment modalities to increase life expectancy and to develop minimal invasive methods for an earlier detection of NSCLC.

In 2013, immunotherapy was elected as the "breakthrough of the year" for the treatment of cancer by the journal "Science" (6). The basis for this was the increase in knowledge in the detection of tumor-specific traits that have the potential to serve as tumor-specific targets for immunotherapeutic approaches. Along this line, our laboratory investigated the potential of the major stress-inducible heat-shock protein 70 (Hsp70, HSPA1A) as a tumor-specific target. Hsp70 is frequently overexpressed in many different tumor types like hematological malignancies, breast, prostate, colon, brain, and lung cancer (7, 8). Hsp70 assists protein folding, prevents protein aggregation and apoptotic cell death under physiological conditions and following stress (9, 10). Tumor cells compared to normal cells not only express significantly higher levels of Hsp70 in the cytosol (7, 8), but also exhibit an unusual plasma membrane localization of Hsp70 (11). Therefore, mHsp70 has the potential as a tumor-specific target for immunological approaches. Additionally, we have shown recently that mHsp70 positive tumor cells actively secrete Hsp70 in lipid vesicles, most likely exosomes, that mirror the membrane orientation of the cell from which they are derived (12). Based on these findings, liposomal Hsp70 which is found in the peripheral blood circulation can reflect the mHsp70 status of the tumor. We have established the lipHsp70 ELISA (13), which enables the detection of Hsp70 in the serum and plasma of patients. The use of the monoclonal antibody (mAb) cmHsp70.1 (14, 15) in this ELISA allows a quantitative determination of free and liposomal Hsp70 in the blood, whereas other commercially available Hsp70 ELISA tests only detect free Hsp70.

A mHsp70-positive tumor phenotype exerts dual functions, on the one hand, a high mHsp70 density is associated with a high aggressiveness of the tumor (16) and the potential of metastatic spread; on the other hand, mHsp70 on tumor cells serves as a target for activated natural killer (NK) cells, which have been incubated either with Hsp70 protein or TKD a 14mer peptide derived from Hsp70 in combination with low-dose IL-2 (TKD/IL-2) (12, 17, 18). Following activation, these NK cells regain the capacity to kill mHsp70-positive tumor cells *in vitro* (19) and *in vivo* (15, 20) via granzyme B-mediated apoptosis (21).

For a better understanding of this duality of mHsp70, we addressed the question whether serum Hsp70 levels are associated with clinical parameters, such as gross tumor volume (GTV) at diagnosis and after radiochemotherapy (RCT), and whether serum Hsp70 levels can have impact on the immune phenotype of squamous cell and adeno NSCLC (18).

MATERIALS AND METHODS

Patient Material

Blood samples of healthy human donors and NSCLC patients of the Klinikum rechts der Isar, TUM (patient collective #1; **Table 1**) and the Martin Luther University Hospital Halle-Wittenberg (patient collective #2, **Table 2**) were collected between 2008 and 2015. In patient collective #1, blood was taken from patients with squamous cell ($n = 25$) and adenocarcinoma ($n = 18$) of the lung at diagnosis and directly after RCT ($n = 6$), and from age- and gender-matched healthy human volunteers ($n = 126$) as a control group. Tumor biopsies were obtained from nine NSCLC patients, six in stage IV, and three in stage 3 (patient collective #1). The

TABLE 1 | Patient collective #1.

		Number
Gender	Female	11
	Male	32
Histology	Squamous cell	25
	Adeno	18
UICC stage	Ia	1
	Ib	1
	IIa	0
	IIb	0
	IIIa	13
	IIIb	13
	IV	15

Clinico-pathological characteristics of 43 NSCLC patients treated at the Klinikum rechts der Isar, TU München, Munich, Germany.

TABLE 2 | Patient collective #2.

		Number
Gender	Female	8
	Male	47
Histology	Squamous cell	28
	Adeno	24
	Large cell	1
	Other	1
	No histology	1
UICC stage	Ia	1
	Ib	0
	IIa	2
	IIb	0
	IIIa	18
	IIIb	34
	IV	0

Clinico-pathological characteristics of 55 NSCLC patients treated at the Martin-Luther University Hospital, Halle-Wittenberg.

median age of all patients of patient collective #1 was 64 years and ranged from 23 to 95 years. In a screening study, NSCLC patients are stratified for their tumor stage and Hsp70 phenotype to enter a phase II clinical trial at the TUM, which is entitled "Targeted NK cell based adoptive immunotherapy for the treatment of patients with NSCLC after radiochemotherapy (RCT)" (18). In patient collective #2, blood was taken from 55 patients (median age 63 years, range 47–86 years) with advanced stage, inoperable NSCLC with an indication for primary RCT. These patients were recruited into a pilot study entitled "Potential plasma hypoxia markers in the radiotherapy of non-small cell lung cancer" (22). Characteristics of both patient collectives are summarized in **Tables 1** and **2**. Briefly, blood was collected in two EDTA KE/9 ml tubes and one Serum Z/9 ml separator tube (S-Monovette, Sarstedt, Nümbrecht, Germany). For the serum, blood was allowed to clot for 15 min at room temperature. After collecting 1.4 ml of EDTA blood for flow cytometry, plasma and serum were obtained by centrifugation at 750 *g* for 10 min. Aliquots of 100–300 µl were stored at −80°C for further analysis. The studies were approved by the local Ethics Committee of the Medical Faculties of both Universities (TUM, Halle-Wittenberg) and written informed consent was obtained from all patients before entering the trial. All procedures were performed in accordance to the Declaration of Helsinki, 1975, as revised in 2008. Clinical stage was determined according to the UICC TNM classification, seventh edition.

Radiochemotherapy and Volumetric Parameters

Three-dimensional conformal RT (3D-RT) was given normofractionated (5 fractions/week) with curative intent (66 Gy total dose, 2 Gy single dose; Siemens Primus, Germany). Chemotherapy consisted of cisplatin (20 mg/m^2 body surface on days 1–5) and vinorelbine (25 mg/m^2 body surface on day 1) in treatment week 1 and 5 (2 courses). RT was CT based (Siemens Lightspeed RT, Germany) and all patients received a PET-scan (Philips Accel, USA) before RT. CT and PET images were merged and GTV was defined as the primary tumor and involved nodes (pathologic confirmed, highly suspicious by CT and PET). GTV was delineated by an experienced radiation oncologist at planning CT before RT and all image data were registered in the Oncentra Masterplan external beam planning software (Nucletron, USA) used for RT plan calculation.

Detection of Hsp70 in Serum/Plasma Using the lipHsp70 ELISA

The Hsp70 content in the blood of NSCLC patients and healthy donors was determined using the lipHsp70 ELISA, which is equally suitable for serum and plasma samples (13). Using the monoclonal cmHsp70.1 antibody as a detection reagent (15), it is possible to detect both, soluble-free and lipid-bound Hsp70 in the serum/plasma of patients and healthy human individuals. This ELISA allows a quantitative analysis of the total amount of Hsp70 in the circulation blood (13). Briefly, 96-well MaxiSorp Nunc-Immuno plates (Thermo, Rochester, NY, USA) were coated overnight with 2 µg/ml rabbit polyclonal antibody (Davids, Biotechnologie, Regensburg, Germany), directed against human Hsp70 in sodium carbonate buffer (0.1 M sodium carbonate, 0.1 M sodium hydrogen carbonate, pH 9.6). After washing three times with phosphate-buffered saline (PBS, Life Technologies, Carlsbad, CA, USA) with 0.05% Tween-20 (Calbiochem, Merck, Darmstadt, Germany), wells were blocked with 2% milk powder (Carl Roth, Karlsruhe, Germany) in PBS for 1.5 h at 27°C. Following another washing step, serum samples diluted 1:5 in CrossDown Buffer (AppliChem, Chicago, IL, USA) were added to the wells for 2 h at 27°C. Then, the wells were washed again and incubated with 4 µg/ml of the biotinylated mouse mAb cmHsp70.1 (multimmune, Munich, Germany) in 2% milk powder in PBS for 2 h at 27°C. Finally, after another washing step, 0.2 µg/ml horseradish peroxidase-conjugated streptavidin (Pierce, Thermo, Rockford, IL, USA) in 1% bovine serum albumin (Sigma-Aldrich, St. Louis, MO, USA) was added for 1 h at 27°C. Binding was quantified by adding substrate reagent (R&D Systems, Minneapolis, MN, USA) for 30 min at 27°C and absorbance was read at 450 nm, corrected by absorbance at 570 nm, in a Microplate Reader (BioTek, Winooski, VT, USA). An eight-point standard curve was determined for each ELISA test using 0–50 ng/ml recombinant Hsp70 diluted in CrossDown Buffer. Each sample was measured in triplicates.

Immunohistochemical Staining

Immunohistochemical staining was performed on formalin-fixed and paraffin-embedded specimen of lung tumors ($n = 9$). Sections were cut, dewaxed and hydrated, heated for 30 min in a microwave oven in 600 ml DAKO retrieval buffer, then washed for 5 min in H_2O. After washing twice with T-PBS buffer, specimens were blocked for 1 h in 10% rabbit serum in PBS containing 1% BSA. Immunohistochemistry was done with streptavidine–biotin complex (StreptABC) using mouse mAb cmHsp70.1 (multimmune, Munich Germany) at a dilution of 1:200 overnight 2 h at 4°C.

Analysis of the Lymphocyte Subpopulations with Flow Cytometry

In order to determine the proportion of different lymphocyte subpopulations, flow cytometric (FACS) analysis was performed using freshly collected EDTA blood (1.4 ml). Therefore, blood (100 µl) was transferred into 14 test tubes and then fluorescently labeled antibodies were added. The antibody combinations that were used for the FACS analysis are summarized in **Table 3**. After an incubation time of 15 min in the dark, the tubes were centrifuged for 5 min at 500 *g* at room temperature after adding 2 ml of PBS/10% FCS washing buffer. In order to eliminate erythrocytes, cells were incubated with lysing buffer (1:9 dilution of BD Lysing Solution Cat. 3490202 with millipore H_2O) for 10 min at the room temperature in the dark. The respective percentages of B, T, and NK cell subpopulations are defined as the proportion of cells within the lymphocyte gate R1 (see **Figure 3**). For the determination of regulatory T cells, buffer A (1:10 dilution of component A with H_2O) was added to the respective tubes. After two washing steps, cells were permeabilized with buffer C (1:50 dilution of buffer A with component B) for 30 min in the dark. Following another two washing steps, a PE-conjugated antibody

TABLE 3 | Panel of antibodies and 14 antibody combinations used in the study.

Specificity	Antibody	Clone	Company	Cat No.	Volume
Ctrl	IgG1-FITC	X40	BD	345815	5
	IgG1-PE	X40	BD	345816	5
	IgG1-PerCP	X40	BD	345817	5
	IgG1-APC	X40	Caltag/Invitrogen	MG 105	1
T/NK	CD94-FITC	HP-3D9	BD	555888	5
	CD56-PE	NCAM16.2	BD	345811	5
	CD3-PerCP	SK7	BD	345766	10
	CD45-APC	HI30	Caltag/Invitrogen	MHCD 4505	1
B/T/NK	CD56-FITC	NCAM16.2	BD	345811	5
	CD19-PE	HIB19	BD	555413	20
	CD3-PerCP	SK7	BD	345766	10
	CD45-APC	HI30	Caltag/Invitrogen	MHCD 4505	1
T/NK	CD56-FITC	NCAM16.2	BD	345811	5
	CD16-PE	3G8	BD	555407	10
	CD3-PerCP	SK7	BD	345766	10
	CD45-APC	HI30	Caltag/Invitrogen	MHCD 4505	1
T/NK	CD56-FITC	NCAM16.2	BD	555518	5
	NKG2D-PE	149810	R&D	FAB139P	10
	CD3-PerCP	SK7	BD	345766	10
	CD69-APC	L78	BD	340560	5
T/NK	CD56-FITC	NCAM16.2	BD	345811	5
	NKp30-PE	IM3709	BC	PN 3709	10
	CD3-PerCP	SK7	BD	345766	10
	CD69-APC	L78	BD	340560	5
T/NK	CD56-FITC	NCAM16.2	BD	345811	5
	NKp46-PE	IM3711	BC	PN 3711	10
	CD3-PerCP	SK7	BD	345766	10
	CD69-APC	L78	BD	340560	5
T/NK	CD94-FITC	HP-3D9	BD	555888	5
	NKG2D-PE	149810	R&D	FAB139P	10
	CD3-PerCP	SK7	BD	345766	10
	CD56-APC	B159	BD	555518	10
T/NK	CD94-FITC	HP-3D9	BD	555888	5
	NKp30-PE	IM3709	BC	PN 3709	10
	CD3-PerCP	SK7	BD	345766	10
	CD56-APC	B159	BD	555518	10
T/NK	CD94-FITC	HP-3D9	BD	555888	5
	NKp46-PE	IM3711	BC	PN 3711	10
	CD3-PerCP	SK7	BD	345766	10
	CD56-APC	B159	BD	555518	10
CD4/CD8 T	CD4-FITC	RPA-T4	BD	555346	20
	CD8-PE	RPA-T8	BD	555366	20
	CD3-PerCP	SK7	BD	345766	10
	CD45-APC	HI30	Caltag/Invitrogen	MHCD 4505	1
Ctrl	IgG1-FITC	X40	BD	345815	5
	IgG1-PE	X40	BD	345816	5
	IgG1-PerCP	X40	BD	345817	5
	IgG1-APC	X40	Caltag/Invitrogen	MG 105	1
CD4 Treg	CD4-PE	RPA-T4	BD	555346	20
	FoxP3-FITC	259/C7	BD	560046	20
	CD3-PerCP	SK7	BD	345766	10
	CD25-APC	2A3	BD	340907	5
CD8 Treg	CD8-PE	RPA-T8	BD	555366	20
	FoxP3-FITC	259/C7	BD	560046	20
	CD3-PerCP	SK7	BD	345766	10
	CD25-APC	2A3	BD	340907	5

APC, allophycocyanin; B, B lymphocyte; BD, Becton Dickinson Biosciences; BC, Beckman Coulter; CD, cluster of differentiation; COPD, chronic obstructive pulmonary disease; Ctrl, control; FITC, fluorescein isothiocyanate; NK, natural killer cell; PE, phycoerythrin; T, T lymphocyte; Treg, regulatory T cells.

directed against the intracellular transcription factor forkhead box P3 (FoxP3) was added for another 30 min. After another two washing steps, 5×10^4 cells were analyzed on a FACScalibur instrument (Becton Dickinson, Heidelberg, Germany).

Statistical Analysis

Statistical analysis was performed using the IBM SPSS 20.0 software package for windows (SPSS Inc., USA). Statistically significant differences between Hsp70 levels of patients with high and low GTV and high and low CD94 expression, lymphocyte subpopulations of healthy donors, patients with squamous cell and adenocarcinoma as well as between the percentage of all lymphocytes of patients with high and low Hsp70 expression were determined with Mann–Whitney's *U*-test. Correlation between serum Hsp70 levels and GTV was evaluated using Spearman's Rank Correlation Coefficient. Potential differences in Hsp70 serum levels in NSCLC patients before and after RCT were determined with the Wilcoxon Rank-Sum Test. Comparison of Hsp70 levels in the serum of two patient groups (squamous cell and adeno NSCLC) and a group of healthy donors was also performed using the Kruskal–Wallis test with a Dunn multiple comparison test. A value of $p < 0.05$ was considered as statistically significant.

RESULTS

Comparison of Hsp70 Levels in Patients with Squamous Cell, Adeno NSCLC, and Healthy Human Individuals

Serum samples derived from 25 squamous cell and 18 adeno NSCLC patients (patient collective #1), and 126 age- and gender-matched healthy donors were analyzed to determine the Hsp70 levels in the peripheral blood. As shown in **Figure 1A**, patients with squamous cell and adeno NSCLC (NSCLC; $n = 43$) have significantly higher serum Hsp70 levels ($p \leq 0.001$) compared to healthy control controls (healthy; $n = 126$), as determined with the lipHsp70 ELISA, at diagnosis. The mean serum Hsp70 levels of patients with squamous cell and adeno NSCLC, 16.69 ± 2.7 ng/ml and 14.51 ± 2.49 (median 12.15 vs. 12.20 ng/ml), respectively, did not differ significantly from each other ($p = 0.825$), but both tumor types differed significantly ($p \leq 0.001$) from that of healthy controls (7.0 ng/ml) as shown in **Figure 1B**. A representative image of an Hsp70 positive tumor section of a squamous cell (upper graph) and an adeno (lower graph) NSCLC in stage IV is illustrated in **Figure 1C**. All nine tumor sections of NSCLC patients (six in stage IV and three in stage III) had elevated Hsp70 serum levels and exhibited a strong Hsp70 staining in the tumor cells but not in the connective tissue. Studies are ongoing that aim to analyze a potential correlation between cytosolic and serum Hsp70 levels in a larger panel of patients.

To investigate whether RCT impacts on serum Hsp70 levels in a small subgroup of patients ($n = 6$), blood was collected before start of therapy and directly after completion of therapy. Although Hsp70 levels after RCT remained significantly higher compared to those of healthy human individuals, a slight drop, which did not reach statistical significance ($p = 0.463$; Wilcoxon Rank-Sum Test), was detectable in the serum Hsp70 levels after completion of RCT (**Figure 1D**).

Correlation of Hsp70 Levels at Diagnosis with Tumor Volume in NSCLC Patients

A comparison of free and lipid-bound Hsp70 in the circulation of tumor patients revealed that a major part of Hsp70 is bound to lipid vesicles, most likely exosomes, which are actively secreted by viable tumor cells carrying Hsp70 on their cell surface (12, 23). Therefore, we studied a potential correlation of the detected serum Hsp70 levels with the GTV of 55 NSCLC patients (patient collective #2; **Table 2**) that was determined by PET-imaging before start of RCT. The average tumor size of these patients was 219.9 ± 32.3 ml and the mean Hsp70 level was 11.2 ± 1.7 ng/ml. The Spearman's Rank Correlation Coefficient revealed a significant correlation ($p = 0.03$) between these two metric parameters. Regarding the median GTV of 143.6 ml, these patients were subdivided into a group with low (≤143.6 ml) and high (>143.6 ml) median GTV. As shown in **Figure 2**, patients in the high GTV group had significantly higher serum Hsp70 levels than patients with a low tumor volume ($p < 0.05$).

Differences in the Immune Phenotype of Healthy Human Donors, Patients with Squamous Cell and Adenocarcinoma of the Lung

Nowadays, it is well accepted that an intact immune system plays a key role in long-term tumor control and in prevention of distant metastasis (24). Therefore, we comparatively investigated differences in the relative amount of lymphocytes and lymphocyte subpopulations, such as B, T, and NK cells, in the EDTA blood of healthy human donors ($n = 10$) and NSCLC patients (patient collective #1; $n = 43$; Table 1) at diagnosis, using multi-color FACS analysis. The panel of fluorescence-labeled antibodies and antibody combinations that were used in the study, is summarized in **Table 3**. Compared to blood of healthy human donors, the relative number of lymphocytes was significantly lower in patients with squamous cell ($n = 25$; $p = 0.001$) and adeno ($n = 18$; $p = 0.008$) NSCLC, although the percentage of lymphocytes in patients with different histology was very similar (22.4 ± 1.6% for squamous cell and 21.8 ± 2.4% for adenocarcinoma patients vs. 34.5 ± 1.77% in healthy controls) (**Figure 3**). The gating strategy of the lymphocytes is exemplified in the lower part of **Figure 3**. Gate R1 refers to the gated population of lymphocytes, whereas gate R2 represents granulocytes. The population of $CD14^+$ monocytes is localized between the gates R1 and R2.

With respect to $CD19^+$ B cells, patients with squamous cell carcinoma had significantly lower percentages of B cells than healthy donors ($p = 0.001$) and adenocarcinoma patients ($p = 0.02$) (**Figure 4A**). A comparison of different $CD3^+$ T cell subpopulations, such as $CD4^+$, $CD8^+$, $CD4^+/CD25^+$ regulatory, $NKG2D^+$, and $CD94^+$ T cells revealed no major differences, apart from a significant increase in the subpopulation of $CD3^+/CD56^+$ NKT cells in patients with adeno lung carcinomas compared to healthy controls ($p = 0.038$) (**Figure 4B**). The activation marker

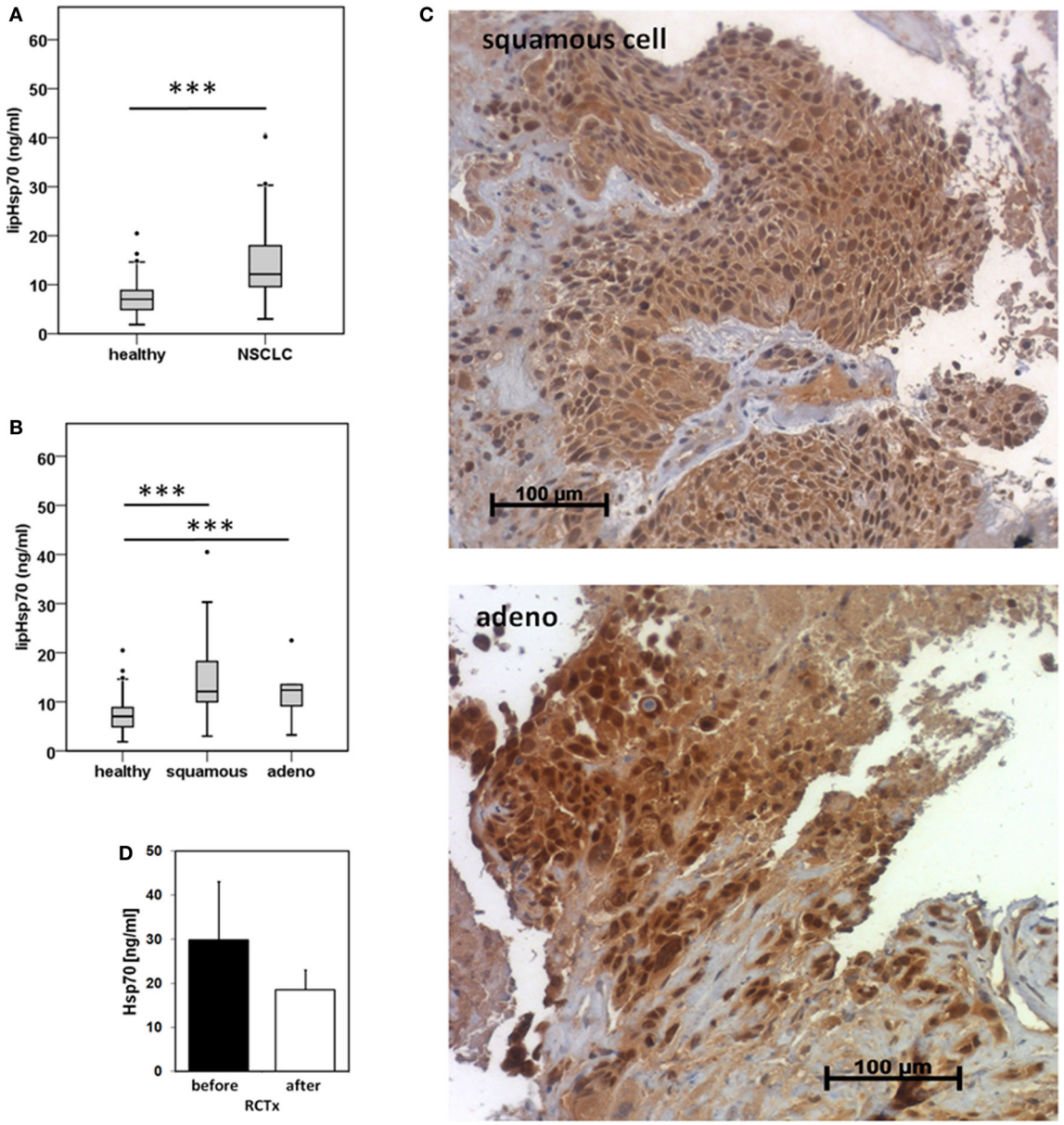

FIGURE 1 | Hsp70 serum levels (nanogram per milliliter) in healthy human individuals and patients with squamous cell and adeno NSCLC at diagnosis and directly after RCT therapy. **(A)** Serum Hsp70 levels of healthy donors (healthy; $n = 126$; median Hsp70 level: 7.03 ng/ml, 95th percentile: 13.84 ng/ml) and NSCLC patients (NSCLC; $n = 43$; median Hsp70 level: 12.15 ng/ml, 95th percentile = 40.20 ng/ml) (patient collective #1) at diagnosis measured with the lipHsp70 ELISA; ***p < 0.001 (Mann–Whitney U-Test). **(B)** Serum Hsp70 levels of healthy donors (healthy; $n = 126$) and patients with squamous cell (squamous; $n = 25$; median Hsp70 level: 12.10 ng/ml; 95th percentile: 40.50 ng/ml) and adeno (adeno; $n = 18$; median Hsp70 level: 12.38 ng/ml; 95th percentile: 40.20 ng/ml) NSCLC (patient collective #1) at diagnosis measured with the lipHsp70 ELISA; ***$p < 0.001$ (Kruskal–Wallis test with Dunn's multiple comparison test). **(C)** Representative immunohistochemical images of a squamous cell and adeno NSCLC section stained with cmHsp70.1 antibody; 20× magnification (patient collective #1). The upper graph shows a squamous cell NSCLC and the lower graph an adeno NSCLC section. Only the tumor tissue but not the surrounding tissue shows an Hsp70 staining. **(D)** Serum Hsp70 levels of NSCLC patients ($n = 6$; patient collective #1) at diagnosis (before) and directly after RCT (after).

CD69 appeared to be slightly, but not significantly, elevated on $CD3^+$ T cells of patients with squamous cell ($p = 0.81$) and adenocarcinoma ($p = 0.197$) patients compared to healthy controls (**Figure 4B**). A representative picture of the strategy to analyze $CD3^+/CD4^+$ T cells is illustrated in the inset of **Figure 4B**. In contrast to the T cell subpopulations, significant differences were observed with respect to $CD3^-$ NK cell subpopulations regarding the activation marker CD69 and the C-type lectin receptor CD94. Patients with squamous cell NSCLC had significantly higher percentages of $CD3^-/CD56^+/CD69^+$ ($p = 0.016$) and $CD3^-/CD56^+/CD94^+$ ($p = 0.028$) NK cells than healthy controls (**Figure 4C**). Although not significantly different, it also appeared

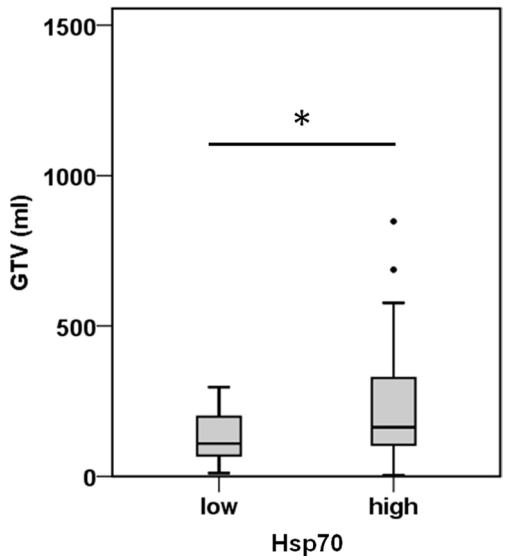

FIGURE 2 | Hsp70 serum levels and gross tumor volume (GTV) in NSCLC patients. According to their median Hsp70 levels, NSCLC patients ($n = 55$; patient collective #2) were divided into patients with low GTV (≤143.6 ml; median GTV: 109.40 ml; 95th percentile: 296.30 ml) and high GTV (>143.6 ml; median GTV: 163.50 ml; 95th percentile: 688.00 ml); $^{*}p < 0.05$ (Mann–Whitney *U*-test).

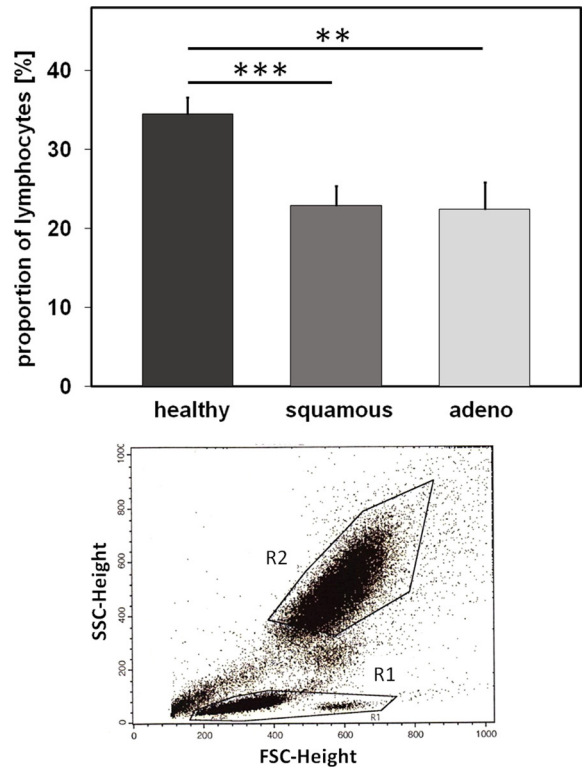

FIGURE 3 | Relative amounts of lymphocytes (%) in healthy human individuals and patients with squamous cell and adeno NSCLC. Comparison of the percentage of peripheral blood lymphocytes (PBL) in healthy human individuals ($n = 10$) and patients with squamous cell ($n = 25$) and adeno ($n = 18$) NSCLC at diagnosis (patient collective #1); $^{**}p < 0.01$, $^{***}p < 0.001$ (Mann–Whitney U-test). Graph below: gate R1 refers to the population of PBL which is analyzed by FACS, G2 refers to the population of granulocytes.

that patients with squamous cell NSCLC had elevated ratios of $CD3^{-}/CD56^{+}$ NK cells and $CD3^{-}/NKG2D^{+}$ NK cells in general, compared to healthy controls ($p = 0.053$) and adenocarcinoma patients (**Figure 4C**).

Correlation of Hsp70 Serum Levels with Lymphocyte Subpopulations in Squamous Cell and Adenocarcinoma Patients

$CD3^{-}/CD94^{+}$ NK cells were found to be significantly elevated in squamous cell carcinoma of the lung (**Figure 4C**). Furthermore, we have shown earlier that the C-type lectin receptor CD94 plays a key role in the recognition of Hsp70 by NK cells (17). To investigate the influence of serum Hsp70 on the ratio of $CD3^{-}/CD94^{+}$ NK cells, patients with squamous cell ($n = 25$) and adenocarcinoma ($n = 18$) were divided into groups with high (≥8.5% in squamous cell and ≥6.5% in adenocarcinoma) and low (<8.5% in squamous cell and <6.5% in adenocarcinoma) median percentages of $CD3^{-}/CD94^{+}$ NK cells. It appeared that patients with squamous cell NSCLC with a high $CD3^{-}/CD94^{+}$ NK cell ratio had significantly lower serum Hsp70 levels than the corresponding group with a low ratio of $CD3^{-}/CD94^{+}$ NK cell ratio ($p = 0.048$) (**Figure 5A**). The $CD94^{+}$ NK cell population was also found to be positive for CD69, which indicates that these NK cells are active. Patients with high percentages of $CD94^{+}/CD69^{+}$ NK cells have low Hsp70 serum levels and also a lower GTV, which indicates that these NK cells might be able to control the growth of mHsp70-positive tumor cells. In contrast, patients with adenocarcinoma showed no significant differences with respect to the ratio of $CD3^{-}/CD94^{+}$ NK cells and serum Hsp70 levels ($p = 0.908$) (**Figure 5B**). These findings might indicate that squamous cell NSCLC is more immunogenic than adeno NSCLC.

DISCUSSION

Many lung tumors are diagnosed at advanced stages, which often restrict curative-intent treatment. In bronchial carcinoma, first diagnosis can be delayed by unspecific symptoms like coughing or dyspnea, which is also seen in inflammatory diseases of the lung, such as chronic obstructive pulmonary disease (COPD) or pneumonia. Apart from that, the majority of patients with the diagnosis COPD are smokers who additionally have an increased risk of developing lung cancer. Consequently, there is an urgent need for novel tumor biomarkers that can distinguish malignant from benign diseases. In contrast to normal cells, tumor cells frequently present Hsp70 on their surface. Membrane Hsp70-positive tumor cells have the capacity to actively secrete Hsp70 in lipid vesicles with molecular characteristics of exosomes (8, 9, 12). In a large variety of different malignant tumor entities,

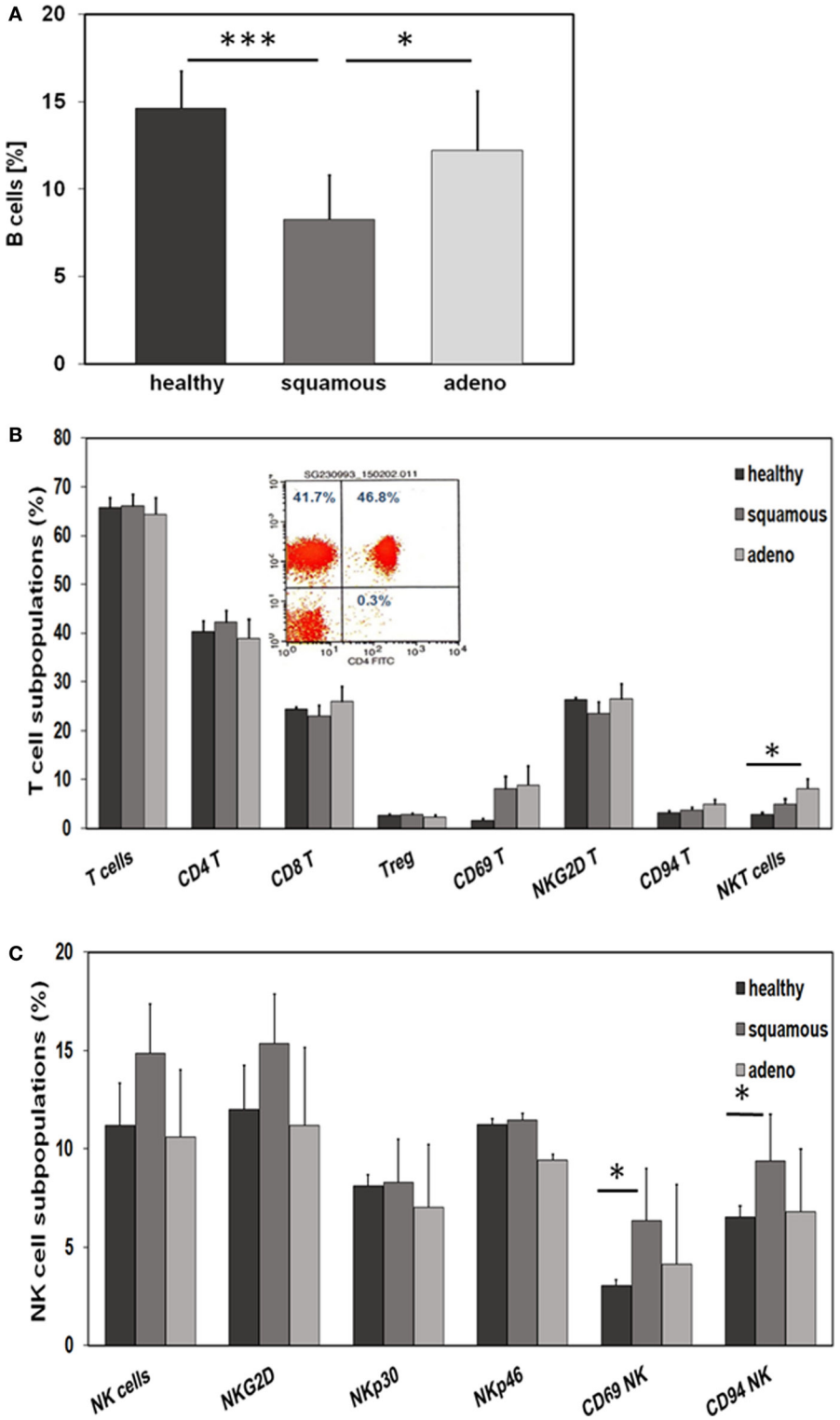

FIGURE 4 | Comparison of the immune phenotype of squamous cell and adeno NSCLC patients with healthy donors. **(A)** Relative amount of B cells in the blood of healthy donors ($n = 10$), squamous cell ($n = 25$) and adeno ($n = 18$) NSCLC patients, as determined by FACS analysis (patient collective #1); $^{*}p < 0.05$, $^{***}p = 0.001$ (Mann–Whitney *U*-test). **(B)** Percentage of T cell subpopulations in the blood of healthy donors ($n = 10$), squamous cell ($n = 25$) and adeno ($n = 18$) NSCLC patients (patient collective #1); $^{*}p < 0.05$ (Mann–Whitney *U*-test). A representative example of the analysis of $CD3^{+}/CD4^{+}$ helper T cells by FACS analysis is shown in the inset (percentages of positively stained cells are shown in each quadrant of the dot blot). **(C)** Percentage of NK cell subpopulations in the blood of healthy donors ($n = 10$), squamous cell ($n = 25$) and adeno ($n = 18$) NSCLC patients (patient collective #1); $^{*}p < 0.05$ (Mann–Whitney *U*-test).

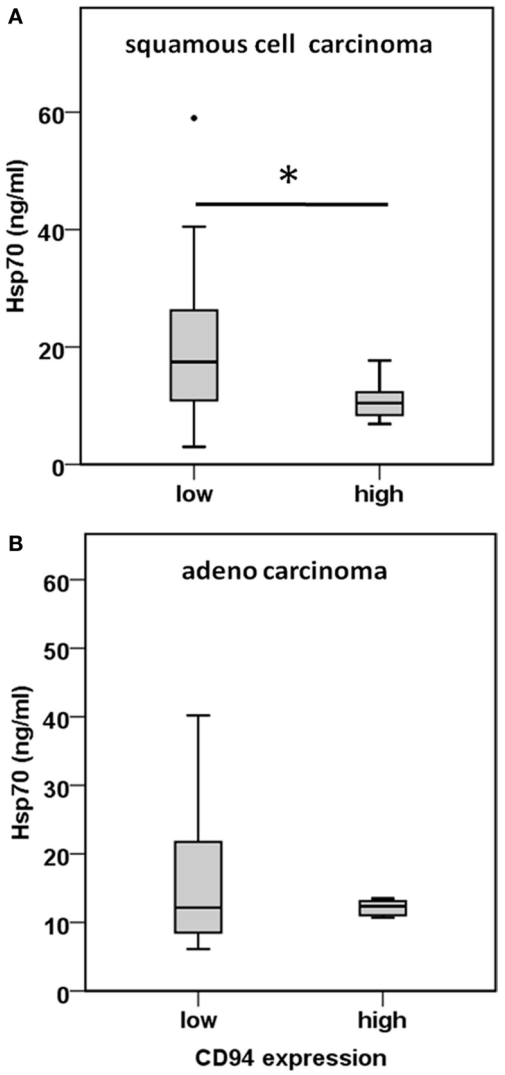

FIGURE 5 | Comparison of the CD94 immune phenotype and Hsp70 serum levels in squamous cell and adeno NSCLC patients.
(A) Correlation of the CD94 expression and serum Hsp70 levels in squamous cell NSCLC patients ($n = 25$) (patient collective #1). NSCLC patients were divided in a group with low (≤8.5% $CD3^-/CD94^+$ NK cells; median Hsp70 level: 17.45 ng/ml; 95th percentile: 59.00 ng/ml) and high (>8.5% $CD3^-/CD94^+$ NK cells; median Hsp70 level: 10.45 ng/ml; 95th percentile: 17.70 ng/ml) percentage of $CD3^-/CD94^+$ NK cells; $^*p < 0.05$ (Mann–Whitney *U*-test).
(B) Correlation of the CD94 expression and serum Hsp70 levels in adeno NSCLC patients ($n = 18$) (patient collective #1). NSCLC patients were divided in a group with low (≤6.5% $CD3^-/CD94^+$ NK cells; median Hsp70 level: 12.15 ng/ml; 95th percentile: 40.20 ng/ml) and high (>6.5% $CD3^-/CD94^+$ NK cells; median Hsp70 level: 12.35 ng/ml; 95th percentile: 22.50 ng/ml) percentage of $CD3^-/CD94^+$ NK cells; $^*p < 0.05$ (Mann–Whitney *U*-test).

elevated Hsp70 levels in the serum could be detected (4, 5) which reflect a mHsp70-positive tumor phenotype. Herein, we could show significantly elevated levels of Hsp70 in the peripheral blood circulation of patients with squamous cell and adeno NSCLC when compared to healthy individuals. Previous work of our group has demonstrated that differences exist in Hsp70 serum levels in patients with inflammatory diseases, such as chronic hepatitis or liver cirrhosis and tumors, such as hepatocellular carcinoma (HCC) (25). All patients exhibited elevated Hsp70 levels in the serum compared to healthy controls, but the highest Hsp70 levels were detected in the group of tumor patients. In line with these findings, it has been demonstrated that NSCLC patients have higher Hsp70 levels in the blood than patients with COPD (26). These findings might provide a first hint that Hsp70 could have the potential as a tumor-specific biomarker, which is able to distinguish inflammatory and tumor diseases.

Since liposomal Hsp70, which can be quantified in the serum and plasma of patients, is derived from viable tumor cells (13, 27), we were interested to study the impact of RCT on serum Hsp70 levels in a small cohort of six NSCLC patients diagnosed with NSCLC stage IIIA and IIIB from whom blood was taken at diagnosis and after RCT. Despite a slight drop directly after completion of RCT, serum Hsp70 levels remained significantly higher than those in healthy individuals. This means that it might be possible to determine the Hsp70 tumor phenotype in the serum of patients not only at diagnosis but also during RCT.

Tumor staging in the follow-up period (2–3 months after RCT) revealed clinical responses, such as partial response or stable disease in these patients. Future studies on a larger patient cohort will elucidate whether clinical responses can be determined by a drop in the serum Hsp70 levels since the major part of circulating Hsp70 is actively released in a lipid-bound form by viable tumor cells (13). In order to further test this hypothesis, the GTV was compared to the serum Hsp70 levels. Herein, we could show that a small GTV was associated with low Hsp70 and a large GTV with high serum Hsp70 levels in NSCLC patients ($n = 55$; collective #2). Furthermore, a significant correlation between serum Hsp70 levels and PET-based GTV was shown using Spearman's Rank Order Correlation. A potential correlation of the Hsp70 levels with the UICC stage has to be performed in a patient cohort with a more balanced distribution of different UICC stages. Studies of Zimmermann et al. (26) have shown that the Hsp27 and Hsp70 serum levels could discriminate clinical stages in NSCLC and the group of Bauer et al. (28) has shown that the tumoral expression of both HSPs might provide useful biomarkers for risk stratification of UICC stage I/II colon cancer. Considering the potential prognostic and predictive quality of tumor volume and its changes during RT of cancer (29, 30), serial GTV registrations at different time points before, during and after RT by CT, MRI, or PET will be determined together with serum Hsp70 levels in ongoing studies.

Nevertheless, further research is necessary to assess in more detail how homogeneously membrane Hsp70 is expressed in tumor cells within one tumor or in tumors of different patients in order to validate a direct correlation between serum Hsp70 levels and the viable tumor mass. Immunohistochemistry data reveal that tumor cells, but not the surrounding normal tissue, are Hsp70 positive. Equally important is to determine which factors can influence the active secretion of Hsp70-containing vesicles by tumor cells. In the tissue of patients with squamous cell carcinoma of the head and neck, a high membrane Hsp70 expression on viable tumor cells was found to be associated with high serum Hsp70 levels (31). Salamuta S. Mambula observed a re-binding of extracellular Hsp70 to the cell surface of prostate

carcinoma cells after its release (32). This phenomenon might also have an impact on circulating levels of Hsp70.

Apart from the fact that high membrane Hsp70 expression levels are associated with and aggressive tumor phenotype, radioresistance (16), and tumor progression (33), Hsp70 can also provide a target for the innate immune system (11, 34, 35). In general, the immune system of each individual human blood donor is highly individual, depending on the genetic constitution combined with the exposition to various antigens during life. Patients with solid tumors often show an immunosuppressed immune phenotype due to a variety of tumor immune escape mechanisms (36). In the present study, we intended to detect differences in the immune phenotype of patients with NSCLC of different histology and healthy human individuals. Considering that patients with squamous cell and adenocarcinoma had significantly lower percentages of lymphocytes in the peripheral blood than healthy controls (**Figure 4A**), our findings confirm that the immune system is essential for tumor control. Since membrane Hsp70 acts as a recognition structure for Hsp70-peptide pre-activated NK cells (35), we asked the question whether lipid-bound, circulating Hsp70 has an impact on the immune phenotype of peripheral blood lymphocytes (PBL). Flow cytometric analysis of the blood of patients with squamous cell carcinoma showed decreased percentages of B cells but elevated percentages of activated NK cell subpopulations in patients with squamous cell, but not adeno NSCLC. Significantly increased percentages of $CD69^+/CD94^+$ NK cells were found in these patients compared to the healthy donors and adenocarcinoma patients. We could show that high serum Hsp70 levels are associated with a larger GTV in squamous cell but not adeno NSCLC. Regarding **Figures 5A,B**, patients with a lower percentage of $CD94^+/CD69^+$ activated NK cells have higher Hsp70 serum levels in squamous cell NSCLC. Since high Hsp70 serum levels are associated with a larger GTV we speculate that $CD94^+/CD69^+$ activated NK might be able to control growth of membrane Hsp70-positive tumor cells. Depending on its subcellular localization Hsp70 exerts dual functions. On the one hand, high intracellular and membrane-bound Hsp70 levels protect tumor cells from apoptotic cell death and thus mediate therapy resistance; on the other hand, membrane Hsp70 acts as a recognition structure for activated NK cells. Highly malignant tumor cells that secrete large amounts of Hsp70 might escape protective antitumor immunity by inducing tolerance, and therefore high Hsp70 levels that are associated with a larger GTV might be associated with a suppression of C-type lectin-positive NK cells. Vice versa, high percentages of $CD94^+/CD69^+$ NK cells can control growth of mHsp70-positive squamous cell carcinomas and thus serum levels of Hsp70 are lower. In case of adeno NSCLC, no correlation of the percentage of $CD94^+/CD69^+$ NK cells and serum Hsp70 levels were observed. This finding might be attributed to the fact that adenocarcinomas are less immunogenic.

Previously, it has been demonstrated that the cell surface density of the C-type lectin receptor CD94 was up-regulated on NK cells after stimulation with Hsp70-peptide TKD ($aa_{450–463}$) and low-dose IL-2 (17). Apart from Hsp70, it is known that CD94 interacts with non-classical HLA-E molecules (37), and serves either as an activating or inhibitory receptor depending on the NKG2C or NKG2A co-receptor (38). In Hsp70 membrane-positive SCCHN patients, even 2 years after surgery and radiation therapy, the expression density of CD94 and NKG2D on NK cells was found to be significantly up-regulated (31). An increased expression of CD69 on NK cells is associated with an increased cytotoxic activity, proliferation, TNF-α production and the induction of further activation markers, such as CD25 and ICAM-1 (39). Our present data indicate that an increased percentage of CD69 and CD94 positive NK cells is only present in the blood of patients with squamous cell but not of adeno NSCLC patients and a significant association of the CD94 expression with serum Hsp70 could be also only detected in the group of squamous cell NSCLC patients (**Figures 5A,B**).

According to the diversity of their gene expression patterns, adenocarcinoma can be divided into subgroups with different outcome in overall survival (40). In squamous cell carcinoma of the lung, a reinforcement of the innate immune response by danger signals, such as circulating Hsp70, might be favorable. NK cells are not only able to detect "missing self" on malignant cells (41), but also can recognize membrane Hsp70 if expressed in a tumor-specific manner (42). Experimental mouse models indicate that the development of tumor-specific $CD8^+$ cytotoxic T cell responses is highly dependent on the NK cell-mediated elimination of tumor cells (43, 44) through the secretion of IFN-γ. Also macrophages and dendritic cells are activated by IFN-γ and TNF. An 11-year follow-up epidemiologic survey has shown that the paucity of activated NK cells was associated with an increased risk to develop cancer (45). Taken together our data indicate that NK cells as the first line of defense might play a major role in the control of squamous cell NSCLC. The danger molecule Hsp70 in the presence of pro-inflammatory cytokines, such as IL-2, might support the immune system to reinforce immunity against cancer.

CONCLUSION

We could show that Hsp70 detected by the lipHsp70 ELISA can serve as a tumor biomarker in liquid biopsies of patients with squamous cell and adeno NSCLC. Due to the fact that vesicular, lipid-bound Hsp70 predominantly originates from viable tumor cells, a correlation of serum Hsp70 levels with GTV was found. This finding is in accordance to the result that changes in tumor volume during radiotherapy in NSCLC patients have potential prognostic and predictive value (46, 47).

Compared to healthy individuals, NSCLC patients have decreased lymphocyte counts in general. However, a comparison of lymphocyte subpopulations in NSCLC patients with different histology revealed elevated percentages of $CD69^+/CD94^+$ NK cells in squamous cell but not adeno NSCLC patients. This might provide a hint that squamous cell NSCLC is more immunogenic than adeno NSCLC. High serum Hsp70 levels are associated with a larger GTV and lower percentage of $CD69^+/CD94^+$ NK cells. This might indicate that activated NK cells might be able to control growth of mHsp70-positive tumors in squamous cell NSCLC patients. If tumor escape

mechanism suppress NK cell activation mHsp70-positive tumors cannot be killed.

AUTHOR CONTRIBUTIONS

SG and CO contributed equally to the study; SG, CO, DV, and GM conceived and designed the experiments and wrote the paper; SG, SS, HS, PM, MJ, and FP performed the experiments, and or analyzed the data; DV and SC did proof-reading of the paper and gave clinical advice.

ACKNOWLEDGMENTS

The work of the team at the TUM was supported by the EU-CELLEUROPE (315963); BMBF (Strahlenkompetenz, 02NUK007E; 02NUK031B; Innovative Therapies, 01GU0823; NSCLC, 16GW0030), DFG – Cluster of Excellence: Munich Centre for Advanced Photonics; DFG –SFB824/2; DFG – INST 95/980-1 FUGG; DFG – INST 411/37-1 FUGG. The work of the team at the Martin Luther University Halle-Wittenberg was supported by the Wilhelm-Sander Foundation (FKZ: 2007.123.2).

REFERENCES

1. Worldwide Cancer Statistics Cancer Research UK. Available from: http://www.cancerresearchuk.org/health-professional/cancer-statistics/worldwide-cancer#heading-Zero
2. Mirsadraee S, Oswal D, Alizadeh Y, Caulo A, van Beek EJ. The 7th lung cancer TNM classification and staging system: review of the changes and implications. *World J Radiol* (2012) **4**:128–34. doi:10.4329/wjr.v4.i4.128
3. Parkin DM, Bray F, Ferlay J, Pisani P. Estimating the world cancer burden: Globocan 2000. *Int J Cancer J Int Cancer* (2001) **94**:153–6. doi:10.1002/ijc.1440
4. Pass HI, Carbone DP, Johnson DH, Minna JD, Scagliotti GV, Turrisi AT. *Principles and Practice of Lung Cancer: The Official Reference Text of the International Association for the Study of Lung Cancer (IASLC)*. Philadelphia: Lippincott Williams & Wilkins (2012).
5. Oberije C, De Ruysscher D, Houben R, van de Heuvel M, Uyterlinde W, Deasy JO, et al. A validated prediction model for overall survival from stage III non-small cell lung cancer: toward survival prediction for individual patients. *Int J Radiat Oncol Biol Phys* (2015) **92**:935–44. doi:10.1016/j.ijrobp.2015.02.048
6. Breakthrough of the Year 2013 Science/AAAS News. Available from: http://news.sciencemag.org/breakthrough-of-the-year-2013#.Vb38J_nwh_8
7. Hantschel M, Pfister K, Jordan A, Scholz R, Andreesen R, Schmitz G, et al. Hsp70 plasma membrane expression on primary tumor biopsy material and bone marrow of leukemic patients. *Cell Stress Chaperones* (2000) **5**:438–42. doi:10.1379/1466-1268(2000)005<0438:HPMEOP>2.0.CO;2
8. Pfister K, Radons J, Busch R, Tidball JG, Pfeifer M, Freitag L, et al. Patient survival by Hsp70 membrane phenotype: association with different routes of metastasis. *Cancer* (2007) **110**:926–35. doi:10.1002/cncr.22864
9. Lindquist S, Craig EA. The heat-shock proteins. *Annu Rev Genet* (1988) **22**:631–77. doi:10.1146/annurev.ge.22.120188.003215
10. Hartl FU. Molecular chaperones in cellular protein folding. *Nature* (1996) **381**:571–9. doi:10.1038/381571a0
11. Gehrmann M, Marienhagen J, Eichholtz-Wirth H, Fritz E, Ellwart J, Jäättelä M, et al. Dual function of membrane-bound heat shock protein 70 (Hsp70), Bag-4, and Hsp40: protection against radiation-induced effects and target structure for natural killer cells. *Cell Death Differ* (2005) **12**:38–51. doi:10.1038/sj.cdd.4401510
12. Gastpar R, Gehrmann M, Bausero MA, Asea A, Gross C, Schroeder JA, et al. Heat shock protein 70 surface-positive tumor exosomes stimulate migratory and cytolytic activity of natural killer cells. *Cancer Res* (2005) **65**:5238–47. doi:10.1158/0008-5472.CAN-04-3804
13. Breuninger S, Ertl J, Bayer C, Knape C, Gunther S, Regel I, et al. Quantitative analysis of liposomal heat shock protein 70 (Hsp70) in the blood of tumor patients using a novel lipHsp70 ELISA. *J Clin Cell Immunol* (2015) **5**:4–10. doi:10.4172/2155-9899.1000264
14. Multhoff G, Hightower LE. Distinguishing integral and receptor-bound heat shock protein 70 (Hsp70) on the cell surface by Hsp70-specific antibodies. *Cell Stress Chaperones* (2011) **16**:251–5. doi:10.1007/s12192-010-0247-1
15. Stangl S, Gehrmann M, Riegger J, Kuhs K, Riederer I, Sievert W, et al. Targeting membrane heat-shock protein 70 (Hsp70) on tumors by cmHsp70.1 antibody. *Proc Natl Acad Sci U S A* (2011) **108**:733–8. doi:10.1073/pnas.1016065108
16. Murakami N, Kühnel A, Schmid TE, Ilicic K, Stangl S, Braun IS, et al. Role of membrane Hsp70 in radiation sensitivity of tumor cells. *Radiat Oncol* (2015) **10**:149. doi:10.1186/s13014-015-0461-1
17. Krause SW, Gastpar R, Andreesen R, Gross C, Ullrich H, Thonigs G, et al. Treatment of colon and lung cancer patients with *ex vivo* heat shock protein 70-peptide-activated, autologous natural killer cells: a clinical phase I trial. *Clin Cancer Res* (2004) **10**:3699–707. doi:10.1158/1078-0432.CCR-03-0683
18. Specht HM, Ahrens N, Blankenstein C, Duell T, Fietkau R, Gaipl US, et al. Heat shock protein 70 (Hsp70) peptide activated natural killer (NK) cells for the treatment of patients with non-small cell lung cancer (NSCLC) after radiochemotherapy (RCTx) – from preclinical studies to a clinical phase II trial. *Front Immunol* (2015) **6**. doi:10.3389/fimmu.2015.00162
19. Gastpar R, Gross C, Rossbacher L, Ellwart J, Riegger J, Multhoff G. The cell surface-localized heat shock protein 70 epitope TKD induces migration and cytolytic activity selectively in human NK cells. *J Immunol* (2004) **172**:972–80.
20. Moser C, Schmidbauer C, Gürtler U, Gross C, Gehrmann M, Thonigs G, et al. Inhibition of tumor growth in mice with severe combined immunodeficiency is mediated by heat shock protein 70 (Hsp70)-peptide-activated, CD94 positive natural killer cells. *Cell Stress Chaperones* (2002) **7**:365–73. doi:10.1379/1466-1268(2002)007<0365:IOTGIM>2.0.CO;2
21. Gross C, Koelch W, DeMaio A, Arispe N, Multhoff G. Cell surface-bound heat shock protein 70 (Hsp70) mediates perforin-independent apoptosis by specific binding and uptake of granzyme B. *J Biol Chem* (2003) **278**:41173–81. doi:10.1074/jbc.M302644200
22. Ostheimer C, Bache M, Güttler A, Kotzsch M, Vordermark D. A pilot study on potential plasma hypoxia markers in the radiotherapy of non-small cell lung cancer. Osteopontin, carbonic anhydrase IX and vascular endothelial growth factor. *Strahlenther Onkol Organ Dtsch Röntgenges Al* (2014) **190**:276–82. doi:10.1007/s00066-013-0484-1
23. Vega VL, Rodríguez-Silva M, Frey T, Gehrmann M, Diaz JC, Steinem C, et al. Hsp70 translocates into the plasma membrane after stress and is released into the extracellular environment in a membrane-associated form that activates macrophages. *J Immunol* (2008) **180**:4299–307.
24. Dunn GP, Old LJ, Schreiber RD. The immunobiology of cancer immunosurveillance and immunoediting. *Immunity* (2004) **21**:137–48. doi:10.1016/j.immuni.2004.07.017
25. Gehrmann M, Cervello M, Montalto G, Cappello F, Gulino A, Knape C, et al. Heat shock protein 70 serum levels differ significantly in patients with chronic hepatitis, liver cirrhosis, and hepatocellular carcinoma. *Front Immunol* (2014) **5**:307. doi:10.3389/fimmu.2014.00307
26. Zimmermann M, Nickl S, Lambers C, Hacker S, Mitterbauer A, Hoetzenecker K, et al. Discrimination of clinical stages in non-small cell lung cancer patients by serum HSP27 and HSP70: a multi-institutional case-control study. *Clin Chim Acta* (2012) **413**:1115–20. doi:10.1016/j.cca.2012.03.008
27. Schwarzer J, Multhoff G. Commentary to: "a comparison of two commercially available ELISA methods for the quantification of human plasma heat shock protein 70 during rest and exercise stress" by Lee et al. 2015. *Cell Stress Chaperones* (2015) **20**:865–6. doi:10.1007/s12192-015-0626-8
28. Bauer K, Nitsche U, Slotta-Huspenina J, Drecoll E, von Weyhern CH, Rosenberg R, et al. High HSP27 and HSP70 expression levels are independent adverse prognostic factors in primary resected colon cancer. *Cell Oncol (Dordr)* (2012) **35**:197–205. doi:10.1007/s13402-012-0079-3
29. Yuh WTC, Mayr NA, Jarjoura D, Wu D, Grecula JC, Lo SS, et al. Predicting control of primary tumor and survival by DCE MRI during early therapy in cervical cancer. *Invest Radiol* (2009) **44**:343–50. doi:10.1097/RLI.0b013e3181a64ce9

30. Huang Z, Mayr NA, Yuh WTC, Lo SS, Montebello JF, Grecula JC, et al. Outcome prediction of cervical cancer: kinetic model of tumor regression during radiation therapy. *Cancer Res* (2010) **70**:463. doi:10.1158/0008-5472.CAN-09-2501
31. Gehrmann M, Specht HM, Bayer C, Brandstetter M, Chizzali B, Duma M, et al. Hsp70 – a biomarker for tumor detection and monitoring of outcome of radiation therapy in patients with squamous cell carcinoma of the head and neck. *Radiat Oncol* (2014) **9**:131. doi:10.1186/1748-717X-9-131
32. Mambula SS, Calderwood SK. Heat shock protein 70 is secreted from tumor cells by a nonclassical pathway involving lysosomal endosomes. *J Immunol* (2006) **177**:7849–57. doi:10.4049/jimmunol.177.11.7849
33. Juhasz K, Lipp A-M, Nimmervoll B, Sonnleitner A, Hesse J, Haselgruebler T, et al. The complex function of hsp70 in metastatic cancer. *Cancers (Basel)* (2013) **6**:42–66. doi:10.3390/cancers6010042
34. Gehrmann M, Schmetzer H, Eissner G, Haferlach T, Hiddemann W, Multhoff G. Membrane-bound heat shock protein 70 (Hsp70) in acute myeloid leukemia: a tumor specific recognition structure for the cytolytic activity of autologous NK cells. *Haematologica* (2003) **88**:474–6.
35. Botzler C, Li G, Issels RD, Multhoff G. Definition of extracellular localized epitopes of Hsp70 involved in an NK immune response. *Cell Stress Chaperones* (1998) **3**:6–11. doi:10.1379/1466-1268(1998)003<0006:DOELEO>2.3.CO;2
36. Blankenstein T, Coulie PG, Gilboa E, Jaffee EM. The determinants of tumour immunogenicity. *Nat Rev Cancer* (2012) **12**:307–13. doi:10.1038/nrc3246
37. Braud VM, Allan DS, O'Callaghan CA, Söderström K, D'Andrea A, Ogg GS, et al. HLA-E binds to natural killer cell receptors CD94/NKG2A, B and C. *Nature* (1998) **391**:795–9. doi:10.1038/35869
38. López-Botet M, Pérez-Villar JJ, Carretero M, Rodríguez A, Melero I, Bellón T, et al. Structure and function of the CD94 C-type lectin receptor complex involved in recognition of HLA class I molecules. *Immunol Rev* (1997) **155**:165–74. doi:10.1111/j.1600-065X.1997.tb00949.x
39. Borrego F, Robertson MJ, Ritz J, Pena J, Solana R. CD69 is a stimulatory receptor for natural killer cell and its cytotoxic effect is blocked by CD94 inhibitory receptor. *Immunology* (1999) **97**:159–65. doi:10.1046/j.1365-2567.1999.00738.x
40. Garber ME, Troyanskaya OG, Schluens K, Petersen S, Thaesler Z, Pacyna-Gengelbach M, et al. Diversity of gene expression in adenocarcinoma of the lung. *Proc Natl Acad Sci U S A* (2001) **98**:13784–9. doi:10.1073/pnas.241500798
41. Johansson MH, Bieberich C, Jay G, Kärre K, Höglund P. Natural killer cell tolerance in mice with mosaic expression of major histocompatibility complex class I transgene. *J Exp Med* (1997) **186**:353–64. doi:10.1084/jem.186.3.353
42. Multhoff G, Botzler C, Jennen L, Schmidt J, Ellwart J, Issels R. Heat shock protein 72 on tumor cells: a recognition structure for natural killer cells. *J Immunol* (1997) **158**:4341–50.
43. Diefenbach A, Jensen ER, Jamieson AM, Raulet DH. Rae1 and H60 ligands of the NKG2D receptor stimulate tumour immunity. *Nature* (2001) **413**:165–71. doi:10.1038/35093109
44. Kelly JM, Darcy PK, Markby JL, Godfrey DI, Takeda K, Yagita H, et al. Induction of tumor-specific T cell memory by NK cell-mediated tumor rejection. *Nat Immunol* (2002) **3**:83–90. doi:10.1038/ni746
45. Imai K, Matsuyama S, Miyake S, Suga K, Nakachi K. Natural cytotoxic activity of peripheral-blood lymphocytes and cancer incidence: an 11-year follow-up study of a general population. *Lancet* (2000) **356**:1795–9. doi:10.1016/S0140-6736(00)03231-1
46. Fox J, Ford E, Redmond K, Zhou J, Wong J, Song DY. Quantification of tumor volume changes during radiotherapy for non-small-cell lung cancer. *Int J Radiat Oncol Biol Phys* (2009) **74**:341–8. doi:10.1016/j.ijrobp.2008.07.063
47. Wang JZ, Mayr NA, Zhang D, Li K, Grecula JC, Montebello JF, et al. Sequential magnetic resonance imaging of cervical cancer: the predictive value of absolute tumor volume and regression ratio measured before, during, and after radiation therapy. *Cancer* (2010) **116**:5093–101. doi:10.1002/cncr.25260

Conflict of Interest Statement: The authors declare that the research was conducted in the absence of any commercial or financial relationships that could be construed as a potential conflict of interest.

frontiers in Immunology

ORIGINAL RESEARCH
published: 18 October 2017
doi: 10.3389/fimmu.2017.01305

Dynamics of Heat Shock Protein 70 Serum Levels As a Predictor of Clinical Response in Non-Small-Cell Lung Cancer and Correlation with the Hypoxia-Related Marker Osteopontin

Christian Ostheimer[1†], Sophie Gunther[2†], Matthias Bache[1], Dirk Vordermark[1] and Gabriele Multhoff[2]*

[1] Department of Radiation Oncology, Martin Luther University Halle-Wittenberg, Halle, Germany, [2] Department of Radiation Oncology, Klinikum rechts der Isar, Technische Universität München (TUM), Munich, Germany

OPEN ACCESS

Edited by:
Willem Van Eden, Utrecht University, Netherlands

Reviewed by:
Albrecht Piiper, Universitätsklinikum Frankfurt, Germany
Carlos De Torre, IMIB-Arrixaca, Spain

***Correspondence:**
Gabriele Multhoff
gabriele.multhoff@tum.de

[†]These authors have contributed equally to this work.

Specialty section:
This article was submitted to Inflammation, a section of the journal Frontiers in Immunology

Received: *28 June 2017*
Accepted: *27 September 2017*
Published: *18 October 2017*

Citation:
Ostheimer C, Gunther S, Bache M, Vordermark D and Multhoff G (2017) Dynamics of Heat Shock Protein 70 Serum Levels As a Predictor of Clinical Response in Non-Small-Cell Lung Cancer and Correlation with the Hypoxia-Related Marker Osteopontin. Front. Immunol. 8:1305. doi: 10.3389/fimmu.2017.01305

Hypoxia mediates resistance to radio(chemo)therapy (RT) by stimulating the synthesis of hypoxia-related genes, such as osteopontin (OPN) and stress proteins, including the major stress-inducible heat shock protein 70 (Hsp70). Apart from its intracellular localization, Hsp70 is also present on the plasma membrane of viable tumor cells that actively release it in lipid vesicles with biophysical characteristics of exosomes. Exosomal Hsp70 contributes to radioresistance while Hsp70 derived from dying tumor cells can serve as a stimulator of immune cells. Given these opposing traits of extracellular Hsp70 and the unsatisfactory outcome of locally advanced lung tumors, we investigated the role of Hsp70 in the plasma of patients with advanced, non-metastasized non-small-cell lung cancer (NSCLC) before (T1) and 4–6 weeks after RT (T2) in relation to OPN as potential biomarkers for clinical response. Plasma levels of Hsp70 correlate with those of OPN at T1, and high OPN levels are significantly associated with a decreased overall survival (OS). Due to a therapy-induced reduction in viable tumor mass after RT Hsp70 plasma levels dropped significantly at T2 ($p = 0.016$). However, with respect to the immunostimulatory capacity of Hsp70 derived from dying tumor cells, patients with higher post-therapeutic Hsp70 levels showed a significantly better response to RT ($p = 0.034$) than those with lower levels at T2. In summary, high OPN plasma levels at T1 are indicative for poor OS, whereas elevated post-therapeutic Hsp70 plasma levels together with a drop of Hsp70 between T1 and T2, successfully predict favorable responses to RT. Monitoring the dynamics of Hsp70 in NSCLC patients before and after RT can provide additional predictive information for clinical outcome and therefore might allow a more rapid therapy adaptation.

Keywords: heat shock protein 70, osteopontin, radio(chemo)therapy, non-small-cell lung cancer, therapy response, overall survival

INTRODUCTION

Lung cancer is the second most common tumor type in the Western world that accounts for the majority of cancer-related deaths worldwide (1, 2). The lack of specific symptoms limits the possibilities to diagnose lung cancer at an early stage when radical surgery or stereotactic ablative radiotherapy can assure long-term tumor control and cure (3). As a result, most patients are diagnosed in advanced tumor stages where curative-intended treatment options are limited (4, 5). Cure of locally advanced (inoperable) NSCLC after definitive RT (4, 5), as the gold standard, have failed to improve survival significantly (6). Immune-based therapies are in the scientific focus (7) for their remarkable clinical responses that have been reported for some tumor types (8–10). Particularly the treatment with immune checkpoint inhibitors such as nivolumab (11–16) caused a paradigm shift in the therapy of NSCLC. Despite promising remission rates, overall survival (OS) still remains dismal at only 10–20% in almost all patients. This emphasizes the medical need for integration of immune-oncologic approaches into other treatment concepts that are based on an improved patient stratification (17, 18).

Evidence is accumulating that apart from direct cytotoxic effects, RT can elicit systemic antitumor immune responses (19, 20) by modulating the tumor and its microenvironment (21–24). However, the patient's individual immune competence and immune escape mechanisms often hamper radio(chemo) therapy (RT)-induced abscopal effects (25). These findings further accentuate the necessity of a pretreatment patient stratification (26, 27), and a continuous monitoring of immune responses during therapy (28). Presently, circulating proteins, exosomes, microRNAs and immune cell subpopulations are discussed as potential prognostic and predictive markers (29–33). We studied the dynamics of extracellular heat shock protein 70 (Hsp70) levels and correlated it with osteopontin (OPN) plasma levels at diagnosis (T1) as predictors for outcome. Elevated levels of these biomarkers are generally associated with an aggressive tumor phenotype (34, 35). OPN is reported to be associated with reduced intratumoral pO_2 levels, which is prognostic for NSCLC patients (36–38). In a randomized double-blinded trial, elevated OPN plasma levels were able to identify patients with head and neck cancer who showed clinical benefit from a hypoxia sensitizer after RT (39). For NSCLC patients, an additive prognostic value after radical RT could be determined for the co-detection of hypoxia- and angiogenesis-related markers OPN, vascular endothelial growth factor (VEGF), and carbonic anhydrase IX (CAIX) (30). Furthermore, the serial detection of circulating OPN plasma levels provided additional prognostic information for NSCLC patients in stage III with respect to the risk to relapse (31).

Heat shock protein 70 fulfils different tasks, depending on its associated partners and its sub- or extracellular localization. Vaccination with Hsp70-peptide complexes isolated from tumor cells can elicit $CD8^+$ T cell specific antitumor immune responses (40, 41), membrane-bound Hsp70 serves as a tumor-specific target for Hsp70-activated natural killer (NK) cells (42–45), and circulating Hsp70 can act as a biomarker for monitoring outcome in patients with head and neck cancer (46). Extracellular Hsp70 can originate from two major sources, exosomal Hsp70 which is actively released by viable, membrane Hsp70-positive tumor cells and free Hsp70 which most likely originates from dying cells (47, 48). By using lipHsp70 enzyme-linked immunosorbent assay (ELISA), it is possible to detect both forms of Hsp70 quantitatively in serum and plasma (49). Recent data of our group demonstrated a significant correlation of Hsp70 levels and vital tumor mass, but also provided evidence that free extracellular Hsp70 in a pro-inflammatory cytokine milieu can activate innate immunity in NSCLC patients (50).

In this prospective clinical trial, we evaluated the predictive quality of circulating pre- and post-therapeutic Hsp70 and OPN levels at T1 in patients with non-metastasized advanced NSCLC.

PATIENTS AND METHODS

Patients and Treatment

A total of 44 patients with advanced NSCLC (M0) were prospectively recruited into a clinical study at the hospital of Martin Luther University Halle-Wittenberg. The inclusion criteria were (i) age $\geq$ 18 years, (ii) histologically confirmed, nonoperable NSCLC, (iii) no prior treatment, and (iv) indication for RT, as determined by the interdisciplinary tumor board. The Ethics Committee of the Medical Faculty of the Martin Luther University Halle-Wittenberg approved the study protocol. Written informed consent was obtained from all patients before start of the study. All procedures were in accordance with the Helsinki Declaration of 1975 (as revised in 2008). Staging was based on the TNM classification of malignant tumors (7th edition) and treatment was carried out at the Department of Radiation Oncology of the Medical Faculty of the Martin Luther University Halle-Wittenberg. Depending on the World Health Organization performance status and comorbidities, treatment consisted of a three-dimensional conformal, normofractionated (5 Fx/week) definite RT (single dose 2 Gy, total dose 66 Gy, Siemens Primus, Germany) $\pm$ double-agent based chemotherapy (cisplatin 20 mg/m^2 body surface, day 1–5 and 29–33; vinorelbine 25 mg/m^2 body surface, used on day 1 and 29) in treatment week one and five (2 courses). RT was computed tomography-based (GE Healthcare) and all patients received a FDG positron emission tomography-scan prior to RT which was used for target volume delineation (Oncentra Masterplan External Beam software, Nucletron, Elekta, USA). The first follow-up of the patients was performed 4–6 weeks after end of RT to evaluate their post-radiotherapeutic response at the Department of Radiation Oncology, University Hospital Halle-Wittenberg. Thereafter,

Abbreviations: AUC, area under the curve; CAIX, carbonic anhydrase IX; CD, cluster of differentiation; CT, computed tomography; ELISA, enzyme-linked immunosorbent assay; Hsp70, heat shock protein 70; HIF1α, hypoxia-inducible factor 1α; IL-2, interleukin 2; NK cells, natural killer cells; NSCLC, non-small-cell lung cancer; OPN, osteopontin, PAI-1, plasminogen activator inhibitor type 1; PBS, phosphate buffered saline; PET, positron emission tomography; RT, radio(chemo) therapy; ROC curve, receiver operating characteristic; SCC, squamous cell carcinoma; uPAR, urokinase type plasminogen activator receptor; WHO, World Health Organization; VEGF, vascular endothelial growth factor.

patients were followed up regularly every 3 months for a period of 5 years according to RT guidelines. The mean follow-up period in patients alive was 34 (22–48) months. The survival status of patients was continuously monitored in cooperation with local citizen registration offices.

A positive therapy response was defined as complete remission, implying a disappearance of all target lesions, or partial remission which commonly signifies a decrease of at least 30% in the lesion with the largest diameter. A negative therapy response is defined by stable or progressive disease.

Plasma Samples

Blood samples of NSCLC patients were collected by peripheral venous puncture before start of RT (T1) and 4–6 weeks after the end of RT (T2). Briefly, blood was collected in two S-Monovette EDTA KA/9 ml tubes (Sarstedt, Nümbrecht, Germany). Blood was anti-coagulated and centrifuged at 4°C for 10 min with 4,000 rpm. Aliquots of 150–300 µl were prepared and directly stored at −80°C for further analysis.

Detection of Hsp70 and OPN

Heat shock protein 70 concentrations were determined using the lipHsp70 ELISA, which is capable to detect both, lipid-bound and free Hsp70 in serum and plasma. The use of cmHsp70.1 as detection antibody (49, 51) allows quantitative analysis of total content of circulating Hsp70 in the blood. 96-well MaxiSorp Nunc-Immuno plates (Thermo, Rochester, NY, USA) were coated overnight with 2 µg/ml rabbit polyclonal antibody (Davids, Biotechnologie, Regensburg, Germany) directed against human Hsp70 in sodium carbonate buffer (0.1 M sodium carbonate, 0.1 M sodium hydrogen carbonate, pH 9.6). After three washing steps with phosphate buffered saline (PBS, Life Technologies, Carlsbad, CA, USA) with 0.05% Tween 20 (Calbiochem, Merck, Darmstadt, Germany), wells were blocked with 2% milk powder (Carl Roth, Karlsruhe, Germany) in PBS for 1.5 h at 27°C. After another washing step, samples diluted 1:5 in CrossDown Buffer (Applichem, Chicago, IL, USA) were added to the wells for 2 h at 27°C. After another washing, wells were incubated with 4 µg/ml of the biotinylated mouse-anti-human monoclonal antibody cmHsp70.1 (multimmune, Munich, Germany) in 2% milk powder in PBS for 2 h at 27°C. After a last washing step, 0.2 µg/ml horseradish peroxidase-conjugated streptavidin (Pierce, Thermo, Rockford, IL, USA) in 1% bovine serum albumin (Sigma-Aldrich, St. Louis, MO, USA) was added for 1 h at 27°C. Binding was quantified by adding substrate reagent (R&D Systems, Minneapolis, MN, USA) for 30 min at 27°C and absorbance was read at 450 nm, corrected by absorbance at 570 nm, in a Microplate Reader (BioTek, Winooski, VT, USA). Each sample was measured in duplicates in three independent experiments. An eight-point standard curve using recombinant Hsp70 diluted in CrossDown Buffer at concentrations ranging from 0 to 50 ng/ml, as well as reference plasma samples were used as internal controls for each individual assay.

For OPN, the "Human Osteopontin Assay" ELISA (IBL Ltd., Japan) was performed and optical density was measured blinded and in duplicate according to manufacturer's instructions. To determine the OPN concentration, the standard curve supplied by the kit was used and OPN plasma concentration is reported in ng/ml (±1 SD). None of the two markers shows an age- and/or gender-related association.

Statistical Analysis

All statistical analyses were performed using the SPSS PASW software package for windows (SPSS Inc., USA, version 19.0) and statistical significance was accepted with two-sided p-values ($p < 0.05$). Median Hsp70 plasma levels were used as cutoff values.

Non-parametric tests (Mann–Whitney U test, Kruskal–Wallis H test) were used to determine statistically significant differences in patient subgroups with low and high Hsp70 concentration with and without response. Differences in Hsp70 levels in patients with and without therapy response were investigated using Pearson's chi-squared test. Coherences between Hsp70 and OPN as a hypoxia-related marker were evaluated using Pearson's rank correlation coefficient and paired samples test assessed potential differences in plasma Hsp70 levels before and after RT. Survival analysis was performed using the Kaplan–Meier product limit method with the log-rank test. The survival status of the patients was monitored and determined with the help of local citizen registration offices. Overall survival (OS) was calculated from start of radiotherapy until death or last seen in follow-up.

Therapy response was the primary endpoint, classified in responding (complete or partial remission after RT) vs. non-responding patients (progressive or stable disease after RT). For univariate and multivariate analysis, the Cox proportional hazard regression model was used to calculate the relative risk and hazard ratio and its 95% confidence interval (CI). Receiver operating characteristic (ROC) curves illustrate the performance of Hsp70 plasma levels as a binary classifier system in the prediction of therapy response after RT.

RESULTS

Pre-Therapeutic (T1) OPN Levels Correlate with Hsp70 Plasma Levels in Patients with NSCLC

A total of 44 NSCLC patients (6 females, 38 males) with NSCLC (M0) were enrolled into the study for T1. The clinico-pathological characteristics of all patients ($n = 44$) are summarized in **Table 1** and that of non-responding and responding patients is shown in **Table 2**. With respect to tumor volume ($p = 0.086$), age ($p = 0.114$), gender ($p = 0.306$), histology ($p = 0.158$), and UICC

TABLE 1 | Clinico-pathological characteristics of all non-small-cell lung cancer patients ($n = 44$) at M0 (Martin Luther University Hospital, Halle-Wittenberg).

		Counts	
Gender	Female	6	14%
	Male	38	86%
Histological type	Squamous cell carcinoma	23	52%
	Adeno ca	19	43%
	Other	2	5%
UICC stage	I–II	2	5%
	IIIa	16	36%
	IIIb	26	59%

stage ($p = 0.175$), no statistically significant differences have been determined in non-responding and responding patients.

Plasma levels of OPN and Hsp70 were determined pre-therapeutically (T1, before RT) in all patients (**Table 3**). As already shown for a larger patient cohort (30), also in a subgroup of non-metastasized NSCLC patients, high pre-therapeutic OPN plasma levels (above median, $n = 22$) significantly correlated with inferior OS compared to low (below median, $n = 22$) levels (13 [5–66] vs. 23 [5–61]; $p < 0.05$). Both biomarkers, OPN and Hsp70, revealed a positive correlation according to the Pearson's correlation coefficient ($r = 0.422$, $p = 0.005$) for T1. According to the Mann–Whitney *U* test (**Figure 1**), patients whose median Hsp70 values were above 9.30 ng/ml showed significantly higher OPN values, compared to those with median Hsp70 values below 9.30 ng/ml ($n = 43$, $p = 0.021$). A direct comparison of the OPN and Hsp70 values also revealed a correlation ($r = 0.42$), as shown in the Supplementary material (Figure S1 in Supplementary Material).

Hsp70 Plasma Levels Drop after RT in Patients with NSCLC

To investigate the impact of RT on Hsp70 plasma levels, pre- (T1) and post- (T2) therapeutic Hsp70 plasma levels were compared in 26 patients from whom plasma samples were available at both time-points. As summarized in **Table 4**, median Hsp70 levels dropped significantly from 10.35 before RT to 6.05 ng/ml after RT (paired samples test, $p = 0.016$). According to the Pearson's correlation coefficient, a significant positive correlation was determined ($r = 0.659$, $p < 0.0001$).

The drop in circulating Hsp70 after RT was also detected by mean Hsp70 levels (T1 vs. T2: 14.94 vs. 9.02 ng/ml). However, compared to a cohort of 114 healthy donors (7.8 ng/ml) which was published previously (49), mean Hsp70 values in NSCLC patients remained to be significantly upregulated before (T1) and after (T2) RT ($p < 0.05$).

High Post-Therapeutic Hsp70 Plasma Levels Predict Clinical Response to RT

To address the question whether Hsp70 might be predictive for clinical response, pre- (T1) and post- (T2) therapeutic Hsp70 plasma levels were associated with response to RT. As expected, patients who responded to therapy showed a significantly improved OS compared to non-responding patients (23 vs. 9 months, $p = 0.026$,

TABLE 2 | Clinico-pathological characteristics of non-responding and responding non-small-cell lung cancer patients at M0 (Martin Luther University Hospital, Halle-Wittenberg).

		Non-responder		Responder	
		Counts		Counts	
Gender	Female	0		6	17.6%
	Male	10	100%	28	82.4%
Histological type	Squamous cell carcinoma	7	70%	16	47%
	Adeno ca	2	20%	17	50%
	Other	1	10%	1	3%
UICC stage	I–II	1	10%	1	2.9%
	IIIa	4	40%	12	35.3%
	IIIb	5	50%	21	61.8%

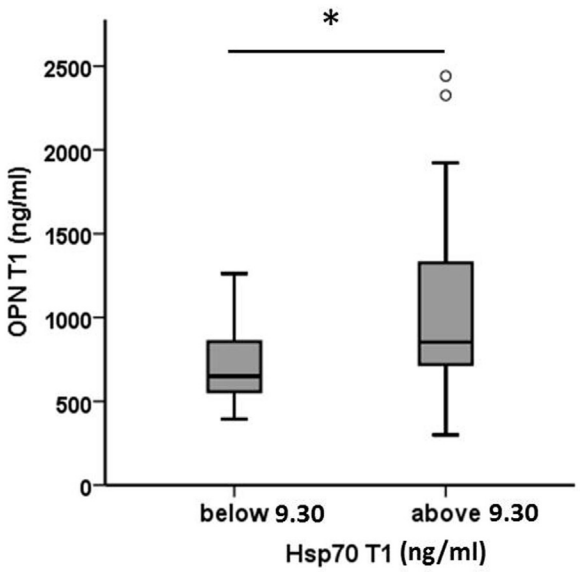

FIGURE 1 | Comparison of pre-therapeutic (T1) osteopontin (OPN) levels in non-small-cell lung cancer patients (M0) with high and low median heat shock protein 70 (Hsp70) plasma levels. According to the median Hsp70 plasma level of 9.30 ng/ml the patient cohort ($n = 43$) was divided into two subgroups with median Hsp70 plasma levels below or above 9.30 ng/ml; Mann–Whitney *U* test, $p = 0.021$.

TABLE 3 | Comparison of pre-therapeutic (T1) osteopontin (OPN) and heat shock protein 70 (Hsp70) plasma levels in non-small-cell lung cancer patients (M0; $n = 44$) in relation to overall survival.

	OPN T1 (ng/ml)	Hsp70 T1 (ng/ml)
N (missing)	44 (0)	43 (1)
Mean	872.14	12.13
SEM	71.63	2.02
Median	752.45	9.30
SD	475.11	13.26
Maximum	2441.00	67.50
Minimum	299.30	0.20
Paired samples test (overall survival)	$p < 0.05$	

TABLE 4 | Comparison of heat shock protein 70 (Hsp70) plasma levels before (T1) and 4–6 weeks after (T2) radio(chemo)therapy in non-small-cell lung cancer patients (M0).

	Hsp70 T1 (ng/ml)	Hsp70 T2 (ng/ml)
N	26	26
Mean	14.94	9.02
SEM	3.02	1.81
Median	10.35	6.05
SD	15.41	9.24
Maximum	67.50	46.20
Minimum	0.20	0.80
Paired samples test	$p = 0.016$	

log-rank Mantel Cox) who had an increased risk of death ($r = 2.11$, CI [0.94–4.57], $p = 0.58$).

A comparison of Hsp70 plasma levels before (T1) and 4–6 weeks after RT (T2) in non-responding ($n = 7$, 9.76 vs. 4.03 ng/ml) and responding patients ($n = 19$, 16.85 vs. 10.87 ng/ml) demonstrated that in both patient subgroups, mean and median Hsp70 plasma levels declined after RT (**Figure 2**). In general, responding patients had significantly higher (mean/median) Hsp70 plasma levels compared to non-responding patients at T1 and T2 (**Figure 2**).

As depicted in **Figure 3**, all patients who responded to therapy had significantly higher median Hsp70 plasma levels at T2 (median 8.6 ng/ml, range 0.8–46.2) after RT compared to those who showed no response (median 2.8, range 1.5–12.2) 4–6 weeks after therapy (T2) (Mann–Whitney *U* test, $p = 0.013$). The median Hsp70 values, revealed similar results with respect to both time-points in responding (11.10 ng/ml at T1 vs. 8.60 ng/ml at T2) and non-responding (5.30 ng/ml at T1 vs. 2.80 ng/ml at T2) patients (paired samples test $p = 0.034$).

In line with these findings, a subdivision of the patient cohort into subgroups with median Hsp70 plasma levels above and below 5.0 ng/ml at T2 revealed that patients with Hsp70 plasma levels above the threshold had significantly higher response rates than those below the threshold (92.9 vs. 50%, Pearson Chi-Square $p = 0.02$) (**Table 5**). Based on these findings, plasma Hsp70 levels were analyzed for their potential to predict therapy response after RT. The related ROC curve analysis (**Figure 4**) showed a significant predictive function ($p = 0.014$) of plasma Hsp70 levels for therapy response with an area under the curve (AUC) of 0.82. The optimal cutoff value which determines a positive therapy response is a value of ≤4.35 ng/ml with a sensitivity of 0.895 and a false positive rate of 0.143. Plasma Hsp70 levels which were taken before start of therapy (T1) showed a similar trend, but failed statistical significance.

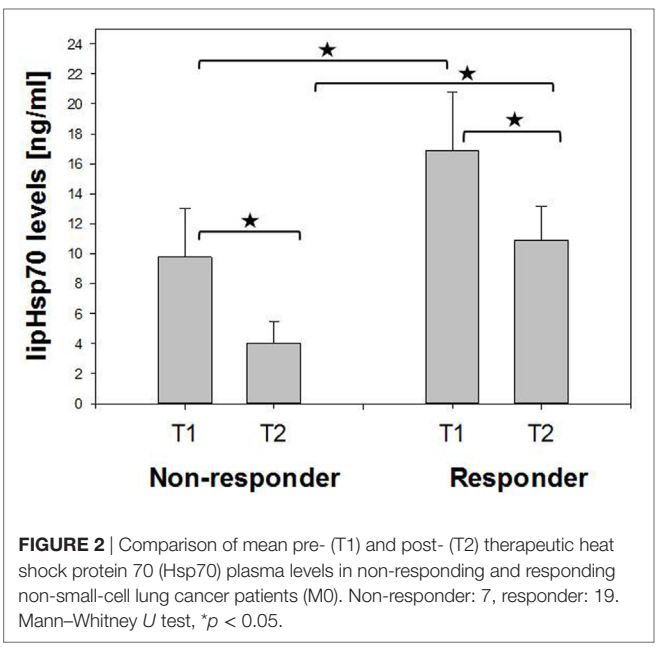

FIGURE 2 | Comparison of mean pre- (T1) and post- (T2) therapeutic heat shock protein 70 (Hsp70) plasma levels in non-responding and responding non-small-cell lung cancer patients (M0). Non-responder: 7, responder: 19. Mann–Whitney *U* test, *$p < 0.05$.

DISCUSSION

Post-Therapeutic Hsp70 Plasma Levels As a Biomarker for Therapy Response

The patient's endogenous immune defense is able to attack tumor cells. However, tumors as well as its microenvironment have developed mechanisms that allow immune escape against tumor cells (52–55). Therefore, novel therapeutic approaches aim to reactivate the patient's immune defense by inhibiting tumor-induced immune checkpoints that impair immune responses against malignantly transformed cells (56, 57). Another strategy to reinforce the patient's immune system is based on the activation of immune effector cells against tumor-specific targets that are overexpressed in tumor cells, presented on the cell surface and released in a tumor-selective manner (58). Tumor cells of different types including NSCLC (34) frequently overexpress Hsp70, present it on their plasma membrane, and actively release

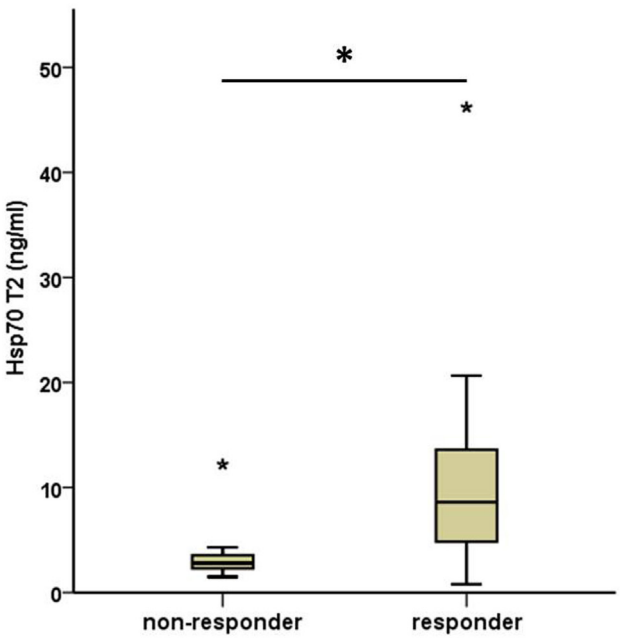

FIGURE 3 | Comparison of median post- (T2) therapeutic heat shock protein 70 (Hsp70) plasma levels in non-responding and responding non-small-cell lung cancer patients (M0). Non-responder: 7, responder: 19. Mann–Whitney *U* test, asterisks above the box plots indicate outliers; *$p = 0.013$.

TABLE 5 | Comparison of post- (T2) therapeutic heat shock protein 70 (Hsp70) plasma levels in non-responding and responding non-small-cell lung cancer patients (M0).

Therapy response (T2)	Median Hsp70 above 5 ng/ml	Median Hsp70 below 5 ng/ml
N	14	12
Non-responder	1 (7%)	6 (50%)
Responder	13 (93%)	6 (50%)
Pearson chi-square	$p = 0.02$	

Patients were divided into two subgroups with high and low median Hsp70 levels.

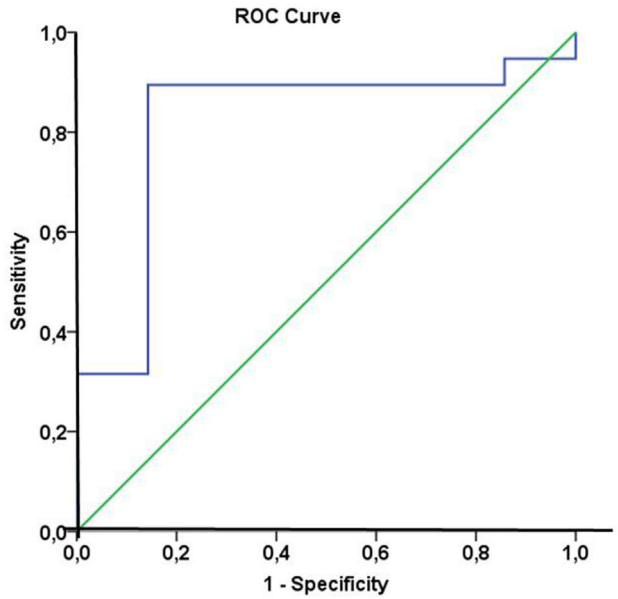

FIGURE 4 | Receiver operating characteristic (ROC) curve analysis of heat shock protein 70 (Hsp70) plasma levels of non-small-cell lung cancer (NSCLC) patients (M0) to predict therapy response. Area under the curve = 0.82, $p = 0.014$. The optimal cutoff value for distinction of responders and non-responders was an Hsp70 plasma level of 4.35 ng/ml with a sensitivity of 0.895 and a false positive rate of 0.143.

it in tumor exosomes (46, 58–60). However, dying tumor cells also release Hsp70, most likely as a free protein (47, 48). High intracellular Hsp70 levels have been found to interfere with apoptotic pathways and thereby protect tumor cells from programmed cell death following stress (61). Hence, we assume that therapy-resistant tumor cells with high cytosolic Hsp70 levels can better compensate RT-induced damage and thus mediate tumor cell survival.

Murakami et al. showed that in addition to cytosolic also membrane-bound Hsp70 supports protection of tumor cells against RT-induced cell death (62), although the expression density of cytosolic and membrane-bound Hsp70 are not associated. Therefore, membrane Hsp70 fulfils dual roles, on the one hand, it acts as a tumor-specific target for Hsp70-activated NK cells (43, 44, 50, 63), on the other hand it mediates therapy resistance. An ongoing phase II clinical trial using *ex vivo* Hsp70-activated NK cells for the treatment of patients with NSCLC after RT is presently testing whether the immunostimulatory capacity of NK cells can overrule therapy resistance of membrane Hsp70-positive NSCLC (44).

In the present trial, we investigated the role of circulating Hsp70 as a prognostic marker to predict outcome of RT in patients with NSCLC (M0) at different time-points. A comparison of pre- and post-therapeutic plasma levels revealed significantly elevated Hsp70 levels in responding compared to non-responding patients.

The lipHsp70 ELISA (52) detects both, lipid-bound and free Hsp70. We hypothesize that high Hsp70 levels at diagnosis predominantly originate from exosomal Hsp70 released by viable tumor cells. This is in line with our finding that Hsp70 plasma levels before start of therapy reflect vital gross tumor volume (50). In contrast, elevated post-therapeutic Hsp70 plasma levels rather originate from dying tumor cells (47, 48) that might be able to stimulate the immune system. Analysis of the concentration of cytosolic proteins in the exosomal versus non-exosomal plasma fraction after ultracentrifugation of responding non-metastasized NSCLC patients in stage IIIa/b ($N = 4$) before (T1) and after RT (T2) showed a significant ($p < 0.05$) protein drop in the exosomal fraction and an increase in the non-exosomal fraction after therapy (data not shown) which reflects the reduction in viable tumor mass after therapy. In summary, pre- and post-treatment Hsp70 levels are indicative for different tumor characteristics such as vital tumor mass, intrinsic tumor aggressiveness, and RT-induced tumor cell death that can cause immunostimulation.

Previous work of our group demonstrated that membrane Hsp70 serves as a target for NK cells that have been pre-stimulated with an Hsp70-peptide plus low-dose interleukin 2 (42). The stimulation of NK cells is associated with an upregulated expression of activatory NK receptors, including the C-type lectin receptor CD94/NKG2C (64) that in turn induces the production of the pro-apoptotic enzyme granzyme B (63). With respect to these findings, we speculate that high post-therapeutic Hsp70 plasma levels derived from dying tumor cells in a pro-inflammotory environment after RT might be able to stimulate Hsp70-reactive NK cells that mediate favorable therapeutic outcome. Elevated pre-therapeutic exosomal Hsp70 plasma levels might be predictive for a superior outcome because they reflect an aggressive, but yet immunogenic tumor type. This is in accordance with the finding that Hsp70-bearing exosomes isolated from membrane Hsp70-positive tumor cells, but not from their Hsp70-negative counterparts, can induce the migratory and cytolytic activity of NK cells (65).

The high predictive value of post-therapeutic Hsp70 plasma levels for the response of an individual patient could be demonstrated by ROC analysis with an AUC of 0.82 ($p = 0.014$). Identical analyses have been performed for Hsp70 plasma levels before start of therapy. Although a similar trend was observed, pre-therapeutic levels failed to show statistical significance as a biomarker for clinical response. This might be explained by the fact that pre-therapeutic Hsp70 plasma levels predominantly originate from viable tumor cells and thus represent vital tumor mass rather than therapy response.

To obtain a better view on the exact dynamics and prognostic relevance of circulating Hsp70 levels, further pre- and post-therapeutic measurements of Hsp70 at different time-points have to be correlated with clinical response in larger patient cohorts.

Role of Hsp70 in the Context of Hypoxia-Related Markers of the Tumor Microenvironment

Another parameter that co-determines OS of patients after RT is the tumor microenvironment. The presence of hypoxic stress impacts prognosis and therapy response to RT adversely. The molecular effects induced by RT involve the production of

DNA radicals which are normally fixed by oxygen. Hence, DNA damage decreased under hypoxic stress and hypoxia-inducible factor 1α (HIF1α) is stabilized which in turn leads to promotion of tumor cell survival. HIF1α also has been shown to impair membrane Hsp70 expression on tumor cells, and therefore might negatively affect NK cell recognition (66).

Tumor hypoxia is also associated with an overexpression of OPN. Physiologically, OPN is involved in the process of bone remodeling (67); however, many tumor cells show an overexpression of this protein (68) as an aggression marker. Plasma levels of OPN correlate with tumor hypoxia in NSCLC (38), and previously we demonstrated that high OPN levels before RT and increasing OPN levels after RT translate into poor OS in NSCLC after radical RT (30, 31). With respect to the prediction of therapy response, OPN as a single marker failed to show significance. Only in combination with VEGF and CAIX, the prognostic impact of OPN could be augmented (30). Hypoxic stress also has been shown to increase the release of exosomes (69) that contain large amounts Hsp70. Therefore, the present study evaluated the prognostic and predictive value of Hsp70 levels in relation to OPN. Due to a positive correlation of Hsp70 and OPN plasma levels at diagnosis, the association of OPN and OS was re-evaluated in the subgroup of non-metastasized NSCLC patients ($n = 44$) that was also analyzed for Hsp70. In line with previous results of a larger, more heterogenous NSCLC patient cohort (31), non-metastastized NSCLC patients also revealed a significant correlation of high OPN values at T1 with a decreased OS.

CONCLUSION

Our findings illustrate the differential prognostic and predictive relevance of pre- and post-treatment Hsp70 levels in NSCLC patients after RT. Being actively released by viable tumor cells in exosomes, high pre-therapeutic Hsp70 levels (T1) are most likely be indicative for viable tumor mass. Therapy response that was associated with a reduction in tumor size results in a significant drop in exosomal Hsp70 plasma levels from 21.7 ± 2.8 to 15.6 ± 1.3 ng/ml ($p < 0.05$, data not shown), as determined by lipHsp70 ELISA in 4 responding patients who were not included into the trial. However, with respect to the immunostimulatory capacity of Hsp70 derived from dying tumor cells, elevated post-therapeutic Hsp70 levels also can predict beneficial outcome to RT. Although elevated OPN levels significantly correlate with decreased OS, reduced lung function, and weight loss (30), OPN as a single parameter is unable to predict therapy response (30, 31). Therefore, the co-detection of both biomarkers before and/or after RT integrates prognostic (OPN) and predictive (Hsp70) information for therapy response that allows a more rapid therapy adaptation to improve clinical outcome of NSCLC patients.

ETHICS STATEMENT

The Ethics Committee of the Medical Faculty of the Martin Luther University Halle-Wittenberg approved the study protocol. Written informed consent was obtained from all patients before start of the study. All procedures were in accordance with the Helsinki Declaration of 1975 (as revised in 2008).

AUTHOR CONTRIBUTIONS

CO and SG equally contributed to the study; CO, SG, and MB conceived and designed the experiments, analyzed data, and wrote the paper; DV gave clinical advice; and GM did proofreading, designed and revised the study.

FUNDING

We want to thank Anett Lange for excellent editorial support. The work at the TUM was supported by DFG (SFB824/3, MAP, INST411/37-1FUGG, INST95/980-1FUGG, STA1520/1-1), BMBF (01GU0823, 02NUK038A), BMWi (AiF), and DKTK-ROG. This work was supported by the German Research Foundation (DFG) and the Technische Universität München within the funding programme Open Access Publishing. The work of the Martin Luther University Halle-Wittenberg was supported by the Wilhelm Sander Stiftung (FKZ: 2007.123.2).

SUPPLEMENTARY MATERIAL

The Supplementary Material for this article can be found online at http://www.frontiersin.org/article/10.3389/fimmu.2017.01305/full#supplementary-material.

REFERENCES

1. Parkin DM, Bray F, Ferlay J, Pisani P. Estimating the world cancer burden: Globocan 2000. *Int J Cancer* (2001) 94:153–6. doi:10.1002/ijc.1440
2. Cancer Research UK. *Worldwide Cancer Statistics*. (2015). Available from: http://cancerresearchuk.org/health-professional/cancer-statistics/worldwide-cancer#heading-Zero
3. Guckenberger M, Allgauer M, Appold S, Dieckmann K, Ernst I, Ganswindt U, et al. Safety and efficacy of stereotactic body radiotherapy for stage 1 non-small-cell lung cancer in routine clinical practice: a patterns-of-care and outcome analysis. *J Thorac Oncol* (2013) 8:1050–8. doi:10.1097/JTO.0b013e318293dc45
4. Pass HI, Carbone DP, Johnson DH, Minna JD, Scagliotti GV, Turrisi AT. *Principles and Practice of Lung Cancer: The Official Reference Text of the International Association for the Study of Lung Cancer (IASLC)*. Lippincott Williams & Wilkins (2012).
5. Mirsadraee S, Oswal D, Alizadeh Y, Caulo A, van Beek E Jr. The 7th lung cancer TNM classification and staging system: review of the changes and implications. *World J Radiol* (2012) 4:128–34. doi:10.4329/wjr.v4.i4.128
6. Oberije C, De Ruysscher D, Houben R, van de Heuvel M, Uyterlinde W, Deasy JO, et al. A validated prediction model for overall survival from stage III non-small cell lung cancer: toward survival prediction for individual patients. *Int J Radiat Oncol Biol Phys* (2015) 92:935–44. doi:10.1016/j.ijrobp.2015.02.048
7. *Breakthrough of the Year 2013| Science/AAAS | News*. (2015). Available from: http://news.sciencemag.org/breaktrough-of-the-year-2013#.Vb38J_nwh_8
8. Deeks ED. Nivolumab: a review of its use in patients with malignant melanoma. *Drugs* (2014) 74:1233–9. doi:10.1007/s40265-014-0234-4
9. Wolchok JD, Kluger H, Callahan MK, Postow MA, Rizvi NA, Lesokhin AM, et al. Nivolumab plus ipilimumab in advanced melanoma. *N Engl J Med* (2013) 369:122–33. doi:10.1056/NEJMoa1302369

10. Marquez-Rodas I, Cerezuela P, Soria A, Berrocal A, Riso A, Gonzalez-Cao M, et al. Immune checkpoint inhibitors: therapeutic advances in melanoma. *Ann Transl Med* (2015) 3:267. doi:10.3978/j.issn.2305-5839.2015.10.27
11. Anagnostou VK, Brahmer JR. Cancer immunotherapy: a future paradigm shift in the treatment of non-small cell lung cancer. *Clin Cancer Res* (2015) 21:976–84. doi:10.1158/1078-0432.CCR-14-1187
12. Schmid-Bindert G, Jiang T. First-line nivolumab (anti-PD-1) monotherapy in advanced NSCLC: the story of immune checkpoint inhibitors and "the sorcerers apprentice". *Transl Lung Cancer Res* (2015) 4:215–6. doi:10.3978/j.issn.2218-6751.2015.01.12
13. Soria JC, Marabelle A, Brahmer JR, Gettinger S. Immune checkpoint modulation for non-small cell lung cancer. *Clin Cancer Res* (2015) 21:2256–62. doi:10.1158/1078-0432.CCR-14-2959
14. Bustamante Alvarez JG, Gonzalez-Cao M, Karachaliou N, Santarpia M, Viteri S, Teixido C, et al. Advances in immunotherapy for treatment of lung cancer. *Cancer Biol Med* (2015) 12:209–22. doi:10.7497/j.issn.2095-3941.2015.0032
15. Brahmer JR, Pardoll DM. Immune checkpoint inhibitors: making immunotherapy a reality for the treatment of lung cancer. *Cancer Immunol Res* (2013) 1:85–91. doi:10.1158/2326-6066.CIR-13-0078
16. Forde PM, Brahmer JR, Kelly RJ. New strategies in lung cancer: epigenetic therapy for non-small cell lung cancer. *Clin Cancer Res* (2014) 20:2244–8. doi:10.1158/1078-0432.CCR-13-2088
17. Massarelli E, Papadimitrakopoulou V, Welsh J, Tang C, Tsao AS. Immunotherapy in lung cancer. *Transl Lung Cancer Res* (2014) 3:53–63. doi:10.3978/j.issn.2218-6751.2014.01.01
18. Rangachari D, Brahmer JR. Targeting the immune system in the treatment of non-small-cell lung cancer. *Curr Treat Options Oncol* (2013) 14:580–94. doi:10.1007/s11864-013-0250-8
19. Postow MA, Callahan MK, Barker CA, Yamada Y, Yuan J, Kitano S, et al. Immunologic correlates of the abscopal effect in a patient with melanoma. *N Engl J Med* (2012) 366:925–31. doi:10.1056/NEJMoa1112824
20. Rödel F, Frey B, Multhoff G, Gaipl U. Contribution of the immune system to bystander and non-targeted effects of ionizing radiation. *Cancer Lett* (2015) 356:105–13. doi:10.1016/j.canlet.2013.09.015
21. Gaipl US, Multhoff G, Scheithauer H, Lauber K, Hehlgans S, Frey B, et al. Kill and spread the word: stimulation of antitumor immune responses in the context of radiotherapy. *Immunotherapy* (2014) 6:597–610. doi:10.2217/imt.14.38
22. Siva S, MacManus MP, Martin RF, Martin OA. Abscopal effects of radiation therapy: a clinical review for the radiobiologist. *Cancer Lett* (2015) 356:82–90. doi:10.1016/j.canlet.2013.09.018
23. Hanna GG, Coyle VM, Prise KM. Immune modulation in advanced radiotherapies: targeting out-of-field effects. *Cancer Lett* (2015) 368:246–51. doi:10.1016/j.canlet.2015.04.007
24. Golden EB, Demaria S, Schiff PB, Chachoua A, Formenti SC. An abscopal response to radiation and ipilimumab in a patient with metastatic non-small cell lung cancer. *Cancer Immunol Res* (2013) 1:365–72. doi:10.1158/2326-6066.CIR-13-0115
25. Schmid TE, Multhoff G. Non-targeted effects of photon and particle irradiation and the interaction with the immune system. *Front Oncol* (2012) 2:80. doi:10.3389/fonc.2012.00080
26. Sun R, Sbai A, Ganem G, Boudabous M, Collin F, Marcy PY, et al. [Non-targeted effects (bystander, abscopal) of external beam radiation therapy: an overview for the clinician]. *Cancer Radiother* (2014) 18:770–8. doi:10.1016/j.canrad.2014.08.004
27. Simone CB II, Burri SH, Heinzerling JH. Novel radiotherapy approaches for lung cancer: combining radiation therapy with targeted and immunotherapies. *Transl Lung Cancer Res* (2015) 4:545–52. doi:10.3978/j.issn.2218-6751.2015.10.05
28. Kao CJ, Wurz GT, Lin YC, Vang DP, Griffey SM, Wolf M, et al. Assessing the effects of concurrent versus sequential cisplatin/radiotherapy on immune status in lung tumor-bearing C57BL/6 mice. *Cancer Immunol Res* (2015) 3:741–50. doi:10.1158/2326-6066.CIR-14-0234
29. Sage EK, Schmid TE, Sedelmayr M, Gehrmann M, Geinitz H, Duma MN, et al. Comparative analysis of the effects of radiotherapy versus radiotherapy after adjuvant chemotherapy on the composition of lymphocyte subpopulations in breast cancer patients. *Radiother Oncol* (2015) 118:176–80. doi:10.1016/j.radonc.2015.11.016
30. Ostheimer C, Bache M, Guttler A, Kotzsch M, Vordermark D. A pilot study on potential plasma hypoxia markers in the radiotherapy of non-small cell lung cancer. Osteopontin, carbonic anhydrase IX and vascular endothelial growth factor. *Strahlenther Onkol* (2014) 190:276–82. doi:10.1007/s00066-013-0484-1
31. Ostheimer C, Bache M, Guttler A, Reese T, Vordermark D. Prognostic information of serial plasma osteopontin measurement in radiotherapy of non-small-cell lung cancer. *BMC Cancer* (2014) 14:858. doi:10.1186/1471-2407-14-858
32. Jasinski-Bergner S, Mandelboim O, Seliger B. The role of microRNAs in the control of innate immune response in cancer. *J Natl Cancer Inst* (2014) 106. doi:10.1093/jnci/dju257
33. Mima K, Nishihara R, Nowak JA, Kim SA, Song M, Inamura K, et al. MicroRNA MIR21 and T cells in colorectal cancer. *Cancer Immunol Res* (2016) 4:33–40. doi:10.1158/2326-6066.CIR-15-0084
34. Hantschel M, Pfister K, Jordan A, Scholz R, Andreesen R, Schmitz G, et al. Hsp70 plasma membrane expression on primary tumor biopsy material and bone marrow of leukemic patients. *Cell Stress Chaperones* (2000) 5:438–42. doi:10.1379/1466-1268(2000)005<0438:HPMEOP>2.0.CO;2
35. Gunther S, Ostheimer C, Specht HM, Erl J, Breuninger S, Combs S, et al. Development of a novel LipHsp70 ELISA for screening exosomal Hsp70 in the blood of NSCLC patients. *Strahlenther Onkol* (2015) (Suppl 1):S72.
36. Ostheimer C, Vordermark D. Osteopontin – an indicator of tumor hypoxia and treatment resistance. In: Vordermark D, editor. *Hypoxia: Causes, Types and Management*. New York: Nova Publishers (2013). p. 255–318.
37. Zhu Y, Denhardt DT, Cao H, Sutphin PD, Koong AC, Giaccia AJ, et al. Hypoxia upregulates osteopontin expression in NIH-3T3 cells via a Ras-activated enhancer. *Oncogene* (2005) 24:6555–63. doi:10.1038/sj.onc.1208800
38. Le QT, Chen E, Salim A, Cao H, Kong CS, Whyte R, et al. An evaluation of tumor oxygenation and gene expression in patients with early stage non-small cell lung cancers. *Clin Cancer Res* (2006) 12:1507–14. doi:10.1158/1078-0432.CCR-05-2049
39. Overgaard J, Eriksen JG, Nordsmark M, Alsner J, Horsman MR; Danish Head and Neck Cancer Study Group. Plasma osteopontin, hypoxia, and response to the hypoxia sensitiser nimorazole in radiotherapy of head and neck cancer: results from the DAHANCA 5 randomised double-blind placebo-controlled trial. *Lancet Oncol* (2005) 6:757–64. doi:10.1016/S1470-2045(05)70292-8
40. Gao Y, Gao W, Chen X, Cha N, Wang X, Jia X, et al. Enhancing the treatment effect on melanoma by heat shock protein 70-peptide complexes purified from human melanoma cell lines. *Oncol Rep* (2016) 36:1243–50. doi:10.3892/or.2016.4947
41. Blachere NE, Li Z, Chandawarkar RY, Suto R, Jaikaria NS, Basu S, et al. Heat shock protein-peptide complexes, reconstituted in vitro, elicit peptide-specific cytotoxic T lymphocyte response and tumor immunity. *J Exp Med* (1997) 186:1315–22. doi:10.1084/jem.186.8.1315
42. Multhoff G, Pfister K, Gehrmann M, Hantschel M, Gross C, Hafner M, et al. A 14-mer Hsp70 peptide stimulates natural killer (NK) cell activity. *Cell Stress Chaperones* (2001) 6:337–44. doi:10.1379/1466-1268(2001)006<0337:AMHPSN>2.0.CO;2
43. Krause SW, Gastpar R, Andreesen R, Gross C, Ullrich H, Thonigs G, et al. Treatment of colon and lung cancer patients with ex vivo heat shock protein 70-peptide-activated, autologous natural killer cells: a clinical phase i trial. *Clin Cancer Res* (2004) 10:3699–707. doi:10.1158/1078-0432.CCR-03-0683
44. Specht HM, Ahrens N, Blankenstein C, Duell T, Fietkau R, Gaipl US, et al. Heat shock protein 70 (Hsp70) peptide activated natural killer (NK) cells for the treatment of patients with non-small cell lung cancer (NSCLC) after radiochemotherapy (RCTx) – from preclinical studies to a clinical phase II trial. *Front Immunol* (2015) 6:162. doi:10.3389/fimmu.2015.00162
45. Moser C, Schmidbauer C, Gurtler U, Gross C, Gehrmann M, Thonigs G, et al. Inhibition of tumor growth in mice with severe combined immunodeficiency is mediated by heat shock protein 70 (Hsp70)-peptide-activated, CD94 positive natural killer cells. *Cell Stress Chaperones* (2002) 7:365–73. doi:10.1379/1466-1268(2002)007<0365:IOTGIM>2.0.CO;2
46. Gehrmann M, Specht HM, Bayer C, Brandstetter M, Chizzali B, Duma M, et al. Hsp70 – a biomarker for tumor detection and monitoring of outcome of radiation therapy in patients with squamous cell carcinoma of the head and neck. *Radiat Oncol* (2014) 9:131. doi:10.1186/1748-717X-9-131
47. De Maio A. Extracellular Hsp70: export and function. *Curr Protein Pept Sci* (2014) 15:225–31. doi:10.2174/1389203715666140331113057
48. Radons J, Multhoff G. Immunostimulatory functions of membrane-bound and exported heat shock protein 70. *Exerc Immmunol Rev* (2005) 11:17–33.

49. Breuninger S, Ertl J, Bayer C, Knape C, Gunther S, Regel I, et al. Quantitative analysis of liposomal heat shock protein 70 (Hsp70) in the blood of tumor patients using a novel lipHsp70 ELISA. *J Clin Cell Immunol* (2015) 5:4–10.
50. Gunther S, Ostheimer C, Stangl S, Specht HM, Mozes P, Jesinghaus M, et al. Correlation of Hsp70 serum levels with gross tumor volume and composition of lymphocyte subpopulations in patients with squamous cell and adeno non-small cell lung cancer. *Front Immunol* (2015) 6:556. doi:10.3389/fimmu.2015.00556
51. Stangl S, Gehrmann M, Riegger J, Kuhs K, Riederer I, Sievert W, et al. Targeting membrane heat-shock protein 70 (Hsp70) on tumors by cmHsp70.1 antibody. *Proc Natl Acad Sci U S A* (2011) 108:733–8. doi:10.1073/pnas.1016065108
52. Sun B, Zhang S, Zhao X, Zhang W, Hao X. Vasculogenic mimicry is associated with poor survival in patients with mesothelial sarcomas and alveolar rhabdomyosarcomas. *Int J Oncol* (2004) 25:1609–14. doi:10.3892/ijo.25.6.1609
53. Williamson SC, Metcalf RL, Trapani F, Mohan S, Antonello J, Abbott B, et al. Vasculogenic mimicry in small cell lung cancer. *Nat Commun* (2016) 7:13322. doi:10.1038/ncomms13322
54. Folberg R, Rummelt V, Parys-Van Ginderdeuren R, Hwang T, Woolson RF, Pe'er J, et al. The prognostic value of tumor blood vessel morphology in primary uveal melanoma. *Ophthalmology* (1993) 100:1389–98. doi:10.1016/S0161-6420(93)31470-3
55. Hanahan D, Weinberg RA. Hallmarks of cancer: the next generation. *Cell* (2011) 144:646–74. doi:10.1016/j.cell.2011.02.013
56. Iafolla MAJ, Juergens RA. Update on programmed death-1 and programmed death-ligand 1 inhibition in the treatment of advanced or metastatic non-small cell lung cancer. *Front Oncol* (2017) 7:67. doi:10.3389/fonc.2017.00067
57. Cooling LL, Sherbeck J, Mowers JC, Hugan SL. Development of red blood cell autoantibodies following treatment with checkpoint inhibitors: a new class of anti-neoplastic, immunotherapeutic agents associated with immune dysregulation. *Immunohematology* (2017) 33:15–21.
58. Weidle UH, Maisel D, Klostermann S, Schiller C, Weiss EH. Intracellular proteins displayed on the surface of tumor cells as targets for therapeutic intervention with antibody-related agents. *Cancer Genomics Proteomics* (2011) 8:49–63.
59. Bayer C, Liebhardt ME, Schmid TE, Trajkovic-Arsic M, Hube K, Specht HM, et al. Validation of heat shock protein 70 as a tumor-specific biomarker for monitoring the outcome of radiation therapy in tumor mouse models. *Int J Radiat Oncol Biol Phys* (2014) 88:694–700. doi:10.1016/j.ijrobp.2013.11.008
60. Multhoff G, Botzler C, Wiesnet M, Muller E, Meier T, Wilmanns W, et al. A stress-inducible 72-kDa heat-shock protein (HSP72) is expressed on the surface of human tumor cells, but not on normal cells. *Int J Cancer* (1995) 61:272–9. doi:10.1002/ijc.2910610222
61. Jaattela M, Wissing D, Kokholm K, Kallunki T, Egeblad M. Hsp70 exerts its anti-apoptotic function downstream of caspase-3-like proteases. *EMBO J* (1998) 17:6124–34. doi:10.1093/emboj/17.21.6124
62. Murakami N, Kuhnel A, Schmid TE, Ilicic K, Stangl S, Braun IS, et al. Role of membrane Hsp70 in radiation sensitivity of tumor cells. *Radiat Oncol* (2015) 10:149. doi:10.1186/s13014-015-0461-1
63. Gross C, Koelch W, DeMaio A, Arispe N, Multhoff G. Cell surface-bound heat shock protein 70 (Hsp70) mediates perforin-independent apoptosis by specific binding and uptake of granzyme B. *J Biol Chem* (2003) 278:41173–81. doi:10.1074/jbc.M302644200
64. Gross C, Hansch D, Gastpar R, Multhoff G. Interaction of heat shock protein 70 peptide with NK cells involves the NK receptor CD94. *Biol Chem* (2003) 384:267–79. doi:10.1515/BC.2003.030
65. Gastpar R, Gehrmann M, Bausero MA, Asea A, Gross C, Schroeder JA, et al. Heat shock protein 70 surface-positive tumor exosomes stimulate migratory and cytolytic activity of natural killer cells. *Cancer Res* (2005) 65:5238–47. doi:10.1158/0008-5472.CAN-04-3804
66. Schilling D, Tetzlaff F, Konrad S, Li W, Multhoff G. A hypoxia-induced decrease of either MICA/B or Hsp70 on the membrane of tumor cells mediates immune escape from NK cells. *Cell Stress Chaperones* (2015) 20:139–47. doi:10.1007/s12192-014-0532-5
67. Choi ST, Kim JH, Kang EJ, Lee SW, Park MC, Park YB, et al. Osteopontin might be involved in bone remodelling rather than in inflammation in ankylosing spondylitis. *Rheumatology (Oxford)* (2008) 47:1775–9. doi:10.1093/rheumatology/ken385
68. Rittling SR, Chambers AF. Role of osteopontin in tumour progression. *Br J Cancer* (2004) 90:1877–81. doi:10.1038/sj.bjc.6601839
69. Jung KO, Youn H, Lee CH, Kang KW, Chung JK. Visualization of exosome-mediated miR-210 transfer from hypoxic tumor cells. *Oncotarget* (2017) 8:9899–910. doi:10.18632/oncotarget.14247

Conflict of Interest Statement: The authors declare that the research was conducted in the absence of any commercial or financial relationships that could be construed as a potential conflict of interest.